







Review

# Aspects of Reaction Engineering for Biodiesel Production

Afsanehsadat Larimi <sup>1,\*</sup>, Adam P. Harvey <sup>2,\*</sup>, Anh N. Phan <sup>2</sup>, Mehdi Beshtar <sup>3</sup>, Karen Wilson <sup>4</sup>  
and Adam F. Lee <sup>4,\*</sup>

<sup>1</sup> Department of Chemical Engineering, School of Engineering and Applied Sciences, Swansea University, Swansea SA1 8EN, UK

<sup>2</sup> School of Engineering, Newcastle University, Newcastle upon Tyne NE2 4HH, UK; anh.phan@ncl.ac.uk

<sup>3</sup> Department of Chemical and Petroleum Engineering, Sharif University of Technology, Tehran 11155-1639, Iran; beshtarmahdi@gmail.com

<sup>4</sup> Centre for Catalysis and Clean Energy, Griffith University, Gold Coast, QLD 4222, Australia; karen.wilson6@griffith.edu.au

\* Correspondence: a.larimi@swansea.ac.uk (A.L.); adam.harvey@ncl.ac.uk (A.P.H.); adam.lee@griffith.edu.au (A.F.L.)

**Abstract:** Biodiesel is a non-toxic, drop-in liquid transportation fuel that is amenable to continuous production from sustainable biomass resources using catalytic technologies. A diverse range of catalysts and reactor technologies have been experimentally investigated and computationally modelled, for producing biodiesel (fatty acid methyl esters) from oil feedstocks by their esterification or transesterification with short-chain alcohols. Solid-acid and base catalysts are attractive for biodiesel production from renewable oil feedstocks due to their ease of separation from the desired biodiesel and glycerol by-product, use of Earth's abundant elements, and suitability in continuous processes. Here, we review the technical challenges and opportunities in designing catalytic reactor systems for biodiesel production.

**Keywords:** biodiesel; catalysis; porous solids; process intensification; reactor engineering



**Citation:** Larimi, A.; Harvey, A.P.; Phan, A.N.; Beshtar, M.; Wilson, K.; Lee, A.F. Aspects of Reaction Engineering for Biodiesel Production. *Catalysts* **2024**, *14*, 701. <https://doi.org/10.3390/catal14100701>

Academic Editor: Keith Hohn

Received: 23 August 2024

Revised: 19 September 2024

Accepted: 21 September 2024

Published: 8 October 2024



**Copyright:** © 2024 by the authors. Licensee MDPI, Basel, Switzerland. This article is an open access article distributed under the terms and conditions of the Creative Commons Attribution (CC BY) license (<https://creativecommons.org/licenses/by/4.0/>).

## 1. Introduction

Biomass utilisation will play an important role in achieving the United Nations 2030 Sustainable Development Goals of affordable and clean energy, responsible consumption and production, climate action, and numerous national government targets of net-zero CO<sub>2</sub> emissions [1–5]. Liquid biofuels already make a modest but significant contribution to mitigating carbon emissions from hard-to-abate transport transportation sectors, with bioethanol and biodiesel accounting for the majority of biomass consumption in chemical manufacturing, according to the U.S. Energy Information Administration [6]. Global population growth and pressures to improve living standards have exacerbated the drivers to develop and commercialise renewable and environmentally benign alternatives to fossil fuels [7,8]. Biodiesel is a commercial fuel derived from triglyceride-containing feedstocks such as edible/non-edible plants, waste vegetable oils, microalgae and animal fats [9], with physiochemical properties similar or superior to conventional diesel [10,11]. For instance, biodiesel has a higher cetane number, which improves engine performance by ensuring a more complete fuel combustion and better lubricating properties, which can extend engine life. Additionally, biodiesel has a higher flash point, making it safer to handle and store. However, its calorific value is approximately 9% lower than that of standard diesel, which can impact fuel efficiency. Biodiesel also produces lower emissions of particulate matter, carbon monoxide, carbon dioxide, sulfur oxides, and unburned hydrocarbons, mitigating air pollution [12,13]. Nevertheless, biodiesel is often more expensive than petroleum-derived diesel, with comparative pricing heavily dependent on subsidies, legislation, and geopolitics [14]. Biodiesel is most commonly produced by the (base) acid-catalysed (trans)esterification of triglycerides (TAGs, Figure 1A) with short-chain alcohols to yield

fatty acid alkyl esters and glycerol by-products [15]. Methanol is the most common alcohol for oil transesterification due to its high polarity and reactivity, and it produces fatty acid methyl esters (FAMES). In the presence of a solid-acid catalyst, methanol can also undergo esterification with free fatty acid (FFA) impurities to form FAMES (Figure 1B). Although methanol is the most common alcohol used for biodiesel production, ethanol offers lower toxicity and higher miscibility with vegetable oils [16,17]. For base catalysts, undesired saponification competes with transesterification (Figure 1C).

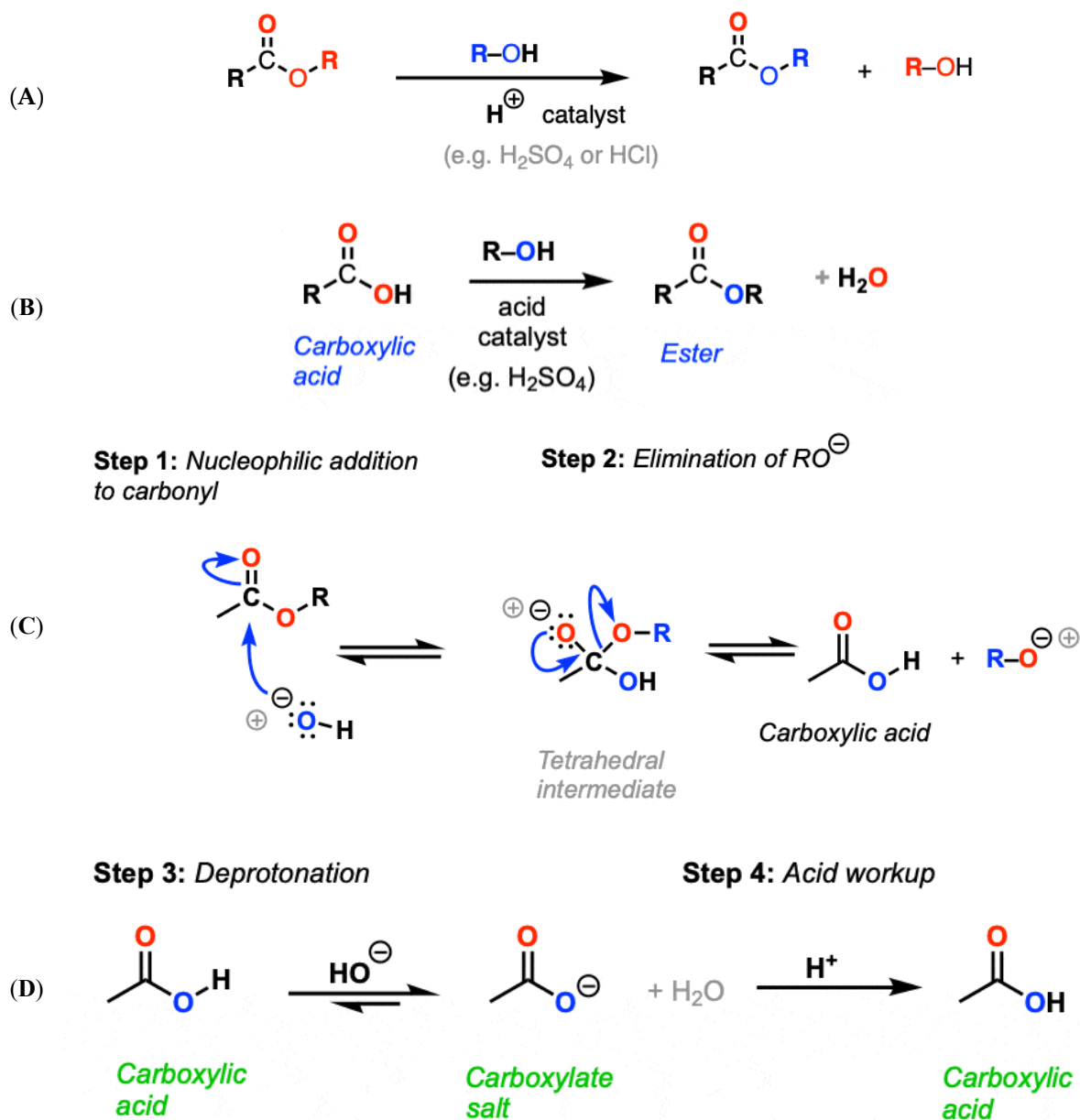


**Figure 1.** Biodiesel production by (A) transesterification and (B) esterification of triglycerides. (C) Saponification of triglycerides with liquid base catalyst. (D) Base catalyst neutralisation by FFAs. Bond-forming (blue), bond scission (red). Adapted from references [18].

A major consideration for biodiesel production is feedstock selection, which influences fuel cost, land use and food security (notably for edible oil crops and/or animal fats in developing countries [19]). Many recent studies, therefore, focus on biomass waste and used cooking oils [15,20–22] or inedible plant and microalgal species [23–26]. The cost implications of different bio-oil and waste cooking oil feedstocks are summarised in Table 1. As shown in Table 1, the production of hundreds of thousands of barrels of diesel per

day requires less than 1% of the land used for soybean and corn cultivation. Algae can yield more oil per hectare of the occupied area compared to traditional biodiesel crops. For example, the yield of algae with 30% oil in dry biomass is up to 58,700 L/hectares/year, which is much higher compared to oilseed rape or soybeans [27]. Palm oil and sunflower oil have the lowest and highest prices, respectively. In the future, if the price of seed oils rises due to population growth and its consequent food crisis, and technological advances are made in the production of algae biodiesel, the algae biodiesel price could compete with the price of B99-B100 and B20. Considering the average plant oil prices and waste cooking oil (WCO) average free on board (FOB) price, WCO is more economical than plant oils but available in much lower quantities than plant oils and hence cannot supply a substantial portion of the global biodiesel demand.

**Table 1.** Economics of biodiesel production from different oil feedstocks [27–32].

<b>Fresh oils</b>			
Oil crop	Average oil yield /L·hectare <sup>-1</sup> ·year <sup>-1</sup>	Average oilseed price /\$·tonne <sup>-1</sup>	Average oil price /\$·tonne <sup>-1</sup>
Palm	5950–1900	-	900
Soybean	446–12,258	420	900
Rapeseed	1190	400	1050
Corn	172	177	1200
Sunflower	952	340	890
Algae	58,700–136,900	-	0.43–24.60 \$/L
<b>Waste cooking oil</b>			
Country	Waste cooking oil average FOB price /\$·tonne <sup>-1</sup>	Waste cooking oil average production /kton·year <sup>-1</sup>	
USA	990	10,000	
China	1000	5000	
India	1050	3000	
UK	1050	200	
<b>Biodiesel</b>			
B99–B100 price /\$·tonne <sup>-1</sup>	B20 price /\$·tonne <sup>-1</sup>	Algae biodiesel /\$·tonne <sup>-1</sup>	
1183	1033	2500	

Waste cooking oils contain water through the dehydration of food, while the oils themselves are exposed to oxygen, heat and light during cooking. These factors drive reactions, including oxidation, polymerisation and hydrolysis. Oxidation of TAGs can decrease the degree of oil saturation, promoting the formation of ketones, aldehydes, hydroperoxides and other degradation products. In the presence of heat, light or heavy metals such as Cu or Fe, unsaturated fatty acids may form dimers and polymers with molecular weights of between 692–1600 g/mol [33], which increases the oil viscosity. After 30 cooking cycles, the viscosity and density of olive oil increased from 25.5 mPas and 892.5 kg/m<sup>3</sup> to 32 mPas and 898 kg/m<sup>3</sup> [34]. Hydrolysis of TAGs can generate FFAs, diglycerides and monoglycerides. Waste cooking oils are thus more complex chemical mixtures than crude or refined bio-oils [35]. Homogenous basic catalysts used for biodiesel production can also react with FFAs to form organic salts via saponification (Figure 1D) [36] which neutralises the catalyst and interferes with the separation process, resulting in loss of product. The amount of FFAs is typically <0.2 wt% in refined bio-oils, but can vary from 1 to 20 wt% in unrefined or waste cooking oils (Table 2), necessitating oil pretreatment if triglycerides are to undergo subsequent base-catalysed transesterification [37]. Homogeneous acids, including H<sub>2</sub>SO<sub>4</sub>, HCl, HF, H<sub>3</sub>PO<sub>4</sub> and *p*-toluene sulfonic acid, have been used for the esterification pretreatment of oils to remove FFAs [38,39]. However, such acids are corrosive,

hazardous to store, transport and handle, and difficult to separate from biodiesel/glycerol products, prompting research on alternative solid-acid catalysts [40].

**Table 2.** Free fatty acid (FFA) content of different types of oils [41,42].

Type of Oil	FFA Content/wt%
Palm kernel oil	2–5
Soybean oil	0.3–0.7
Corn oil	0.1–0.2
Sunflower oil	0.1–0.2
Waste cooking oil	1.2–20
Olive	≤0.8% for extra virgin olive oil
Coconut	0.1–0.5
Avocado	0.1–0.2
Canola	0.1–0.2
Peanut	0.1–0.2
Sesame	0.1–0.2

## 2. Thermodynamics of Transesterification and Esterification

There are two key thermodynamic considerations when considering biodiesel production: thermodynamics of the reaction and thermodynamics of phase separation/mixing.

### 2.1. Reaction

Kinetic analysis of fatty acid and triglyceride respective esterification and transesterification allows the determination of associated thermodynamic parameters [43] via the Eyring-Polanyi equation (Equation (1)):

$$k = \frac{k_b T}{h} \times \exp\left(-\frac{\Delta G^*}{RT}\right) \quad (1)$$

where  $k_b$ ,  $h$  and  $\Delta G^*$  are the Boltzmann constant, Planck constant and Gibbs free energy of activation, respectively. The Gibbs free energy of activation can be expressed as (Equation (2)):

$$\Delta G^* = \Delta H^* - T\Delta S^* \quad (2)$$

where  $\Delta H^*$  and  $\Delta S^*$  represent the enthalpy and entropy of the reaction, respectively. Combining Equations (1) and (2) yields the following expression (Equation (3)) relating kinetic and thermodynamic properties:

$$\ln\left(\frac{k}{T}\right) = \left[\ln\left(\frac{k_b}{h}\right) + \left(\frac{\Delta S^*}{R}\right)\right] - \left(\frac{\Delta H^*}{RT}\right) \quad (3)$$

In this equation, the slope and intercept of the plot of  $\ln k$  versus  $1/T$  yield the respective enthalpy and entropy, from which the Gibbs free energy can then be calculated using Equation (2). Table 3 collates these thermodynamic properties of the different feedstocks and temperatures.

Transesterification is non-spontaneous, endothermic, and endergonic, with high oil conversion possible in all cases (reflecting their common glycerol backbone). Differences in the thermodynamic properties arise from a combination of the unique molecular structure of the triglycerides present in each feedstock and the chosen alcohol. Reaction kinetics are largely controlled by mass transport and mixing, which reflect the physicochemical properties of the individual oils (notably their temperature-dependent viscosity), in addition to the nature of the catalyst active sites, textural properties and reaction mechanisms.

**Table 3.** Comparison of thermodynamic parameters for bio-oil transesterification with methanol.

Feedstock	Temperature Range /°C	$\Delta G$ /kJ·mol <sup>-1</sup>	$\Delta H$ /kJ·mol <sup>-1</sup>	$\Delta S$ /kJ·mol <sup>-1</sup>	Maximum Conversion /%	Kinetic Parameters	Methanol:Oil Molar Ratio	Ref.
<i>S. triguga</i> oil	30–60	82.4–85.6	50.6	−0.10	97 (at 50 °C)	2nd order, k = 0.04–0.23 L·mol <sup>-1</sup> ·min <sup>-1</sup>	3–12	[43]
Waste cooking oil	50–100	93.8	54.1	−0.11	99 (at 100 °C)	1st order, k = 0.059–0.94 min <sup>-1</sup>	10–40	[44]
Castor oil	45–75	90.9–92.7	47.4–46.0	−0.13–−0.14	98 (at 65 °C)	pseudo-1st order	8–18	[45]
<i>Spirulina platensis</i> algal biomass	35–75	92.7	16.4	−0.23	75 (at 55 °C)	1st order, k = 0.001 min <sup>-1</sup>	1–6 (mass:volume)	[46]
Soybean oil	40–65	83.3–87.7	28.3	−0.18	98 (at 57.8 °C)	pseudo-1st order, k = 0.085–0.208 min <sup>-1</sup>	4.5–9	[47]
Rapeseed oil	20–40	75.3–79.1	19.6	−0.19	98 (at 30 °C)	pseudo-1st order, k = 0.081 min <sup>-1</sup>	6–12	[48]
<i>Schleichera triguga</i> oil	55–65	82.4–85.6	50.6	−0.11	90 (at 65 °C)	pseudo-1st order, k = 0.0237–0.0512 min <sup>-1</sup>	6–12	[49]
Refined jatropha oil	100–160	140.0	16.7	−0.28	91 (at 160 °C)	pseudo-1st order, k = 0.0029–0.0072 min <sup>-1</sup>	30	[50]

## 2.2. Separation

The products of oil transesterification using methanol are fatty acid methyl esters (biodiesel) and glycerol, which typically have poor miscibility with alcohol in significant (3–100 fold excess) [51]. Obtaining high-purity biodiesel requires the separation of alcohol, which reduces the fuel flash point [17], and glycerol (EN 14214; EU quality standard, 2008 [52] requires levels of  $\leq 0.02$  wt%) [52]. Knowledge of the phase diagram is, therefore, critical for optimising biodiesel separation [53].

Biodiesel can contain water from either the production process or from storage, as hygroscopic FAMES make biodiesel more hydrophilic than regular diesel. The water content in biodiesel reduces its heat value and its shelf life, as biodiesel with more water has less resistance to oxidation. The more oxidation-prone the biodiesel, the more likely it is to form oxidation products that can damage the engine, especially the injection system, by creating deposits and corroding zinc and chromium. Water can also promote biological growth and ester reactions, which can form soaps and change the biodiesel composition and quality. The miscibility of water in fatty acid esters and biodiesel thus influences fuel quality during production. Experimental data for water solubility in alkyl esters in the temperature range of 288–318 K are listed in Table 4. Oliveira et al. [54] reported such data for eleven fatty acids and six biodiesels spanning 15–50 °C and modelled these data using the Cubic Plus Association (CPA) equation of state [55]. Their CPA model, which accounts for polar interactions between ester and water, predicted water solubility in binary ester systems with a global deviation of less than 7% and in commercial biodiesel (from the Portuguese oil company Galp) with a global deviation of less than 16%. Figure 2 shows the water solubility of ethyl butanoate, methyl tetradecanoate, ethyl decanoate, and commercial biodiesel at different temperatures.

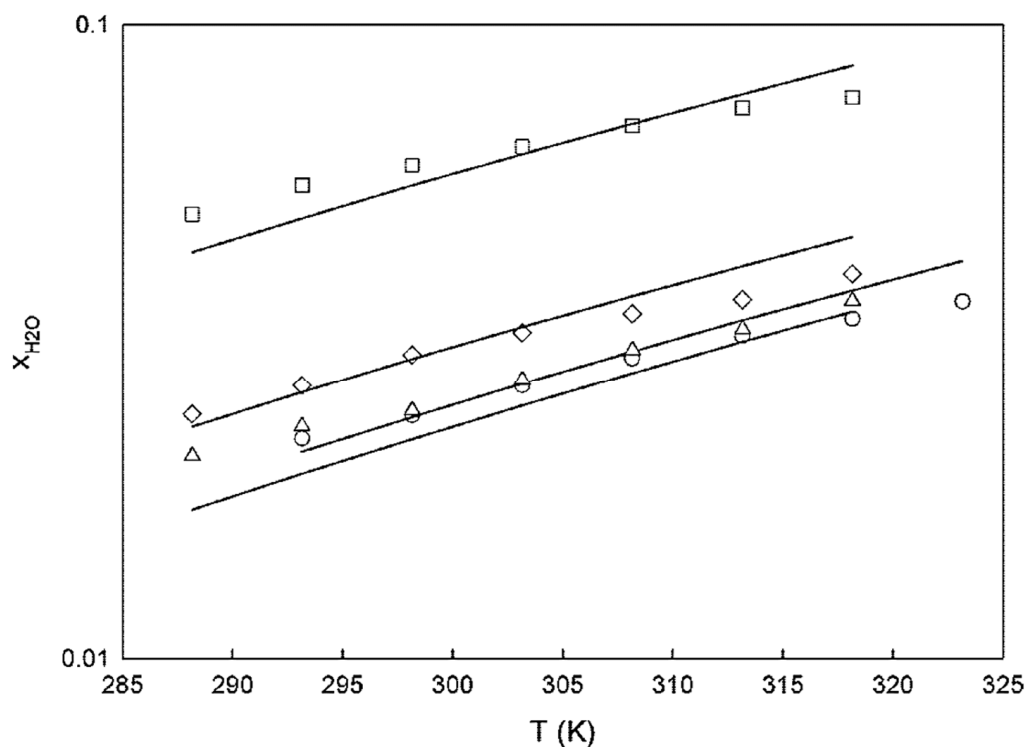


**Figure 2.** Water solubility in ethyl butanoate ( $\square$  experimental; (-), CPA regressed parameters), in methyl tetradecanoate ( $\circ$ , experimental; (-), CPA regressed parameters), in ethyl decanoate ( $\diamond$ , experimental; (-), CPA regressed parameters), and in Biodiesel F ( $\Delta$ , experimental; (-), CPA regressed parameters). Reproduced from [54].

**Table 4.** Experimental data for water miscibility in alkyl esters [54].

T/K	(xH <sub>2</sub> O ± σ <sup>a</sup> )	T/K	(xH <sub>2</sub> O ± σ <sup>a</sup> )	T/K	(xH <sub>2</sub> O ± σ <sup>a</sup> )
	ethyl butanoate		Methyl tetradecanoate		Ethyl decanoate
288.2	0.0504 ± 0.0003	293.2	0.0223 ± 0.0002	288.2	0.0243 ± 0.0005
293.2	0.056 ± 0.001	298.2	0.0242 ± 0.0003	293.2	0.0270 ± 0.0011
298.2	0.060 ± 0.002	303.2	0.0270 ± 0.0002	298.2	0.0302 ± 0.0004
303.2	0.0644 ± 0.0004	308.2	0.0298 ± 0.0004	303.2	0.0327 ± 0.0004
308.2	0.0694 ± 0.0001	313.2	0.0324 ± 0.0003	308.2	0.0351 ± 0.0002
313.2	0.0741 ± 0.0004	318.2	0.0344 ± 0.0002	313.2	0.0370 ± 0.0008
318.2	0.0770 ± 0.0005	323.2	0.0367 ± 0.0004	318.2	0.0405 ± 0.0008

Data for methyl oleate, methanol and glycerol ternary liquid-liquid equilibria at 60 °C [56] were also simulated by UNIFAC and UNIFAC-Dortmund semi-empirical models for predicting non-electrolyte activity in non-ideal mixtures, revealing that (unsurprisingly) the type of catalyst did not significantly influence the solubility of glycerol in fatty acid methyl esters. A ternary soybean oil biodiesel, methanol and glycerol phase diagram has also been reported [57], showing that small temperature differences (10 °C) had little impact on solubility, whereas differences of 45 °C increased glycerol solubility in soybean oil biodiesel. The UNIFAC-Dortmund model has fewer errors and more reliable predictions than the UNIFAC model. The methyl ester + glycerol + water system was successfully modelled by the NRTL equation at 40 °C [58]. This model can provide data and correlation parameters that can be used to enhance the performance and efficiency of separation systems for transesterified biodiesel fuels. UNIQUAC modelling of binary, ternary and quadruple systems, including soybean biodiesel, methanol/ethanol, water and/or glycerol, was performed at 30, 45 and 60 °C [59]. The binodal or coexistence curve defines the temperature and composition at which the phase separation is thermodynamically feasible. Such diagrams can help design and improve biodiesel separation systems. Moreover, obtaining the phase diagrams of the reaction medium represents a fundamental step for the optimisation of the purification process. The temperature dependence of the binodal curve for a biodiesel, water and methanol ternary system [60] indicates that water and biodiesel are immiscible and that water is soluble only in the presence of ~95% methanol. Phase diagrams for the ternary chicha biodiesel, ethanol and glycerol systems were accurately simulated by non-random two-liquid (NRTL) and analytical solutions of groups (ASOG) models at 30, 45 and 60 °C (Figure 3) [61], albeit with small deviations for ethanol-rich mixtures. Temperature has little impact on the two-phase (glycerol-methyl oleate) region unless the temperature difference is large (>10 °C), which is in accordance with other studies [62,63]. The choice of alcohol (methanol or ethanol) has little influence on the ternary phase diagrams.

Thermodynamic simulation is integral to the design and optimisation of the process separation units used in biodiesel production. Such simulations have modelled liquid-liquid equilibria (LLE) for biodiesel/alcohol/glycerol mixtures with high accuracy over a range of temperatures and pressures. These include the NRTL model (Non-Random Two Liquid), UNIQUAC model (UNIversal QUAsi-Chemical) and the UNIFAC (UNIversal quasi-chemical Functional group Activity Coefficient) model. These models can predict LLE using activity coefficients calculated from the functional groups within the mixture. The NRTL model can be applied to ternary (and higher order) systems using regression parameters derived from binary equilibrium data but can incorrectly predict miscibility gaps. The UNIQUAC model is well suited to non-ideal systems at moderate temperatures and pressures and is favoured over the NRTL model due to its simplicity and accuracy in describing liquid-liquid and liquid-vapour equilibria. However, UNIQUAC requires experimental data to estimate the model parameters. UNIFAC has found broad applications and has been adapted to develop improved models, such as UNIFAC-ELL (ELL ≡ liquid-liquid equilibrium). The accuracy and suitability of the model heavily rely on the quality of the available intermolecular interaction parameters. Santos et al. [54] sought to apply



NRTL and UNIQUAC models (to account for the polarity of methanol), however as some binary coefficients of the biodiesel/alcohol/glycerol phase equilibria were unavailable, they also employed UNIFAC-LLE to estimate parameters and facilitate modelling of the ternary liquid mixture. Carmo et al. [64] used a range of thermodynamic models, including UNIFAC, UNIFAC-Dortmund, UNIQUAC, NRTL, and ASOG, to simulate the LLE of biodiesel, glycerol and alcohol mixtures. They suggested that thermal effects on molecular activity were responsible for the accuracy of the predictions, with the quality of LLE modelling following the order UNIFAC-Dortmund > ASOG > UNIFAC-LLE > UNIFAC > UNIQUAC > NRTL. Note that the preceding simulations do not capture the complexity of quaternary (biodiesel/glycerol/ethanol/water) mixtures found in real-world biodiesel manufacturing, wherein the use of low-cost ethanol azeotropes is economically desirable. Some efforts have been made to model soybean oil biodiesel/ethanol/glycerol/NaOH phase equilibria pertinent to homogeneous catalytic processes [65]. Nevertheless, the role of water remains poorly understood despite experimental studies showing that it can promote biodiesel separation from glycerol in some instances [66].

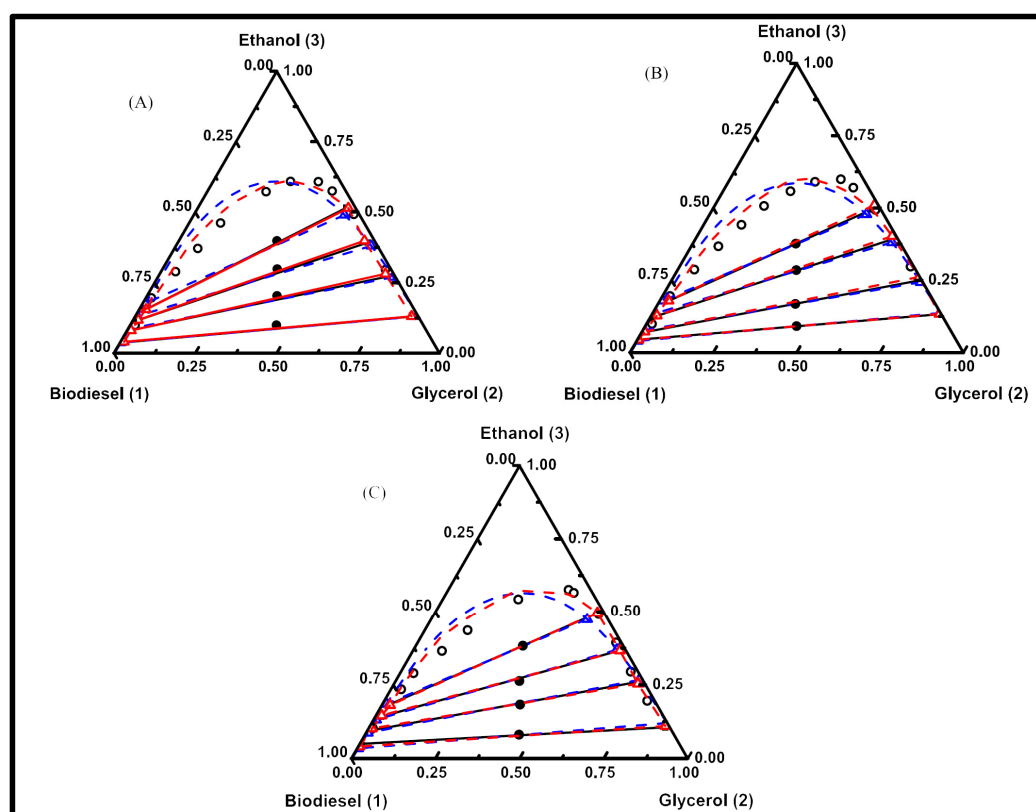


**Figure 3.** Liquid-liquid equilibria for chicha biodiesel (1) + glycerol (2) + ethanol (3) at (A) 30, (B) 45, and (C) 60 °C. Experimental (black), global composition, tie line and binodal points; NRTL model (blue), tie line and binodal curve; and ASOG models (red), tie line and binodal curve. Reproduced from [61].

### 3. Kinetics of Heterogeneously Catalysed Transesterification

Transesterification of a triglyceride with methanol occurs in three consecutive steps (Equations (4)–(6)) [67], involving the formation of diglyceride (D) and monoglyceride (M) intermediates to glycerol (G) and the concomitant formation of methyl fatty ester (MeOOR).





The overall reaction stoichiometry is therefore:



Assuming the following:

The rate-determining step is the first transesterification step (with di- and monoglyceride products rapidly reacting);

- i. excess methanol drives the transesterification equilibrium forward, and hydrolysis is negligible;
- ii. the methanol concentration is constant, and hence, transesterification is pseudo-first-order;
- iii. glycerol does not react with methanol;
- iv. reactions are free from mass-transport limitations, and the reaction mixture is homogeneous;

The reaction rate expression simplifies to:

$$-r = -\frac{dC_T}{dt} = -\frac{1}{3} \frac{dC_{\text{MeOH}}}{dt} = kC_T^\alpha C_{\text{MeOH}}^\beta \quad (8)$$

where  $C_T$  indicates the concentration of triglyceride and  $C_{\text{MeOH}}$  the concentration of methanol,  $k$  the reaction rate constant, and  $\alpha$  and  $\beta$  are the reaction orders with respect to  $T$  and  $\text{MeOH}$ , respectively. As acid-catalysed transesterification is typically performed with a large excess (30–100 fold) of methanol, the alcohol concentration can be considered constant, in which case  $k' = kC_{\text{MeOH}}^\beta$  and Equation (8) can be rewritten as follows:

$$-r = -\frac{dC_T}{dt} = k' C_T^\alpha \quad (9)$$

By rearrangement of Equation (9) we obtain

$$-\frac{dC_T}{C_T^\alpha} = k' dt \quad (10)$$

and the subsequent integration of Equation (10) between reaction time  $t = 0 \rightarrow t$  the following expression is obtained:

$$\int_{C_{T0}}^{C_T} \frac{dC_T}{C_T^\alpha} = \int_0^t dt \quad (11)$$

where,  $C_{T0}$  is the initial concentration of triglycerides at the beginning of the reaction ( $t = 0$ ) and  $C_T$  is the concentration of triglyceride at reaction time  $t$ , where  $\alpha$  can have values of 0, 1 and 2 [68]. If  $\alpha = 0$ , a pseudo-zero-order reaction is obtained, wherein concentration and time are related as follows:

$$C_T = C_{T0} - k't \quad (12)$$

If  $\alpha = 1$  a pseudo-first-order reaction is obtained, then:

$$C_T = C_{T0} e^{-k't} \quad (13)$$

If  $\alpha = 2$  a pseudo-second-order reaction is obtained, then:

$$C_T = \frac{1}{\left(\frac{1}{C_{T0}} + k't\right)} \quad (14)$$

Equations (12)–(14) can be written in terms of triglyceride conversion as Equations (15)–(17):

$$x_T = \frac{k't}{C_{T0}} \quad (15)$$

$$1 - x_T = e^{-k't} \quad (16)$$

$$1 - x_T = \frac{1}{(1 + \frac{k't}{C_{T0}})} \quad (17)$$

where  $x_T = 1 - \frac{C_T}{C_{T0}}$ .

Fitting the experimental data to Equations (15)–(17) enables the determination of the reaction rate constant, from which the activation energy ( $E_a$ ) and pre-exponential factor ( $A$ ) can be obtained from the Arrhenius equation:

$$k' = Ae_a^{-\frac{E_a}{RT}} \quad (18)$$

$$\ln k' = \ln A - \frac{E_a}{RT} \quad (19)$$

A plot of  $\ln k'$  versus  $1/T$  yields the activation energy and pre-exponential factor from the respective slope and intercept. Most systems in the literature have reported pseudo-first-order kinetics for transesterification. Table 5 collates activation energies and pre-exponential factors for different feedstocks and catalysts. It is evident that strong acid and base catalysts offer the lowest activation energies, but other factors such as catalyst cost, reproducibility (particularly when waste-derived), and ease of separation (for  $H_2SO_4$ ) also dictate the catalyst selection.

**Table 5.** Kinetic parameters for catalytic transesterification and esterification of bio-oils.

Feedstock	Catalyst	Model	Pre-Exponential /s <sup>-1</sup>	E <sub>a</sub> /kJ·mol <sup>-1</sup>	Ref.
Waste cooking oil, Methanol	K <sub>3</sub> PO <sub>4</sub> /AC	pseudo-1st order	28.68	34.2	[69]
WCO, Methanol	Waste mussel shells (CaO)	pseudo-1st order	7.8 × 10 <sup>7</sup>	79.8	[70]
Waste cotton seed oil, Methanol	Zn/CaO	pseudo-1st order	0.0275 × 10 <sup>7</sup>	43.0	[71]
Jatropha oil, Ethanol	Molybdenum impregnated calcium oxide	pseudo-1st order	0.26 × 10 <sup>7</sup>	66.0	[72]
Waste cotton seed, Methanol	Li/ZrO <sub>2</sub>	pseudo-1st order	1.35 × 10 <sup>3</sup>	40.8 and 43.1	[73]
Algae, Methanol	H <sub>2</sub> SO <sub>4</sub>	1st order	0.17 × 10 <sup>-3</sup>	14.5	[46]
Waste cooking oil, Methanol	Bentonite-CH <sub>3</sub> ONa	1st order	1.4 × 10 <sup>5</sup>	41.0	[74]
Sunflower oil, Methanol	Al-Sr (nano)	pseudo-1st order	3.38 × 10 <sup>7</sup>	72.9	[75]
Karanja oil, Methanol	BaCeO <sub>3</sub>	pseudo-1st order	0.228 × 10 <sup>3</sup>	36.2	[76]

Three principal mechanisms have been proposed for bimolecular reactions involving solid catalysts [67]: Eley-Rideal (ER), Langmuir-Hinshelwood-Hougen-Watson (LHHW), and Hattori LHHW and ER, all of which have been considered for transesterification [77]. The LHHW mechanism has been studied for Lewis acid/base heterogeneous catalysts, while [78] Hattori et al. [79] and Dossin et al. [80] have explored the ER mechanisms. Some reports have identified methanol adsorption [79–82] as the rate-limiting step in transesterification, while others have proposed the reaction of adsorbed tri-, di-, or monoglycerides with methanol as rate-limiting. The mechanism and rate-limiting step are expected to depend on the catalyst type, loading, concentrations of methanol and triglycerides, and mixing (also a function of reactor configuration) [83]. Intrinsic reaction kinetics can only be determined in the absence of mass transfer limitations [84].

The ER mechanism can be described as follows [67,82]:

- methanol adsorption is rate-limiting;
- quasi-steady-state kinetics can be assumed;
- reaction intermediates are rapidly converted into glycerol.

In the ER mechanism, if methanol adsorption is the limiting step, then methanol is assumed to be adsorbed at an empty active site on the catalyst surface (\*), followed by a direct reaction of the activated methoxy species (Me\*) with a triglyceride molecule (T) in the liquid phase to form an adsorbed diglyceride (D\*) and release a methyl alkyl ester (MeOOR). D\* is then assumed to desorb back into the liquid as a molecular diglyceride (D), undergoing a subsequent reaction with another Me\* species to form a monoglyceride (M\*) and release another molecule of MeOOR. Finally, M\* is released into the liquid phase as a molecular monoglyceride (M), which then reacts with a final Me\* to release glycerol (G) and a third MeOOR molecule [67,82]. This model assumes that D\* and M\* cannot directly react with nearby Me\* species. In this scenario, the elementary reactions are listed in Table 6.

**Table 6.** Elementary reactions in ER mechanism.

Reaction	Equation
$* + \text{CH}_3\text{OH} \rightleftharpoons \text{CH}_3\text{OH}^*$	(20)
$\text{CH}_3\text{OH}^* + \text{T} \rightleftharpoons \text{D}^* + \text{MeOOR}$	(21)
$\text{D}^* \rightleftharpoons \text{D} + *$	(22)
$\text{CH}_3\text{OH}^* + \text{D} \rightleftharpoons \text{M}^* + \text{MeOOR}$	(23)
$\text{M}^* \rightleftharpoons \text{M} + *$	(24)
$\text{CH}_3\text{OH}^* + \text{M} \rightleftharpoons \text{G}^* + \text{MeOOR}$	(25)
$\text{G}^* \rightleftharpoons \text{G} + *$	(26)

The quasi-steady-state case assumes that the catalyst surface is uniform and that there are no inert adsorbates [67]. The adsorption of T, D or M molecules is again omitted, with only the methanol surface activated. In this case, the reaction is considered to be in a quasi-steady state with elementary reactions according to Table 7, wherein k is the rate constant for the surface reaction (SR), adsorption (AD), or desorption (DE) [82].

**Table 7.** Rate expressions for ER quasi-steady-state mechanism [82].

Reaction	Rate Expression	Equation
$* + \text{CH}_3\text{OH} \rightleftharpoons \text{CH}_3\text{OH}^*$	$r_1 = \frac{k_1 \left( \text{Me} - \frac{k_5 \text{DMeOOR}}{k_1 k_2 \text{T}} \right)}{1 + \frac{k_5 \text{DMeOOR}}{k_2 \text{T}} + k_5 \text{D} + k_6 \text{M} + k_7 \text{G}}$	(27)
$\text{CH}_3\text{OH}^* + \text{T} \rightleftharpoons \text{D}^* + \text{MeOOR}$	$r_2 = \frac{k_2 \left( k_1 \text{MeT}^* - \frac{k_5 \text{DMeOOR}}{k_2} \right)}{1 + k_1 \text{Me} + k_5 \text{D} + k_6 \text{M} + k_7 \text{G}}$	(28)
$\text{CH}_3\text{OH}^* + \text{D} \rightleftharpoons \text{M}^* + \text{MeOOR}$	$r_3 = \frac{k_3 \left( k_1 \text{MeD}^* - \frac{k_6 \text{MMeOOR}}{k_3} \right)}{1 + k_1 \text{Me} + k_5 \text{D} + k_6 \text{M} + k_7 \text{G}}$	(29)
$\text{CH}_3\text{OH}^* + \text{M} \rightleftharpoons \text{G}^* + \text{MeOOR}$	$r_4 = \frac{k_4 \left( k_1 \text{MeM}^* - \frac{k_7 \text{GMeOOR}}{k_4} \right)}{1 + k_1 \text{Me} + k_5 \text{D} + k_6 \text{M} + k_7 \text{G}}$	(30)
$\text{D}^* \rightleftharpoons \text{D} + *$	$r_5 = \frac{k_{-5} \left( \frac{k_1 k_2 \text{MeT}^*}{\text{MeOOR}} - k_5 \text{D} \right)}{1 + k_1 \text{Me} + \frac{k_1 k_2 \text{MeT}^*}{\text{MeOOR}} + k_6 \text{M} + k_7 \text{G}}$	(31)
$\text{M}^* \rightleftharpoons \text{M} + *$	$r_6 = \frac{k_{-6} \left( \frac{k_1 k_3 \text{MeD}^*}{\text{MeOOR}} - k_6 \text{M} \right)}{1 + k_1 \text{Me} k_5 \text{D} + \frac{k_1 k_3 \text{MeD}^*}{\text{MeOOR}} + k_7 \text{G}}$	(32)
$\text{G}^* \rightleftharpoons \text{G} + *$	$r_7 = \frac{k_{-7} \left( \frac{k_1 k_4 \text{MeM}^*}{\text{MeOOR}} - k_7 \text{G} \right)}{1 + k_1 \text{Me} + k_5 \text{D} + k_6 \text{M} + \frac{k_1 k_4 \text{MeM}^*}{\text{MeOOR}}}$	(33)

The third case assumes that each of the intermediate reactions is rapid such that the mechanism is simplified to three elementary steps (Table 8) [82].

**Table 8.** Rate expressions for the ER mechanism assuming rapid reaction of intermediates [82].

Reaction	Rate Expression	Equation
$* + \text{CH}_3\text{OH} \rightleftharpoons \text{CH}_3\text{OH}^*$	$r_1 = \frac{k_1 \left( \text{Me} - \frac{k_3 \text{GMeOOR}}{k_1 k_2 \text{T}} \right)}{1 + \frac{k_3 \text{GMeOOR}}{k_2 \text{T}} + k_3 \text{G}}$	(34)
$\text{CH}_3\text{OH}^* + \text{T} \rightleftharpoons \text{G}^* + \text{MeOOR}$	$r_2 = \frac{k_2 \left( k_1 \text{MeT}^* - \frac{k_3 \text{GMeOOR}}{k_2} \right)}{1 + k_1 \text{Me} + k_3 \text{G}}$	(35)
$\text{G}^* \rightleftharpoons \text{G} + *$	$r_3 = \frac{k_{-3} \left( \frac{k_1 k_2 \text{MeT}^*}{\text{MeOOR}} - k_3 \text{G} \right)}{1 + k_1 \text{Me} + \frac{k_1 k_2 \text{MeT}^*}{\text{MeOOR}}}$	(36)

The LHHW mechanism can be described as follows [67,82]:

- bimolecular surface reaction is the limiting step
- methanol adsorption is the limiting step
- the intermediate steps are assumed to be rapid

In the case where the surface reaction is rate limiting, methanol (Me) and triglyceride (T) are assumed to co-adsorb at empty active sites (\*) and react to form diglyceride (D\*) and methyl alkyl ester (MeOOR\*). The adsorbed D\* can react with additional co-adsorbed Me\* to form a monoglyceride (M\*) and methyl alkyl ester, with M\* reacting once more with methanol to produce adsorbed glycerol (G\*) and a third methyl ester molecule. The desorption of reactively formed products regenerates the active sites. The resulting elementary reactions are listed in Table 9, with the corresponding rate equations listed in Table 10 [82].

If the intermediate surface reactions are assumed to be rapid compared to methanol and triglyceride adsorption, their surface reactions, and glycerol and alkyl ester desorption, then the elementary reactions in Table 11 ensue. This is termed the 5-stage LHHW [82]. Rate expressions for the LHHW mechanism assuming fast intermediate steps [82].

In the Hattori mechanism, methanol (Me) and triglyceride (T) co-adsorb on nearby empty active sites (\*) and react to form an intermediate (TCH<sub>3</sub>OH\*), which subsequently transforms into adsorbed diglyceride (D\*) and desorbed methyl ester (MeOOR). The activated D\* then reacts with another methanol to form a second intermediate (DCH<sub>3</sub>OH\*) which again transforms into an activated monoglyceride (M\*) and desorbed methyl ester, repeating until the adsorbed glycerol (G\*) and methyl ester products, and reactively formed diglyceride and monoglyceride desorb [67]. In this mechanism, three molecules of methyl ester are released by consecutive surface reactions from one molecule of adsorbed triglyceride. The elementary reactions and their corresponding rate expressions are presented in Table 12 and Table 13, respectively. (TCH<sub>3</sub>OH)\*, (DCH<sub>3</sub>OH)\*, (MCH<sub>3</sub>OH)\* in this table are intermediates produced by the reaction of methanol with tri-, di- and monoglycerides at the catalyst surface [67].

**Table 9.** Elementary reactions in LHHW mechanism [82].

Reaction	Equation
$\text{Me} + * \rightleftharpoons \text{Me}^*$	(37)
$\text{T} + * \rightleftharpoons \text{T}^*$	(38)
$\text{Me}^* + \text{T}^* \rightleftharpoons \text{D}^* + \text{MeOOR}^*$	(39)
$\text{Me}^* + \text{D}^* \rightleftharpoons \text{M}^* + \text{MeOOR}^*$	(40)
$\text{Me}^* + \text{M}^* \rightleftharpoons \text{G}^* + \text{MeOOR}^*$	(41)
$\text{D}^* \rightleftharpoons \text{D} + *$	(42)
$\text{M}^* \rightleftharpoons \text{M} + *$	(24)
$\text{G}^* \rightleftharpoons \text{G} + *$	(43)
$\text{MeOOR}^* \rightleftharpoons \text{MeOOR} + *$	(44)

**Table 10.** Rate expressions for the LHHW mechanism where the surface reaction is rate limiting [82].

Reaction	Rate Expression	Equation
$\text{Me} + * \rightleftharpoons \text{Me}^*$	$r_1 = \frac{k_1 \left( \text{Me} - \frac{k_6 k_9 \text{DMeOR}}{k_1 k_2 k_3 T} \right)}{1 + \frac{k_6 k_9 \text{DMeOR}}{k_2 k_3 T} + k_2 T + k_6 \text{D} + k_7 \text{M} + k_8 \text{G} + k_9 \text{MeOR}}$	(45)
$\text{T} + * \rightleftharpoons \text{T}^*$	$r_2 = \frac{k_2 \left( \text{T} - \frac{k_6 k_9 \text{DMeOR}}{k_1 k_2 k_3 \text{Me}} \right)}{1 + k_1 \text{Me} + \frac{k_6 k_9 \text{DMeOR}}{k_1 k_3 \text{Me}} + k_6 \text{D} + k_7 \text{M} + k_8 \text{G} + k_9 \text{MeOR}}$	(46)
$\text{Me}^* + \text{T}^* \rightleftharpoons \text{D}^* + \text{MeOR}^*$	$r_3 = \frac{k_3 \left( k_1 k_2 \text{MeT}^* - \frac{k_7 k_9 \text{MMeOR}}{k_3} \right)}{(1 + k_1 \text{Me} + k_2 T + k_6 \text{D} + k_7 \text{M} + k_8 \text{G} + k_9 \text{MeOR})^2}$	(47)
$\text{Me}^* + \text{D}^* \rightleftharpoons \text{M}^* + \text{MeOR}^*$	$r_4 = \frac{k_4 \left( k_1 k_6 \text{MeD}^* - \frac{k_7 k_9 \text{MMeOR}}{k_4} \right)}{(1 + k_1 \text{Me} + k_2 T + k_6 \text{D} + k_7 \text{M} + k_8 \text{G} + k_9 \text{MeOR})^2}$	(48)
$\text{Me}^* + \text{M}^* \rightleftharpoons \text{G}^* + \text{MeOR}^*$	$r_5 = \frac{k_5 \left( k_1 k_7 \text{MeM}^* - \frac{k_8 k_9 \text{GMeOR}}{k_5} \right)}{(1 + k_1 \text{Me} + k_2 T + k_6 \text{D} + k_7 \text{M} + k_8 \text{G} + k_9 \text{MeOR})^2}$	(49)
$\text{D}^* \rightleftharpoons \text{D} + *$	$r_6 = \frac{k_{-6} \left( \frac{k_7 k_9 \text{MMeOR}}{k_1 k_4 \text{Me}} - k_6 \text{D} \right)}{1 + k_1 \text{Me} + \frac{k_7 k_9 \text{MMeOR}}{k_1 k_4 \text{Me}} + k_2 T + k_7 \text{M} + k_8 \text{G} + k_9 \text{MeOR}}$	(50)
$\text{M}^* \rightleftharpoons \text{M} + *$	$r_7 = \frac{k_{-7} \left( \frac{k_8 k_9 \text{GMeOR}}{k_1 k_5 \text{Me}} - k_7 \text{M} \right)}{1 + k_1 \text{Me} + \frac{k_7 k_9 \text{GMeOR}}{k_1 k_5 \text{Me}} + k_2 T + k_6 \text{D} + k_8 \text{G} + k_9 \text{MeOR}}$	(51)
$\text{G}^* \rightleftharpoons \text{G} + *$	$r_8 = \frac{k_{-8} \left( \frac{k_1 k_2 k_7 \text{MeM}^*}{k_9 \text{MeOR}} - k_8 \text{G} \right)}{1 + k_1 \text{Me} + \frac{k_1 k_2 k_7 \text{MeM}^*}{k_9 \text{MeOR}} + k_2 T + k_7 \text{M} + k_6 \text{D} + k_9 \text{MeOR}}$	(52)
$\text{MeOR}^* \rightleftharpoons \text{MeOR} + *$	$r_9 = \frac{k_{-9} \left( \frac{k_1 k_2 k_3 \text{MeT}^*}{k_6 \text{D}} - k_9 \text{MeOR} \right)}{1 + k_1 \text{Me} + \frac{k_1 k_2 k_3 \text{MeT}^*}{k_6 \text{D}} + k_2 T + k_7 \text{M} + k_6 \text{D} + k_8 \text{G}}$	(53)

**Table 11.** Rate expressions for the LHHW mechanism where the surface reaction rate is fast.

Reaction	Rate Expression	Equation
$\text{Me} + * \rightleftharpoons \text{Me}^*$	$r_1 = \frac{k_1 \left( \text{Me} - \frac{k_4 k_5 \text{GMeOR}}{k_1 k_2 k_3 T} \right)}{1 + \frac{(k_4 k_5 \text{GMeOR})}{k_2 k_3 T} + k_2 T + k_4 \text{G} + k_5 \text{MeOR}}$	(54)
$\text{T} + * \rightleftharpoons \text{T}^*$	$r_2 = \frac{k_2 \left( \text{T} - \frac{k_4 k_5 \text{GMeOR}}{k_1 k_2 k_3 \text{Me}} \right)}{1 + \frac{(k_4 k_5 \text{GMeOR})}{k_1 k_3 \text{Me}} + k_1 \text{Me} + k_4 \text{G} + k_5 \text{MeOR}}$	(55)
$\text{Me}^* + \text{T}^* \rightleftharpoons \text{G}^* + \text{MeOR}^*$	$r_3 = \frac{k_3 \left( k_1 k_2 \text{MeT}^* - \frac{k_4 k_5 \text{GMeOR}}{k_3} \right)}{(1 + k_1 \text{Me} + k_2 T + k_4 \text{G} + k_5 \text{MeOR})^2}$	(56)
$\text{G}^* \rightleftharpoons \text{G} + *$	$r_4 = \frac{k_{-4} \left( \frac{k_1 k_2 k_3 \text{MeT}^*}{k_5 \text{MeOR}} - k_4 \text{G} \right)}{1 + k_1 \text{Me} + k_2 T + \frac{k_1 k_2 k_3 \text{MeT}^*}{k_5 \text{MeOR}} + k_5 \text{MeOR}}$	(57)
$\text{MeOR}^* \rightleftharpoons \text{MeOR} + *$	$r_5 = \frac{k_{-5} \left( \frac{k_1 k_2 k_3 \text{MeT}^*}{k_4 \text{G}} - k_5 \text{MeOR} \right)}{1 + k_1 \text{Me} + k_2 T + k_4 \text{G} + \frac{k_1 k_2 k_3 \text{MeT}^*}{k_4 \text{G}}}$	(58)

**Table 12.** Elementary reactions in Hattori mechanism [67].

Reaction	Equation
$* + \text{CH}_3\text{OH} \rightleftharpoons \text{CH}_3\text{OH}^*$	(59)
$\text{T} + * \rightleftharpoons \text{T}^*$	(60)
$\text{CH}_3\text{OH}^* + \text{T}^* \rightleftharpoons (\text{TCH}_3\text{OH})^* + *$	(61)
$(\text{TCH}_3\text{OH})^* \rightleftharpoons \text{D}^* + \text{MeOR}$	(62)
$\text{CH}_3\text{OH}^* + \text{D}^* \rightleftharpoons (\text{DCH}_3\text{OH})^* + *$	(63)
$(\text{DCH}_3\text{OH})^* \rightleftharpoons \text{M}^* + \text{MeOR}$	(64)
$\text{CH}_3\text{OH}^* + \text{M}^* \rightleftharpoons (\text{MCH}_3\text{OH})^* + *$	(65)
$(\text{MCH}_3\text{OH})^* \rightleftharpoons \text{G}^* + \text{MeOR}$	(66)
$\text{D} + * \rightleftharpoons \text{D}^*$	(67)
$\text{M} + * \rightleftharpoons \text{M}^*$	(68)
$\text{G} + * \rightleftharpoons \text{G}^*$	(69)

**Table 13.** Rate expressions for the Hattori mechanism where the methanol adsorption is rate limiting.

Reaction	Rate Expression	Equation
$* + \text{CH}_3\text{OH} \rightleftharpoons \text{CH}_3\text{OH}^*$	$r_1 = \frac{k_1 \left( [\text{CH}_3\text{OH}] - \frac{K_9}{K_1 K_2 K_3 K_4} \frac{[\text{D}][\text{MeOOR}]}{[\text{T}]} \right)}{1 + \frac{K_9}{K_2 K_3 K_4} \frac{[\text{D}][\text{MeOOR}]}{[\text{T}]} + \frac{K_9[\text{D}][\text{MeOOR}]}{K_4} + \frac{K_{10}[\text{M}][\text{MeOOR}]}{K_6} + \frac{K_{11}[\text{G}][\text{MeOOR}]}{k_8} + K_2[\text{T}] + K_9[\text{D}] + K_{10}[\text{M}] + K_{11}[\text{G}]}$	(70)
$\text{T} + * \rightleftharpoons \text{T}^*$	$r_2 = \frac{k_2 \left( [\text{T}] - \frac{K_9}{K_1 K_2 K_3 K_4} \frac{[\text{D}][\text{MeOOR}]}{[\text{CH}_3\text{OH}]} \right)}{1 + K_1[\text{CH}_3\text{OH}] + \frac{K_9[\text{D}][\text{MeOOR}]}{[K_4]} + \frac{K_{10}[\text{M}][\text{MeOOR}]}{K_6} + \frac{K_{11}[\text{G}][\text{MeOOR}]}{K_8} + \frac{K_9[\text{D}][\text{MeOOR}]}{K_1 K_3 K_4 [\text{CH}_3\text{OH}]} + K_9[\text{D}] + K_{10}[\text{M}] + K_{11}[\text{G}]}$	(71)
$\text{CH}_3\text{OH}^* + \text{T}^* \rightleftharpoons (\text{TCH}_3\text{OH})^* + *$	$r_3 = \frac{k_3 \left( K_1 K_2 [\text{CH}_3\text{OH}][\text{T}] - \frac{K_9}{K_3 K_4} [\text{D}][\text{MeOOR}] \right)}{\left( 1 + K_1[\text{CH}_3\text{OH}] + \frac{K_9[\text{D}][\text{MeOOR}]}{[K_4]} + \frac{K_{10}[\text{M}][\text{MeOOR}]}{K_6} + \frac{K_{11}[\text{G}][\text{MeOOR}]}{K_8} + K_2[\text{T}] + K_9[\text{D}] + K_{10}[\text{M}] + K_{11}[\text{G}] \right)^2}$	(72)
$(\text{TCH}_3\text{OH})^* \rightleftharpoons \text{D}^* + \text{MeOL}$	$r_4 = \frac{k_4 \left( K_1 K_2 K_3 [\text{CH}_3\text{OH}][\text{T}] - \frac{1}{K_4 K_9 [\text{D}][\text{MeOOR}]} \right)}{1 + K_1[\text{CH}_3\text{OH}] + K_1 K_2 K_3 [\text{CH}_3\text{OH}][\text{T}] + \frac{K_{10}[\text{M}][\text{MeOOR}]}{K_6} + \frac{K_{11}[\text{G}][\text{MeOOR}]}{K_8} + K_2[\text{T}] + K_9[\text{D}] + K_{10}[\text{M}] + K_{11}[\text{G}]}$	(73)
$\text{CH}_3\text{OH}^* + \text{D}^* \rightleftharpoons (\text{DCH}_3\text{OH})^* + *$	$r_5 = \frac{k_5 \left( K_1 K_9 [\text{CH}_3\text{OH}][\text{D}] - \frac{1}{K_5 K_{10} [\text{M}][\text{MeOOR}]} \right)}{\left( 1 + K_1[\text{CH}_3\text{OH}] + \frac{K_9[\text{D}][\text{MeOOR}]}{K_4} + \frac{K_{10}[\text{M}][\text{MeOOR}]}{K_6} + \frac{K_{11}[\text{G}][\text{MeOOR}]}{K_8} + K_2[\text{T}] + K_9[\text{D}] + K_{10}[\text{M}] + K_{11}[\text{G}] \right)^2}$	(74)
$(\text{DCH}_3\text{OH})^* \rightleftharpoons \text{M}^* + \text{MeOL}$	$r_6 = \frac{k_6 \left( K_1 K_9 K_5 [\text{CH}_3\text{OH}][\text{D}] - \frac{1}{K_6 K_{10} [\text{M}][\text{MeOOR}]} \right)}{1 + K_1[\text{CH}_3\text{OH}] + \frac{K_9[\text{D}][\text{MeOOR}]}{K_4} + K_1 K_9 K_5 [\text{CH}_3\text{OH}][\text{D}] + \frac{K_{11}[\text{G}][\text{MeOOR}]}{K_8} + K_2[\text{T}] + K_9[\text{D}] + K_{10}[\text{M}] + K_{11}[\text{G}]}$	(75)

Table 13. Cont.

Reaction	Rate Expression	Equation
$\text{CH}_3\text{OH}^* + \text{M}^* \rightleftharpoons (\text{MCH}_3\text{OH})^* + *$	$r_7 = \frac{k_7 \left( K_1 K_{10} [\text{CH}_3\text{OH}] [\text{M}] - \frac{1}{\frac{K_7 K_{11}}{K_8} [\text{G}] [\text{MeOOR}]} \right)}{\left( 1 + K_1 [\text{CH}_3\text{OH}] + \frac{K_9 [\text{D}] [\text{MeOOR}]}{K_4} + \frac{K_{10} [\text{M}] [\text{MeOOR}]}{K_6} + \frac{K_{11} [\text{G}] [\text{MeOOR}]}{K_8} + K_2 [\text{T}] + K_9 [\text{D}] + K_{10} [\text{M}] + K_{11} [\text{G}] \right)^2}$	(76)
$(\text{MCH}_3\text{OH})^* \rightleftharpoons \text{G}^* + \text{MeOL}$	$r_8 = \frac{k_8 \left( K_1 K_7 K_{10} [\text{CH}_3\text{OH}] [\text{M}] - \frac{1}{K_8 K_{11} [\text{G}] [\text{MeOOR}]} \right)}{1 + K_1 [\text{CH}_3\text{OH}] + \frac{K_9 [\text{D}] [\text{MeOOR}]}{K_4} + \frac{K_{10} [\text{M}] [\text{MeOOR}]}{K_6} + K_1 K_7 K_{10} [\text{CH}_3\text{OH}] [\text{M}] + K_2 [\text{T}] + K_9 [\text{D}] + K_{10} [\text{M}] + K_{11} [\text{G}]}$	(77)
$\text{D} + * \rightleftharpoons \text{D}^*$	$r_9 = \frac{k_9 \left( \frac{K_{10} [\text{M}] [\text{MeOOR}]}{K_1 K_5 K_6 [\text{CH}_3\text{OH}]} - K_9 [\text{D}] \right)}{1 + K_1 [\text{CH}_3\text{OH}] + \frac{K_9 [\text{D}] [\text{MeOOR}]}{K_4} + \frac{K_{10} [\text{M}] [\text{MeOOR}]}{K_6} + \frac{K_{11} [\text{G}] [\text{MeOOR}]}{K_8} + K_2 [\text{T}] + \frac{K_{10} [\text{M}] [\text{MeOOR}]}{K_1 K_5 K_6 [\text{CH}_3\text{OH}]} + K_{10} [\text{M}] + K_{11} [\text{G}]}$	(78)
$\text{M} + * \rightleftharpoons \text{M}^*$	$r_{10} = \frac{k_{10} \left( \frac{K_{11} [\text{G}] [\text{MeOOR}]}{K_1 K_7 K_8 [\text{CH}_3\text{OH}]} - K_{10} [\text{M}] \right)}{1 + K_1 [\text{CH}_3\text{OH}] + \frac{K_9 [\text{D}] [\text{MeOOR}]}{K_4} + \frac{K_{10} [\text{M}] [\text{MeOOR}]}{K_6} + \frac{K_{11} [\text{G}] [\text{MeOOR}]}{K_8} + K_2 [\text{T}] + K_9 [\text{D}] + \frac{K_{11} [\text{G}] [\text{MeOOR}]}{K_1 K_7 K_8 [\text{CH}_3\text{OH}]} + K_{11} [\text{G}]}$	(79)
$\text{G} + * \rightleftharpoons \text{G}^*$	$r_{11} = \frac{k_{11} \left( \frac{K_1 K_7 K_8 K_{10} [\text{CH}_3\text{OH}] [\text{M}]}{[\text{MeOOR}]} - K_{11} [\text{G}] \right)}{1 + K_1 [\text{CH}_3\text{OH}] + \frac{K_9 [\text{D}] [\text{MeOOR}]}{K_4} + \frac{K_{10} [\text{M}] [\text{MeOOR}]}{K_6} + \frac{K_{11} [\text{G}] [\text{MeOOR}]}{K_8} + K_2 [\text{T}] + K_9 [\text{D}] + K_{10} [\text{M}] + \frac{K_1 K_7 K_8 K_{10} [\text{CH}_3\text{OH}] [\text{M}]}{[\text{MeOOR}]}$	(80)



The most likely and well-known case for the Hattori mechanism is that the methanol adsorption step is rate limiting [67]. Under this condition, methanol ( $\text{CH}_3\text{OH}$ ) and triglyceride (T) are adsorbed on the empty site of the catalyst (\*) and react with each other to form the active species ( $\text{TsCH}_3\text{OH}$ ). In the next step, this active species ( $\text{TsCH}_3\text{OH}$ ) is converted to diglyceride adsorbed on the surface (D) and  $\text{MeOOR}$ . Then, the adsorbed diglyceride (D) reacts with the adsorbed methanol ( $\text{CH}_3\text{OH}$ ) to form the active species ( $\text{DsCH}_3\text{OH}$ ), which turns into monoglyceride on the surface (M) and  $\text{MeOOR}$ . As in the previous steps, the adsorbed monoglyceride (M) and adsorbed methanol ( $\text{CH}_3\text{OH}$ ) react with each other to form the active species ( $\text{MsCH}_3\text{OH}$ ), which turns into glycerol on the surface (G) and  $\text{MeOOR}$ . It should be noted that diglyceride (D), monoglyceride (M) and glycerol (G) are desorbed from the surface of the catalyst [67]. As previously noted, the rate expressions assume that methanol adsorption (Equation (70) in Table 13) is rate limiting [67].

#### 4. Heterogeneously Catalysed Transesterification

Homogeneous and heterogeneous basic and acidic catalysts dominate biodiesel production [85], and the advantages and disadvantages of each process are summarised in Table 14. NaOH and KOH are the most widely used homogeneous base catalysts for transesterification due to their low cost and abundance [86–91]. Base-catalysed transesterification is usually conducted at low temperatures (60–70 °C) and pressure (1 bar), delivering a high product yield. Although less active than their homogeneous counterparts due to lower base site concentrations and poor reactant/product mass transport, solid base catalysts are readily separated from the reaction mixture by filtration, sedimentation or centrifugation, saving energy and capital investment, and minimising waste by-products. Continuous flow operation using a packed or entrained catalyst bed permits in situ catalyst separation, although active site leaching into the product stream may occur. FAME separation from glycerol and unreacted alcohol can be performed by gravitational settling, decantation or filtration, followed by purification by washing with water, acid and/or ether, membrane or solvent extraction with ionic liquids, or the use of absorbents. Simultaneous FAME separation and purification are possible using membrane reactors [92,93]. Acid catalysts can mitigate undesired saponification of triglycerides and are insensitive to FFA contaminants [94]. Hydrochloric (HCl) and sulfuric ( $\text{H}_2\text{SO}_4$ ) acids are the most widely used liquid acid catalysts [95–97], offering very high FAME yields, although the reactions kinetics are sluggish, requiring temperatures  $>100$  °C [98]. In heterogeneous catalysis, contact between the reactants is often hindered by the initial oil/alcohol phase separation. Such phase separation can be compensated using high starting concentrations of alcohol to improve the oil miscibility [99]. Solid-acid catalysts also require higher alcohol:oil molar ratios than heterogeneous basic catalysts to overcome the mass transfer barriers arising from their lower activity and reach thermodynamic equilibrium. However, high alcohol:oil molar ratios incur cost penalties, deliver a more dilute FAME product, and can induce catalyst deactivation [100].

**Table 14.** Catalysts for biodiesel production and their associated advantages and disadvantages.

Catalyst Type	Advantages	Disadvantages
Homogeneous basic catalyst	<ul style="list-style-type: none"> <li>- Higher reaction rate compared to transesterification over acid catalyst [101,102]</li> <li>- Mild reaction conditions and thus less energy required [101,102]</li> <li>- Wide availability of NaOH and KOH [102]</li> </ul>	<ul style="list-style-type: none"> <li>- Very difficult to recycle soluble bases</li> <li>- Sensitivity to the presence of FFA in the oil [102]</li> <li>- Saponification for high FFA content oil (<math>&gt;2</math> wt%) [102]</li> <li>- Lower biodiesel yield due to saponification and consequent product purification [101,102]</li> <li>- High yield of contaminated wastewater through purification [36]</li> </ul>

Table 14. Cont.

Catalyst Type	Advantages	Disadvantages
Heterogeneous basic catalyst	<ul style="list-style-type: none"> <li>- Reusable [103]</li> <li>- Easy product separation [103]</li> <li>- Higher activity for transesterification than acid catalyst [102]</li> <li>- Mild reaction conditions and thus less energy required [102]</li> <li>- Longer catalyst lifetime [101]</li> </ul>	<ul style="list-style-type: none"> <li>- Catalyst poisoning by atmospheric CO<sub>2</sub> [102]</li> <li>- Sensitivity to the presence of FFA in the oil [102]</li> <li>- Saponification for high FFA content oil (&gt;2 wt%) [102]</li> <li>- Lower biodiesel yield due to saponification and consequent product purification [101,102]</li> <li>- High yield of contaminated wastewater through purification step [36]</li> <li>- Poor diffusion of bulky triglycerides [36]</li> <li>- High cost [36]</li> </ul>
Homogeneous acid catalyst	<ul style="list-style-type: none"> <li>- Insensitive to the presence of FFA and water in the oil [94]</li> <li>- Simultaneous FFA esterification and TAG transesterification [102]</li> <li>- No saponification [36]</li> <li>- Higher yield of biodiesel [101]</li> </ul>	<ul style="list-style-type: none"> <li>- Very difficult to recycle soluble acids [102]</li> <li>- Slow reaction kinetics [36,101,102]</li> <li>- Equipment corrosion [36,102]</li> </ul>
Heterogeneous acid catalyst	<ul style="list-style-type: none"> <li>- Reusable [18,36]</li> <li>- Easy product separation [102]</li> <li>- Insensitive to the presence of FFA and water in the oil [94], hence suitable for low-grade oil [102]</li> <li>- Simultaneous FFA esterification and TAG transesterification [102]</li> <li>- No saponification [36]</li> </ul>	<ul style="list-style-type: none"> <li>- Slow reaction kinetics, hence more severe reaction conditions [36,101,102]</li> <li>- High cost [36]</li> <li>- High energy demand [102]</li> <li>- Product contamination by leached active sites [102]</li> <li>- Requires higher alcohol:oil molar ratio [100]</li> </ul>

Acid-catalysed transesterification occurs through protonation of the ester (Figure 4), which favours the subsequent nucleophilic attack of the alcohol, molecular rearrangement to eliminate the diglyceride, and deprotonation of the acid intermediate to form FAME [104,105].

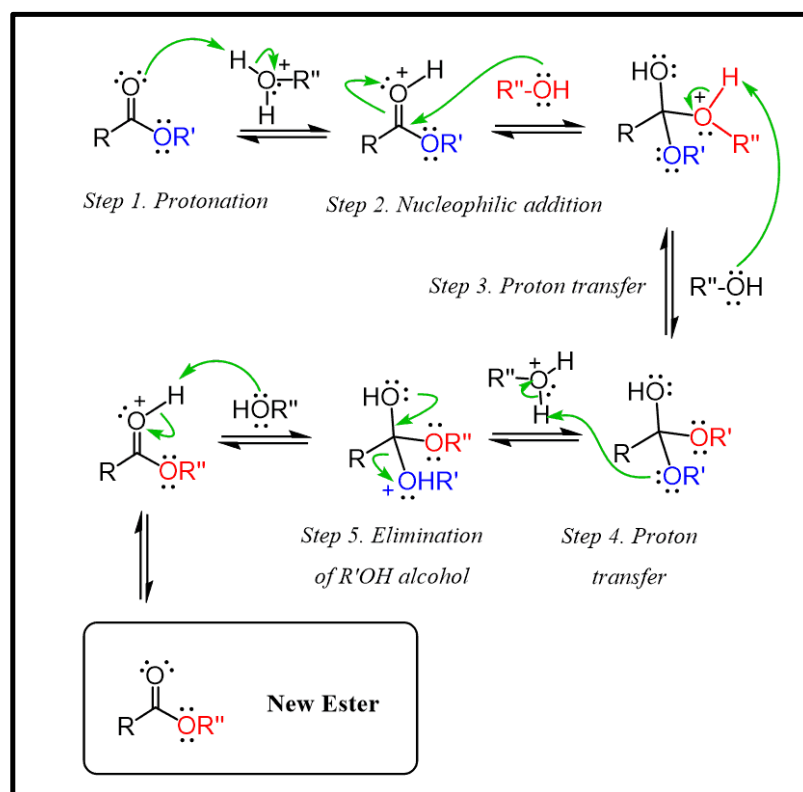
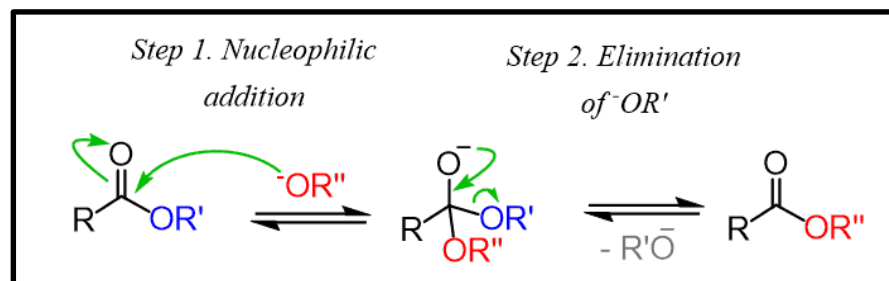


Figure 4. Mechanism of acid-catalysed transesterification.

In the analogous base-catalysed reaction (Figure 5), the alcohol is first deprotonated by the basic catalyst to form an alkoxide, which then undergoes nucleophilic attack by the ester to form FAME and a diglyceride anion (which is then protonated to form the diglyceride) [104,105].



**Figure 5.** Mechanism of base-catalysed transesterification.

The different reaction mechanisms of acid- and base-catalysed transesterification incur different activation barriers, resulting in faster kinetics of base catalysis. Acid catalysts donate a proton to the carbonyl group, whereas base catalysis deprotonates the alcohol to form an alkoxide that undergoes nucleophilic addition to the parent ester. Nucleophilic acyl substitution reactions with basic nucleophiles are favoured when the leaving group is a weaker base than that of the nucleophile. However, if two alkoxides (the nucleophile and leaving group) have comparable basicity, then there is little driving force for FAME production. For example, the conjugate bases of ethanol (pKa 15.9) and methanol (pKa 15.5) have similar basicities, and hence, similar leaving abilities. In acid-base reactions, as soon as a  $CH_3O(-)$  alkoxide is formed, it will react with the  $CH_3CH_2OH$  solvent. However, despite their comparable basicity, the equilibrium will greatly favour  $CH_3CH_2O(-)$  formation, as the concentration of  $CH_3CH_2OH$  is several orders of magnitude higher than that of  $CH_3OH$ .

Transesterification by soluble acids and bases generally has a faster rate than that using their heterogeneous counterparts [106] due to the higher concentration of active sites and superior mass transport for the latter. However, FFAs in animal fats or waste cooking oils can react with homogeneous bases to form soap (saponification), which consumes the catalyst, lowers the biodiesel yield, and complicates downstream separation and purification [107]. Transesterification using homogeneous acids affords slower rates, causes reactor corrosion, and also requires multiple downstream purification steps [102,108,109]. In contrast, solid catalysts offer simpler catalyst recovery and reuse, thereby enhancing biodiesel productivity and cost effectiveness [110,111]. The purification of biodiesel from solid catalysts is also simplified, as these obviate the energy-intensive neutralisation steps and associated wastewater streams required for liquid catalysts [101]. Recovering value from the glycerol by-product remains problematic, although partial hydrogenolysis to propanediols has proven attractive to academic researchers for paint and polymer applications [112]. Further improvements in the design of heterogeneous acid and base catalysts are needed to supplant homogeneous catalysts for commercial biodiesel production [113].

Base-catalysed transesterification of low-grade/cost feedstocks containing high FFA levels, such as WCO, results in a low biodiesel yield due to saponification and emulsification. An acid-catalysed esterification pretreatment offers one solution to this problem [114–116]. In early versions of such two-stage processes, WCO was reacted with methanol in the presence of a liquid acid catalyst (e.g., ferric sulfate), and the reaction mixture was subsequently separated into two layers based on density differences. The lower-density phase comprises excess alcohol, and the denser phase comprises an acid catalyst and esterified oil. Ferric sulfate has a very low solubility in bio-oils and hence settles at the bottom of the reactor, where it can be separated, ashed to remove organic impurities, and reused. Nevertheless, contamination of the esterified bio-oil by soluble metal ions is unavoidable, with metal impurities carrying over to the subsequent transesterification stage where triglycerides react with, e.g., methanol and KOH to form FAME. The reaction mixture again separates into

two layers, the denser layer containing glycerol (and impurities) and the lighter containing FAME and unreacted methanol (which can be removed by vacuum distillation). FAME is subsequently washed with hot water to remove residual glycerol and dried [21,117]. Such a two-step process can be performed in a single reactor by first adding an acid catalyst and then adding an excess of the base catalyst to neutralise the acid catalyst and transesterify the unreacted triglycerides [118]. However, this strategy is wasteful, as the acid catalyst cannot be recovered, and a higher concentration of base catalyst is used than that required for transesterification of the oil. Bifunctional acid/base catalysts have also been reported for the simultaneous (trans)esterification of bio-oils [119], e.g., SrO and ZnO-impregnated alumina [120]; however, the base-active sites remain prone to deactivation by fatty acids. Novel catalyst designs can enable the spatial segregation of antagonistic acid and base sites for the one-pot esterification and transesterification of high FFA-content oils [121]. This approach was recently adapted for the hydrodeoxygenation of fatty acids to alkanes over a Pd-doped hierarchical H-ZSM-5 Brønsted acid zeolite [122]. The use of soluble acid/base catalysts and their contamination of the final biodiesel product causes corrosion of engine components and the formation of incombustible ash in the engine manifold [123–125]. Solid acids can catalyse FFA esterification and triglycerides transesterification and hence, in theory, can produce biodiesel directly from low-grade oils, providing a sufficiently high concentration and strength of acid site can be generated [126]. It is generally accepted that both reactions are catalysed over Brønsted acid sites (polarised hydroxyl groups act as H<sup>+</sup> donors) rather than Lewis acid sites (coordinatively unsaturated cations) which in the presence of polar solvents such as methanol [127].

## 5. Heterogeneous Solid-Acid Catalysis

Heterogeneous solid-acid catalysts are widely used alternatives to homogeneous acid catalysts in the petrochemical industry and are well suited for the production of high-quality biodiesel through (trans)esterification [128,129]. A key advantage of solid-acid catalysts is their water tolerance, ease of separation, and high thermal stability and activity, which are factors mitigating engine corrosion and sensitivity to FFA content [130]. Catalyst efficiency depends on the acid character (Brønsted/Lewis), the number of active sites, and the morphology of the support [131]. Typical solid acids studied for biodiesel production include zeolites, mixed metal oxides, carbon, polyoxometalates, enzymes (lipases), and polymers.

A challenge in benchmarking catalyst performance is the reliance of most academic and patent literature on reporting and comparing oil (or FFA) conversion or FAME yield, neither of which are kinetic parameters nor do they account for differences in catalyst loading (relative to feedstock) or reaction temperature. This does not reflect limitations in methods for analysing biodiesel production, but rather an intentional focus on maximising FAME yield at the expense of insight into the intrinsic catalyst activity. Almost all academic studies employ conventional [132] or ultrafast [133] gas chromatography (GC) or high-performance liquid chromatography (HPLC) [134] to determine the conversion of relatively pure oil or fatty acid feedstock from transesterification and esterification reactions, respectively. Aliquots of the liquid reaction mixture are periodically sampled, diluted, and injected (using either conventional split/splitless or programmable temperature injectors for GC) with conventional flame ionisation (GC) or refractive index and UV detectors (HPLC) to determine the % decrease in the oil/FFA peak area. FAME yields are also typically determined by chromatographic methods in the academic literature, although mid-IR methods are now emerging [135]. However, in all cases, accurate quantification from calibration curves requires access to the appropriate pure FAME reference compound; few such references are available (mainly for plant oils) and are often expensive. Specific activity, i.e., the rate of conversion of triglycerides or FFA molecules normalised to the mass of the total catalyst, is a widely used kinetic parameter for performance benchmarking [136], but neglects the multicomponent nature of the most heterogeneous catalysts, of which the active phase mass only comprises a small mass fraction. Furthermore, the specific activity

is only a reflection of the intrinsic reaction kinetics at low conversion, where mass-transport limitations are absent [137]. In cases where the active site is well-established, for example, pure Brønsted solid acids such as sulfonic acid carbons and silicas possessing low concentrations of isolated sulfonic acid groups, or protonated zeolites, the turnover frequency (TOF, mols of reactant converted per mol of active sites per unit time) is a more valuable comparator. For solid acids, temperature-programmed desorption (TPD) of chemisorbed base probe molecules provides a simple method for quantifying the acid molar loading. However, the most common  $\text{NH}_3$ -TPD method often results in broad desorption peaks and fluctuating baselines that hinder acid-site quantification. In contrast, the Hoffman elimination reaction during *n*-propylamine-TPD (resulting in reactively desorbed propene and  $\text{NH}_3$ ) result in a sharp desorption peak and more accurate acid-site loadings. Recycle tests are critical to assess catalyst deactivation but are often conducted at full conversion, under which little insight is possible other than some initial activity is retained [137]. In addition to kinetic benchmarking, catalyst (and process) effectiveness for commercial development must be assessed through life cycle assessment (LCA) and technoeconomic analysis (TEA) to consider factors such as feedstock abundance, cost, and environmental impact.

### 5.1. Zeolites

Zeolites occur naturally as crystalline aluminosilicates with high surface areas arising from micropore channels, which may host high concentrations of active sites [138]. H-Beta, H-ZSM-5, and H-USY zeolites, in which cations (typically ammonium) used in their synthesis are ion-exchanged for protons, suffer from restricted diffusion of bulky reactants into their micropores [139]. For example, although H-Beta has Lewis and Brønsted acid sites, it is only suitable for FFA esterification pretreatment of WCO, with subsequent transesterification of more sterically challenging TAGs requiring larger-pore solid-acid/base catalysts [140]. Larger-pore H-Y zeolites often possess weak acidity and, hence, are ill-suited for transesterification [139]. Hassani et al. prepared unspecified zeolite pellets using polyvinylalcohol and kaolinite binders for the transesterification of WCO and reported only 46% TAG conversion under optimal conditions (70 °C, 6 h, methanol:oil molar ratio = 5, catalyst loading not reported) [141]. H-Y zeolites partially exchanged with Cs or Na cations achieved 98% FAME yield in sub- and supercritical methanol from used frying oil between 60 and 476 °C in 4 h, with temperatures optimal [142,143]. Surprisingly, the regenerated zeolites showed higher activities than the as-prepared zeolites. A comparison between H-Y-60 and H-ZSM-5 zeolites for palmitic acid esterification with methanol to methyl palmitate revealed superior performance for the former [144], attributed to its wider pores (0.4–0.6 nm vs.  $\leq 0.3$  nm) and higher proportion of Brønsted acid sites (70% vs. 20%). H-ZSM-5, synthesised by Septiani et al., from rice husk ash using a hydrothermal method, was assessed for biodiesel production from (an unspecified) vegetable oil. Transesterification with methanol at 60 °C resulted in 93% FAME for a methanol:oil molar ratio of 3 and catalyst loading of 0.5 wt% [145].

### 5.2. Metal Oxides

Metal oxides are often used as catalyst supports due to their high specific surface areas, large pore volumes and pore sizes, and high thermal stabilities [146]. Abreu et al. [147] synthesised a heterogeneous catalyst comprising nickel and strontium oxides by co-precipitation and evaluated it in biodiesel production from macaw oil. An optimum performance of 97% oil conversion was obtained for 2 wt% catalysts calcined at 1100 °C for 3 h and tested at 65 °C with a methanol:oil molar ratio of 9 over 5 h. Sulfation of transition metal oxides increases their surface acidity for esterification [148] but must be counterbalanced by potential changes in textural properties, such as the crystallisation of bulk sulfates [3]. Sulfated metal oxides, including  $\text{SO}_4/\text{Nb}_2\text{O}_5$ ,  $\text{SO}_4/\text{TiO}_2$ ,  $\text{SO}_4/\text{ZrO}_2$  and  $\text{SO}_4/\text{Ta}_2\text{O}_5$  have been explored for biodiesel production.  $\text{SO}_4/\text{ZnO}$  synthesised by co-precipitation [149] afforded 80% FAME yield at 65 °C, a methanol:oil molar ratio of 6, and catalyst loading of 4 wt%. A mesoporous sulfated titania silica composite (S-TSC) prepared by a sol-gel



method [150] and subsequently calcined at 550 °C was more active (98% conversion), albeit at 120 °C and a higher methanol:oil molar ratio (20) and catalyst loading (10 wt%). ZrO<sub>2</sub>, ZnO, SO<sub>4</sub>/ZrO<sub>2</sub>, and SO<sub>4</sub>/SnO<sub>2</sub> have been studied for the transesterification of palm kernel and crude coconut oils [151], with the superacidic SO<sub>4</sub>/ZrO<sub>2</sub> exhibiting the highest FAME yield (92%). Surface sulfation is typically associated with the high loadings of strong Brønsted acid sites [152–155]. However, excessive sulfation lowers the active surface area and promotes sulfate leaching, resulting in acid-contaminated biodiesel products [156–160]. Incorporation of a magnetic component into sulfated metal oxides (e.g., as a core@shell structure) can assist their rapid separation from the biodiesel product and subsequent reuse [161–165]. However, care must be taken to prevent particle aggregation due to anisotropic dipolar interactions and, hence, loss of active surface area [166,167]. This problem can be partially mitigated by coating a catalytically active surface with porous oxides or polymers that limit aggregation [157,160,168]. Sulfated zirconia has also been used for palm oil esterification and transesterification with methanol under near- and supercritical conditions [169]. The effects of sulfur loading and calcination temperature (500 °C and 700 °C) were investigated; temperature-programmed ammonia desorption showed that the acid density increased with S loading ≤ 2 wt%, while high-temperature calcination lowered the acid density. Biodiesel yields of ≥90% have been reported for SO<sub>4</sub>/ZrO<sub>2</sub> immobilised on alumina [170] and MCM-41 silica [171] for the simultaneous esterification and transesterification of vegetable oils containing high FFA levels (>9 wt%), with negligible leaching of S or Zr. Catalyst activity is linked to the zirconia phase (monoclinic or tetragonal) formed during the calcination of the sulfated precursors. Superacidic SO<sub>4</sub>/ZrO<sub>2</sub>-TiO<sub>2</sub>/La prepared by co-precipitation of TiCl<sub>4</sub>, La(NO<sub>3</sub>)<sub>3</sub>, and ZrOCl<sub>2</sub>·8H<sub>2</sub>O, followed by sulfuric acid treatment, was used for the simultaneous transesterification and esterification of an undefined acid oil containing 60 wt% FFAs and 190 mg KOH/g, achieving a FAME yield >90 wt% at 200 °C, methanol:oil molar ratio of 15:1, and 5 wt% catalyst, being stable over five consecutive runs [172]. Simultaneous esterification and transesterification of waste vegetable oils were also performed on Fe-Zn double-metal cyanide (DMC) complexes (Zn<sub>2</sub>[Fe(CN)<sub>6</sub>]·3H<sub>2</sub>O) prepared by reacting potassium ferrocyanide, zinc chloride, and t-butanol as a complexing agent [173]. The activity for both esterification and transesterification increased as the catalyst crystallinity decreased, which was associated with a higher density of unsaturated Zn<sup>2+</sup> (Lewis acid) active sites. These DMC catalysts catalysed the transesterification of FFA and water-containing oils, possibly due to their hydrophobic surfaces. An SO<sub>4</sub><sup>2-</sup>/SnO<sub>2</sub>-SiO<sub>2</sub> superacid catalyst for the simultaneous esterification and transesterification of *Croton megalocarpus* and *Moringa oleifera* oils [174,175] afforded high biodiesel yields without saponification.

Solid superacid catalysts are thus well suited for continuous biodiesel production from FFA-containing oil feedstocks in a single process [176–180], provided that the acid function is thermochemically stable [156,172,181–190].

### 5.3. Carbon-Based Materials

Carbon catalysts have received considerable attention in organic transformations due to their resistance to coking [127]. Partial hydrothermal carbonisation of β-cyclodextrin to polycyclic aromatic carbon sheets and their subsequent sulfonation (–SO<sub>3</sub>H) created a solid-acid carbon catalyst [191] for simultaneous oleic acid esterification (91% yield in 8 h) and triolein transesterification (80% in 12 h), which retained significant activity for both reactions over six cycles. Sulfonated biochar (using concentrated sulfuric acid and fuming) was assessed for canola oil transesterification [192] but only exhibited modest activity at an unspecified temperature, a high methanol:oil molar ratio of 28, and 5 wt% catalysts after 3 h. A higher activity was observed for FFA esterification. Zhang et al. [193] prepared porous cellulose-based beads using ionic liquid and modified them with different amines (diethylenetriamine (DETA), triethylenetetramine (TETA), 4-aminostyrene (AST), and ethylenediamine (EDA)) as supports to immobilise H<sub>3</sub>PW<sub>12</sub>O<sub>40</sub> (HPW). The esterification reaction of yellow horn oil was investigated at 60 °C with a modest methanol:oil

molar ratio of 10 and 4 wt% catalyst, achieving 96% conversion in 1 h. A lipid-extracted algae, *Dunaliella*, was used as a biochar precursor and treated with  $\text{H}_2\text{SO}_4$  and  $\text{SO}_2\text{Cl}_2$  as a solid-acid catalyst for oleic acid esterification [194]. Biochar modified with  $\text{H}_2\text{SO}_4$  ( $\text{CAT}_\text{H}$ ) was more active than that modified with  $\text{SO}_2\text{Cl}_2$  ( $\text{CAT}_\text{S}$ ), which is attributed to the larger specific surface area and smaller particle size of the former. However,  $\text{CAT}_\text{S}$  retained higher activity after five reaction cycles.

Simultaneous esterification/transesterification of a waste vegetable oil (with high FFA levels) was also performed on solid-acid carbons [195]. These highly active and stable catalysts (obtained by carbonising vegetable oil asphalt followed by sulfonation) possessed a flexible carbonaceous framework and a high density of acid sites due to dispersed polycyclic aromatic hydrocarbons containing sulfonic acid functions. Hydration of the Brønsted acid sites was limited by the catalyst hydrophobicity, although this did not prevent the neutralisation of the surface base site by FFAs.

#### 5.4. Heteropolyacids

Heteropolyacids, which are active for both esterification and transesterification reaction mechanisms, are suitable acid solid catalysts for the production of biodiesel, especially from waste oils, which include Keggin ( $\text{HnXM}_{12}\text{O}_{40}$ ), Heteropoly tungstate, Dawson ( $\text{HnX}_2\text{M}_{18}\text{O}_{62}$ ), and  $\text{H}_3\text{PW}_{12}\text{O}_{40}$  (HPW) among the suitable heteropolyacids [196]. Cao et al. [197] used heteropolyacid  $\text{H}_3\text{PW}_{12}\text{O}_{40} \cdot 6\text{H}_2\text{O}$  ( $\text{PW}_{12}$ ) in the transesterification reaction of cooking wastes, and under optimal conditions, 87% transesterification efficiency was reported (65 °C, 16 h, methanol:oil molar ratio = 70, catalyst loading = 0.1 mmol).  $\text{Cs}_{2.5}\text{H}_{0.5}\text{PW}_{12}\text{O}_{40}$  was used as an SAC by Chai et al. [198] with the aim of producing biodiesel from *Eruca sativa* Gars. Considering that the catalytic activity of  $\text{Cs}_{2.5}\text{H}_{0.5}\text{PW}_{12}\text{O}_{40}$  in vegetable oil is not affected by water content and free fatty acid content, the reaction was faster at a lower temperature. Under optimal reaction conditions (60 °C methanol:oil molar ratio of 5.3, and 0.02 mol% catalyst), 99% conversion was obtained in 1 h. A high conversion was retained over six reaction cycles. A catalyst family based on 12-tungstophosphoric acid on zirconia was prepared by Alcaniz-Monge et al. [199] through a sol-gel method for palmitic acid esterification with methanol. Synthesis of zirconia in the presence of the heteropolyacid altered the morphology and composition of the resulting catalyst; a 30 wt% heteropolyacid/ $\text{ZrO}_2$  was optimal, achieving >90% conversion.

## 6. Solid Base Catalysts

Solid-based catalysts are more active than solid-acid catalysts for transesterification [200,201]; hence, reactions are typically performed at lower temperatures for shorter durations than those using solid-acid catalysts [201–203]. However, base catalysts are prone to saponification of oils with FFA values of >2 wt% [204]. Solid base catalysts are typically pure metal oxides [205], alkali-doped metal oxides [206], layered double hydroxides [207], basic zeolites [208], or obtained from waste residues [209].

#### 6.1. Solid Earth Metal Oxides

Solid earth metal oxides, such as  $\text{BeO}$ ,  $\text{MgO}$ ,  $\text{CaO}$ ,  $\text{SrO}$  and  $\text{BaO}$ , are included in this category, and have been investigated in the various literature with the aim of producing biodiesel in the transesterification reaction. The  $\text{CaO}$  solid base catalyst is very popular due to its high activity, low cost [204], medium reaction conditions (temperature), long life of the catalyst, and eco-friendly is of interest to researchers [210]. The raw materials for the production of  $\text{CaO}$  are calcium hydroxide and calcium nitrate, but natural resources such as egg shells and bones can be used for the purpose of cost-effective production and removing waste from nature [211]. Zhu et al. [212] investigated the performance of  $\text{CaO}$ , which was synthesised through calcination at 900 °C, in the transesterification reaction with the aim of producing biodiesel using *Jatropha curcas* oil, and obtained a conversion of 93% under optimal conditions (70 °C, 2.5 h, methanol:oil molar ratio = 9, catalyst loading = 1.5 wt%). Kouzu et al. [213] synthesised  $\text{CaO}$  using pulverised limestone raw material and calcination



at 900 °C and used it in the transesterification reaction in the presence of waste cooking oil, which achieved 93% conversion in 1 h. They achieved more than 99% in 2 h. Various factors, such as precursors for synthesis, calcination temperature and pore size, have an effect on the catalytic activity of CaO in the transesterification reaction [214]. Using SrO as a catalyst and soybean oil in the transesterification reaction, Liu et al. [215] achieved 95% conversion under the optimal conditions of 70 °C, methanol:oil molar ratio of 12, and 3 wt% catalyst in only 0.5 h. Catalyst recyclability was (surprisingly considering the solubility of alkaline earth hydroxides) good over 10 reaction cycles. Lopez et al. [216] investigated the catalytic performance of MgO calcined at 600 °C in soybean oil transesterification but only observed 18% conversion in 8 h, ascribed to the low MgO surface area of  $0.45 \text{ m}^2 \cdot \text{g}^{-1}$ . Kouzu et al. [213] also compared the performance of CaO, MgO and SrO for soybean oil transesterification (Figure 6), with the strongest base (SrO) affording the highest initial activity.

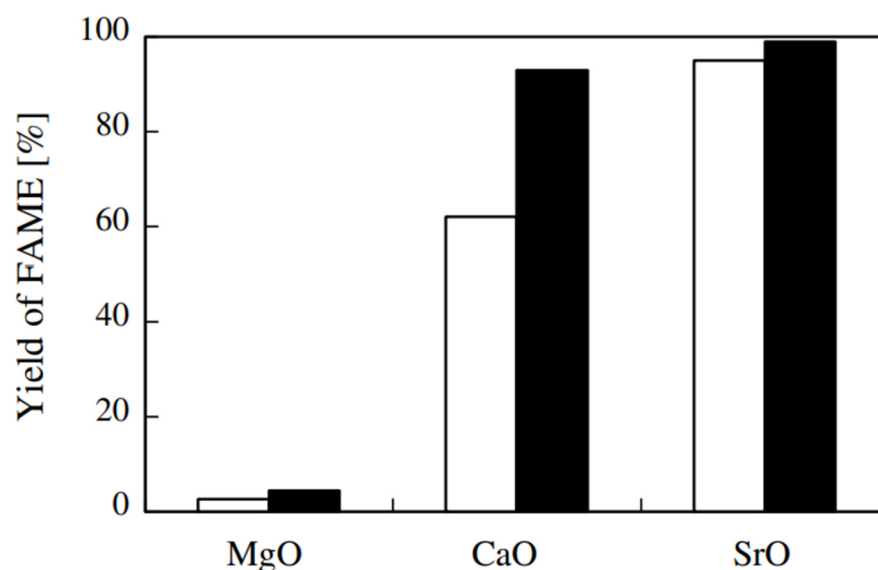


**Figure 6.** FAME yield for edible soybean oil transesterification over MgO, CaO, and SrO catalysts after 0.5 h (□) and 1 h (■) reaction [213].

## 6.2. Alkali-Doped Metal Oxides

Alkali-doping can increase the basicity of metal. Meher et al. [217] investigated the transesterification of Karanja oil using CaO catalyst doped with Li, Na, and K. Li/CaO under optimal conditions of 65 °C, methanol:oil molar ratio of 12, and 2 wt% catalysts resulted in 95% conversion after 8 h. K/CaO and Na/CaO analogues showed slower initial kinetics under the same conditions, but similar conversions after 8 h. In addition, the effect of the FFA content of the oil on the performance of the Li/CaO catalyst was investigated, and by increasing the FFA content to 6% in Karanja oil, the performance of Li/CaO decreased to 90%. Gurunathan et al. [218] investigated the performance of copper-doped zinc oxide (CZO) nanocatalyst in the transesterification reaction of neem oil and obtained a performance of 97% under optimal conditions (55 °C, 1 h, methanol:oil ratio of 12, 10 wt% catalyst), falling to 74% after six reaction cycles. Kinetic studies showed that the experimental data could be fitted to a first-order kinetic model. Torres-Rodríguez et al. [219] synthesised Cs-Na<sub>2</sub>ZrO<sub>3</sub> using ion exchange from Na<sub>2</sub>ZrO<sub>3</sub> and used Cs-Na<sub>2</sub>ZrO<sub>3</sub> as a catalyst in the transesterification reaction of soybean oil and jatropha oil with the aim of producing biodiesel. Under optimal conditions for jatropha oil (65 °C, 1 h, methanol:oil molar ratio of 15, 3 wt% catalyst), a 91% yield was obtained; under optimal conditions for soybean oil (65 °C, a methanol:oil molar ratio of 30, 1 wt% catalyst), a 99% yield was obtained in only 0.25 h using Cs-Na<sub>2</sub>ZrO<sub>3</sub>. Impregnation of Cs on Na<sub>2</sub>ZrO<sub>3</sub> decreased the

specific surface area from  $2.22 \text{ m}^2 \cdot \text{g}^{-1}$  to  $1.65 \text{ m}^2 \cdot \text{g}^{-1}$  accompanied by a change in surface morphology (Figure 7).

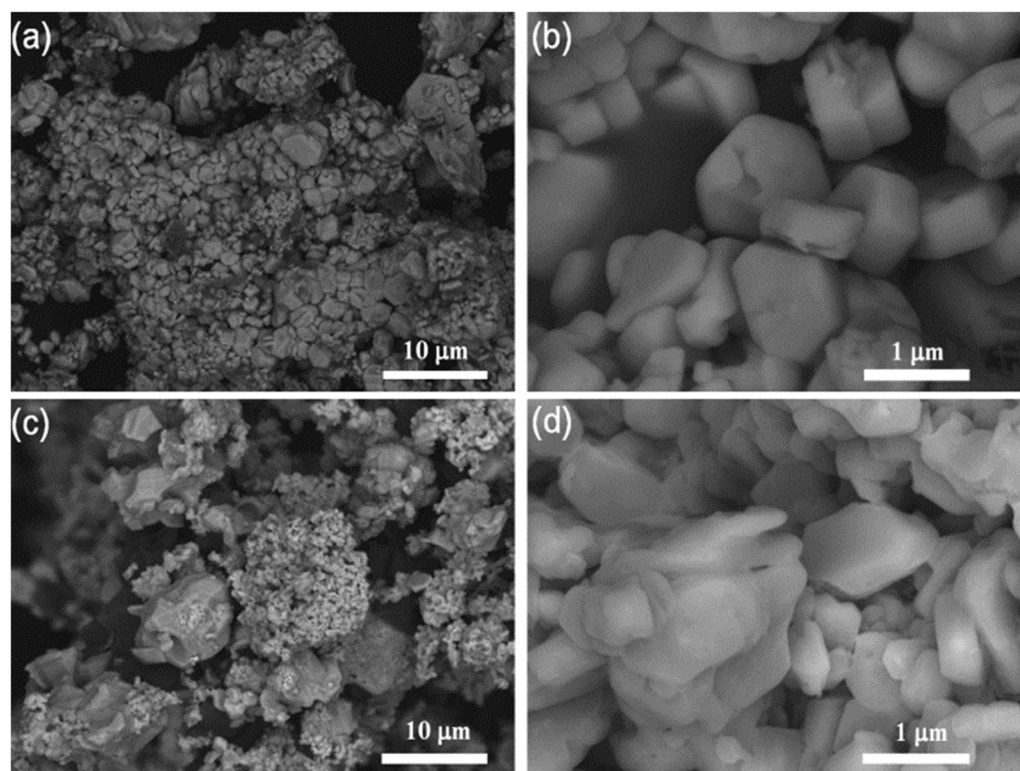


**Figure 7.** SEM images of (a,b)  $\text{Na}_2\text{ZrO}_3$  and (c,d)  $\text{Cs-Na}_2\text{ZrO}_3$  catalysts [219].

With the aim of using ethanol instead of methanol in the process of producing biodiesel from waste cottonseed oil, Kaur et al. [220] prepared  $\text{Li/NiO}$  in an aqueous environment and then calcined it at  $600 \text{ }^\circ\text{C}$ . The optimal value for Li loading with the aim of increasing catalyst strength and catalytic activity was reported to be 5 wt%. Under optimal reaction conditions ( $65 \text{ }^\circ\text{C}$ , 3 h, ethanol:oil molar ratio = 12, 8 wt% catalyst), they obtained 98% yield. Kinetic studies showed that the reaction followed pseudo-first-order kinetics, and the activation energy was reported to be  $74 \text{ kJ} \cdot \text{mol}^{-1}$ . Taufiq-Yap et al. [221] synthesised a  $\text{CaO-MgO}$  catalyst for biodiesel production from *Jatropha curcas* oil with different Ca:Mg atomic ratios, 0.5 being optimal at  $120 \text{ }^\circ\text{C}$ , methanol:oil molar ratio of 25, and 3 wt% catalyst after 3 h (up to 90% conversion falling to 80% after three recycles).

### 6.3. Hydrotalcites

Hydrotalcites (HT) ( $\text{Mg}_6\text{Al}_2(\text{OH})_{16}\text{CO}_3 \cdot 4\text{H}_2\text{O}$ ) are naturally occurring clays and a subset of double-layered hydroxides. The advantages of hydrotalcite include its high density of strong basic sites, high stability, high recyclability, and significant catalytic activity. The two factors of calcination temperature and Mg:Al ratio significantly affect the catalytic activity of hydrotalcite [222,223]. Navajas et al. [224] synthesised magnesium-aluminium (Mg-Al) hydrotalcite by co-precipitation method and then calcined it and evaluated different molar ratios of Mg/Al (Mg/Al) in transesterification reaction of sunflower oil. Under optimal reaction conditions ( $60 \text{ }^\circ\text{C}$ , methanol:oil molar ratio of 48, 2 wt% catalyst), hydrotalcite with a molar ratio of Mg:Al of 5 achieved 96% conversion after 8 h, reflecting their strong basicity ( $\text{H}^-$  values  $> 11$ ) despite their modest surface area ( $32 \text{ m}^2 \cdot \text{g}^{-1}$ ). Xie et al. [222] evaluated magnesium-aluminium (Mg-Al) hydrotalcite in the transesterification reaction of soybean oil after calcination at  $500 \text{ }^\circ\text{C}$  temperature. Under optimal reaction conditions ( $65 \text{ }^\circ\text{C}$ , 9 h, methanol:oil molar ratio of 15, 7.5 wt% catalyst), calcined hydrotalcite with a molar ratio of Mg:Al of 3 achieved 67% conversion. Using the co-precipitation method,

Wang et al. [223] synthesised HT-Ca activated hydrotalcite in a  $\text{Ca}(\text{OH})_2$  aqueous solution and evaluated its performance in the transesterification reaction of jatropha oil. Under optimal reaction conditions (160 °C, 4 h, methanol:oil molar ratio of 30, 5 wt% catalyst), 93% conversion was attained, only dropping to 86% after four cycles. The stability of HT-Ca to FFAs was also evaluated, and the biodiesel efficiency reached 92% in soybean oil, with an acid value (AV) > 12.1. Brito et al. [225] evaluated the performance of double layer Mg-Al catalyst in the transesterification reaction of waste using oil, obtaining 90% conversion under optimal reaction conditions (120 °C, 6 h, methanol:oil molar ratio of 24, 6 wt% catalyst). When employing layered double hydroxides in transesterification, it is important to ensure that there is no entrained alkali in the layers that will leach during the reaction, and synthetic routes using  $\text{NH}_4\text{OH}/(\text{NH}_4)\text{CO}_3$  rather than alkali-based precipitating agents are recommended [226–228].

#### 6.4. Basic Zeolites

Zeolites, such as naturally occurring Phillipsite, Chabazite, Erionite, and Analcime forms, offer a high specific surface area and thermochemical stability. Zeolites, such as Y, A, X, and ZSM-5, can also be synthesised via hydrothermal routes. By changing the metal clusters of zeolites, their chemical properties can be changed, so their basic properties can be changed in order to be used as heterogeneous basic catalysts in the transesterification reaction, which has attracted the attention of many researchers [196]. Du et al. [229] used NaY zeolite-supported  $\text{La}_2\text{O}_3$  catalyst in the form of spherical particles (3–5 mm) with the aim of producing biodiesel in the transesterification reaction of castor oil. Under optimal reaction conditions (70 °C, 50 min, methanol:oil molar ratio of 15, 10 wt% catalyst), they obtained a conversion of 85%. Babajide et al. [230] used FA/Na-X (faujasite zeolite material synthesised from South African class F fly ash) to exchange with ion potassium and prepared FA/K-X as a catalyst in the transesterification of sunflower oil to produce biodiesel. Under optimal reaction conditions (65 °C, 8 h, methanol:oil molar ratio of 6, and 3 wt% catalyst), they obtained 85% conversion. A tuff zeolite was synthesised by Jammal et al. [231] with the aim of producing biodiesel from sunflower oil. After treating zeolite with hydrochloric acid (16%), several catalysts were synthesised by impregnation in KOH solution, and the catalyst impregnated in KOH solution with a molarity of  $1 \times 10^4$  showed the best performance. Under optimal reaction conditions (50 °C, 2 h, methanol to oil molar ratio of 11.5:1), they obtained 97% conversion. Xie et al. [232] evaluated the transesterification reaction of soybean oil with KOH-loaded NaX zeolite. Under optimal reaction conditions (65 °C, 8 h, methanol:oil molar ratio of 10, 3 wt% catalyst), they obtained 86% conversion.

#### 6.5. Natural Waste Sources

Calcium oxide (CaO) obtained from chicken eggshells, bones, crab, lobster shells, and seashells contains 95% calcium carbonate ( $\text{CaCO}_3$ ), which has drawn the attention of many researchers to these natural sources of  $\text{CaCO}_3$  as a heterogeneous catalyst for biodiesel production. Using natural waste sources as heterogeneous catalysts for biodiesel production is considered an eco-friendly method. The simplest calcination method for these natural resources is shown in Figure 8 [196]. Detailed information about the sources that have been used as heterogeneous catalysts in the biodiesel production process in the different literature is reported in Table 15.

**Table 15.** Comparison of CaO sources for the biodiesel production process.

Source	Catalyst	Calcination T/°C	Calcination Time/h	Reaction T/°C	Reaction Time/h	Methanol:Oil Molar Ratio	Catalyst Loading/wt%	Conversion or Yield/%	Ref.
Biont shell	KF-CaO	500	-	70	3	9:1	3	Yield: 98	[232]
Shrimp shell	KF-CaO	450	-	65	3	9:1	2.5	Conversion: 80	[233]
waste mussel shell	CaO	1050	2	60	8	24:1	12	Yield: 94	[234]
combusted oyster shell	CaO	700	3	65–70	5	6:1	25	Yield: 74	[235]
shell of egg	CaO	800	2–4	60	2	18:1	10	Yield: 94	[210]
Coal fly ash loaded with egg shell	CaO-Al <sub>2</sub> O <sub>3</sub>	1000	2	Room temperature	5	6.9:1	1	Yield: 97	[236]
Clamshell	Calcined clamshell	900	3.5	60	3	6.03:1	3 g	Conversion: 97	[237]
river-snail shell	calcined river-snail shell	800	2	65	3	9:1	3	Conversion: 98	[238]
Snail shell	KOH-CaO	800	3	65	3.5	9:1	6	Yield: 96	[239]
Cuttle bone	CaCO <sub>3</sub>	800	2	60	4	18:1	20	Conversion: 24	[240]
Dolomite	CaMg(CO <sub>3</sub> ) <sub>2</sub>	800	2	60	3	30:1	6	Conversion: 99	[240]

Olive cakes/pulps are by-products of olive oil production that contain ~8–10 wt% oil and have been explored as both a source of biodiesel (using soluble KOH and NaOH [241,242]) and as a carbon precursor for the synthesis of heterogeneous carbon catalysts for biodiesel production [243,244].



Figure 8. Calcination of Ca-containing biowastes [196].

## 7. Reactor Engineering

Biodiesel production by transesterification of vegetable oil with methanol is initially a two-phase liquid-liquid reaction, as the oil and methanol are immiscible. To enhance the mass and heat transport and accelerate the rate of biodiesel production reactions, intensified reactors that can efficiently mix such biphasic liquid-liquid mixtures while ensuring effective heat transfer into the reaction mixture are required. The challenge becomes even more pronounced when solid catalysts are added to this mixture, as the system undergoes a three-phase solid-liquid-liquid reaction, typically with a substantial increase in mass transfer limitations.

The majority of commercial biodiesel production processes are conducted in batch reactors [245,246]. Although such reactors are easily operated and modelled at the laboratory scale for both esterification and transesterification [247], they lack operational flexibility and mass transfer limitations are problematic for viscous and/or multiphase reactions, resulting in a limited operating temperature range and long residence times. There are many advantages to using a solid catalyst (ease of product separation and reuse), but in batch reactors, their use exacerbates mass-transport issues, further extending the reaction times [248]. Interphase transport is an important consideration when designing biodiesel reactors for large-scale operation. Batch operation is also labour-intensive and not cost-effective above a certain scale. The process also generates a considerable amount of wastewater due to the downstream purification processes when the reaction is homogeneously catalysed [245,249]. Typically, industrial batch reactors use residence times of 1–2 h, whereas using NaOH, reactions are complete within 10 min at 60 °C and a methanol:triglyceride molar ratio of 6. Batch reactor two-phase reactions are, hence, often mass-transport-limited at a commercial scale. Long reaction times and the cost of downstream processing have resulted in low production efficiencies [107,110]. Continuous processes are superior to batch processes on a large scale due to economies of scale, which reduces the production costs [250]. It has been reported that biodiesel production could be



significantly improved via the use of continuous reactors [251–253]. Generally, continuous processes are more easily adjusted to market needs [245]. The greatest improvement in biodiesel production on a commercial scale would be to develop a continuous system utilising a heterogeneous catalyst with reduced mass transfer limitations. This would improve the process economics, as continuous processes usually have lower running costs, but also because the load on downstream processing would be reduced by eliminating the need to continually remove and process the homogeneous catalyst.

Recently, a variety of intensification strategies have been examined to eliminate or minimise mass transfer limitations, thereby increasing the reaction rate and reducing the reaction time in biodiesel production processes [247,254]. Intensification techniques that have been investigated include microwave and ultrasonic irradiation [254,255], oscillatory baffled reactors [256], hydrodynamic cavitation [257], microreactors [258,259], co-solvents addition [260], operation under supercritical conditions [261], supercritical simultaneous reaction and extraction [262], and utilising dividing-wall columns [263].

### 7.1. Microreactors

Microreactors are of interest for this reaction as they enhance heat and mass transport by using “microchannels” (<1 mm diameter). At such small scales, diffusion becomes the dominant transport mechanism [263]. The microchannels create flows with large interfacial areas between the immiscible liquid phases, thereby increasing the rates of mass transfer and, therefore, accelerating often mass transfer-limited reactions, such as the “biodiesel reaction”. The intensity of fluid mixing in micro-channel reactors is a function of flow regimes and droplet size, which are governed by the physical properties of the fluid and reactor geometry [264,265]. Due to the laminar flow in microreactors, the flow regimes for immiscible liquids are typically in either slug flow or parallel flow [265]. A “slug flow” pattern can be achieved in T-shaped microreactor feed inlets and consists of drops of an organic phase of uniform size separated by uniform lengths of the polar phase.

In micro-channel reactors consisting of straight capillary channels, fluid mixing is mainly due to convective transport arising from recirculation zones and/or diffusion between two immiscible phases [265,266]. In a slug flow, the mechanism for mass transport involves both convective transport and diffusion. Hence, the intensity of mixing in the plug flow can be enhanced by increased recirculation and large interfacial areas for diffusion. The use of microreactors with zigzag channels significantly enhances the formation of vortices and recirculation [259].

Microreactor technology has been applied to intensify mainly homogeneous base-catalysed biodiesel production [259,267,268]. Up to 99–100% conversion was achieved within seconds (28 s for a zigzag microreactor [259] due to the formation of smaller droplets compared to the conventional T-shaped and Y-shaped flow structures [259,266]) to around 5 min (capillary types) compared to 1–2 h in conventional stirred tank reactors (STRs). Microreactors have shown numerous advantages compared with batch-stirred reactors [269–273]. A comparative study of the key process parameters between the microreactors and conventional batch reactors is presented in Table 16. Microreactors require short residence times to achieve high conversions, which leads to higher productivity and smaller equipment. They have shorter characteristic diffusion lengths and higher surface-to-volume ratios, and consequently, higher heat and mass transfer coefficients as well as improved energy conversion efficiencies. Microreactors also have the potential for small-scale mobile and distributed production rather than large-scale, centralised production. This could lead to reduced storage and transportation costs, as well as processing on- or near-site (a farm, for instance). They also offer a reduction in construction and operating costs due to their small size and can be scaled up using the concept of numbering-up.

Clearly, there are benefits, but the economic drivers are probably insufficient to drive changes in the biodiesel industry. The disadvantages of microreactors should not be underestimated: narrow channels are prone to fouling and blockages, meaning that more effort must be devoted to upstream cleaning, filtration and quality assurance of the feed-

stocks. Their use with heterogeneous catalysts would be extremely challenging. Generally, more research should be conducted in order to develop suitable operating procedures for utilising feedstock with a high FFA content while employing heterogeneous catalysts in microreactors [269,273,274]. Figure 9 shows the schematic of the microreactor system for biodiesel production.

**Table 16.** Biodiesel production in batch and microreactor plants (adapted from [272]).

Characteristics	Batch Plant	Microreactor Plant
Plant volume (tonnes/year)	20,000	20,000
Reactor volume (m <sup>3</sup> )	10	$2.4 \times 10^{-3}$
Plant footprint (m <sup>2</sup> )	149	60
Surface area to volume ratio (m <sup>2</sup> /m <sup>3</sup> )	14.9	$2.5 \times 10^4$
Productivity (kg/h/m <sup>3</sup> )	250	$10.4 \times 10^5$
Energy consumption (kJ/kg)	7.1	0.4
Mass transfer coefficient (s <sup>-1</sup> )	$10^{-2}$ – $10$	$2.86 \times 10^6$
Reynolds Number for mixing	$7 \times 10^5$	10
Capital cost (Rm)	8.6	6.5
Manufacturing costs (R/L)	6.6	5.87

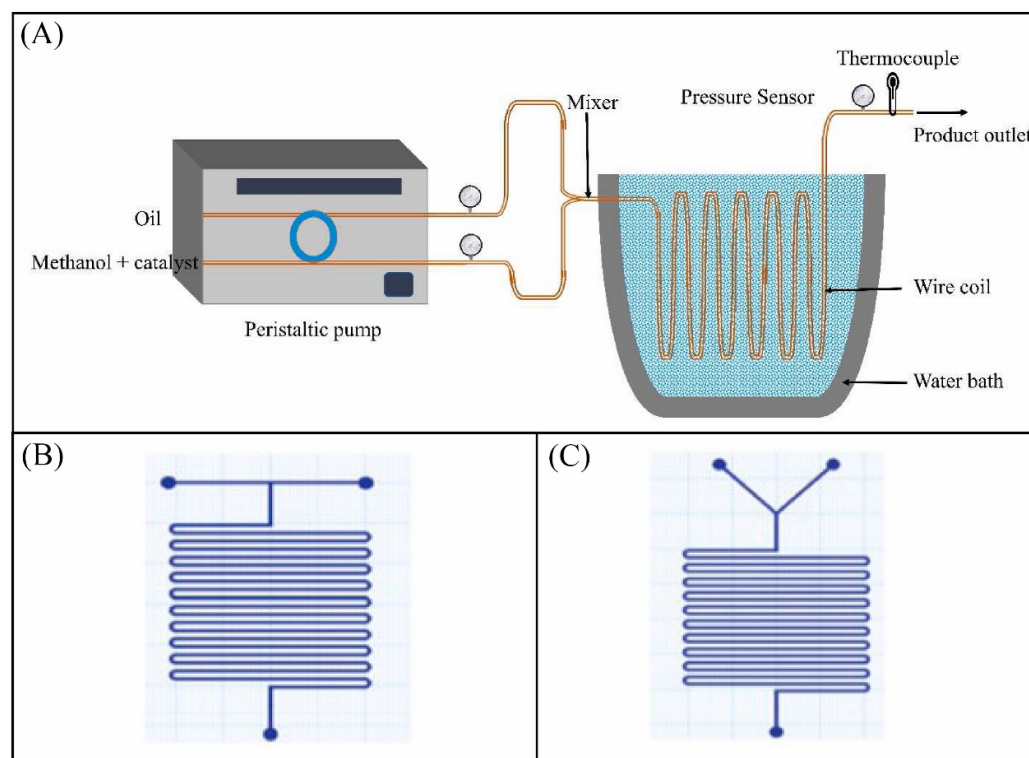


**Figure 9.** (A) Schematic of a micro-channel reactor system for biodiesel production [275], (B) T-shaped and (C) Y-shaped variants [276].

## 7.2. Ultrasonic Reactors

The application of ultrasound, or “sonication”, uses acoustic energy to generate cavitation phenomena necessary for multiphase phase mixing in liquid-liquid reactions. Acoustic reactors use ultrasound in the range of 20–50 kHz [277] to induce the formation and subsequent collapse of bubbles in a process called cavitation. Bubble collapse releases significant amounts of energy in a small volume, resulting in localised extremely high temperatures and pressures, leading to local turbulence and internal circulation [266,277,278], and locally high reaction rates. Fine emulsions can be generated to increase the interfacial area between immiscible liquid phases, such as oil and methanol, in typical biodiesel reactions,



which enhances the reaction rates through improved heat and mass transport. Exposure to ultrasound (“sonication”) can promote both homogeneously or heterogeneously catalysed FFA esterification and triglyceride transesterification in either batch reactors or CSTRs [247,279–283]. Methanol has low solubility in most oils (6–8% at 60 °C), and stirring is usually insufficient to provide a fine emulsion of MeOH-oil [284,285]. Mass transfer between two immiscible phases (e.g., oil and methanol) can be improved by emulsification through ultrasonic irradiation. Emulsification provides a larger surface area for the reaction between the reagents. In addition, a more stable emulsion is generated by sonication, compared to those produced by conventional stirring [286]. Moreover, the reaction rate can be increased as a result of the localised temperature increase occurring by means of cavitation [287]; therefore, less catalyst is required. Thus, ultrasound-assisted processes can provide more than 60% energy savings compared to conventional processes with mechanical stirring [288]. Only a few studies have reported FFA esterification over solid catalysts with ultrasonic irradiation, and it is expected that the microfluidic and ultrasound synergy can significantly improve biodiesel production efficiency when these two technologies are combined for large-scale production (Figure 10). At the same time, the high cost, complexity and design challenges of these technologies on a large scale should not be overlooked.

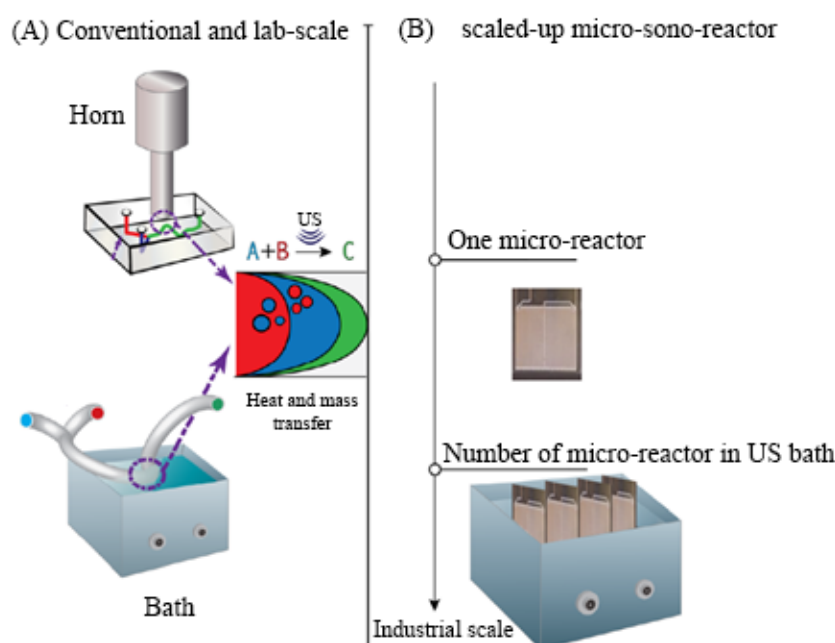


**Figure 10.** (A) Conventional and lab-scale ultrasonic horns and baths to promote chemical reactions, and (B) a scaled-up micro-sonoreactor.

Ultrasonic reactors have been applied to the intensification of homogeneous and transesterification reactions at frequencies of 20–25 kHz. An ultrasonic reactor was used to achieve 98–99% FAME yield in 7–15 min for homogeneously catalysed processes [289–291] or 1–2 h for heterogeneously catalysed reactions [292]. Although ultrasonic reactors are effective for multiphase mixing, such as that required for biodiesel production, they are challenging to scale up [266]. For this reason, the sonicator may be situated externally in a stirred tank, and the reaction mixture flows via an external loop. However, as a whole, this setup is not a fully continuous reactor system.

### 7.3. Rotating Fields

“Spinning” reactors include spinning disc reactors (SDR) and spinning tube reactors (STRs). They intensify reactions by rotating discs or tubes upon which the liquid is dispersed in a thin film. Within this film, reaction/mixing/heat transfer is dominated by diffusion, and the mass and heat transport can be substantially enhanced. SDRs and

STRs have been applied to intensify biodiesel production reactions. FAME yield >98% was achieved after 40 s in an STR for the transesterification of canola oil with methanol at 40–60 °C using a NaOH catalyst [248]. In SDR, about 80% FAME yield was obtained in a few seconds for the transesterification of canola oil (oil:methanol molar ratio of 6, 40 °C, 1000 rpm, and 1 wt% NaOH) [293]. Faster reactions make spinning reactors adaptable to continuous processes in plug flow and with reduced operating costs. As for ultrasound reactions, the challenge for the SDR remains scaling up [294]. There are currently no examples of large-scale SDRs. Solid catalyst particles would be very difficult to handle using this technology; therefore, they would have to be wash-coated onto the disc surface. Figure 11 shows the schematic of the spinning tube, spinning packed bed and spinning disc reactors.

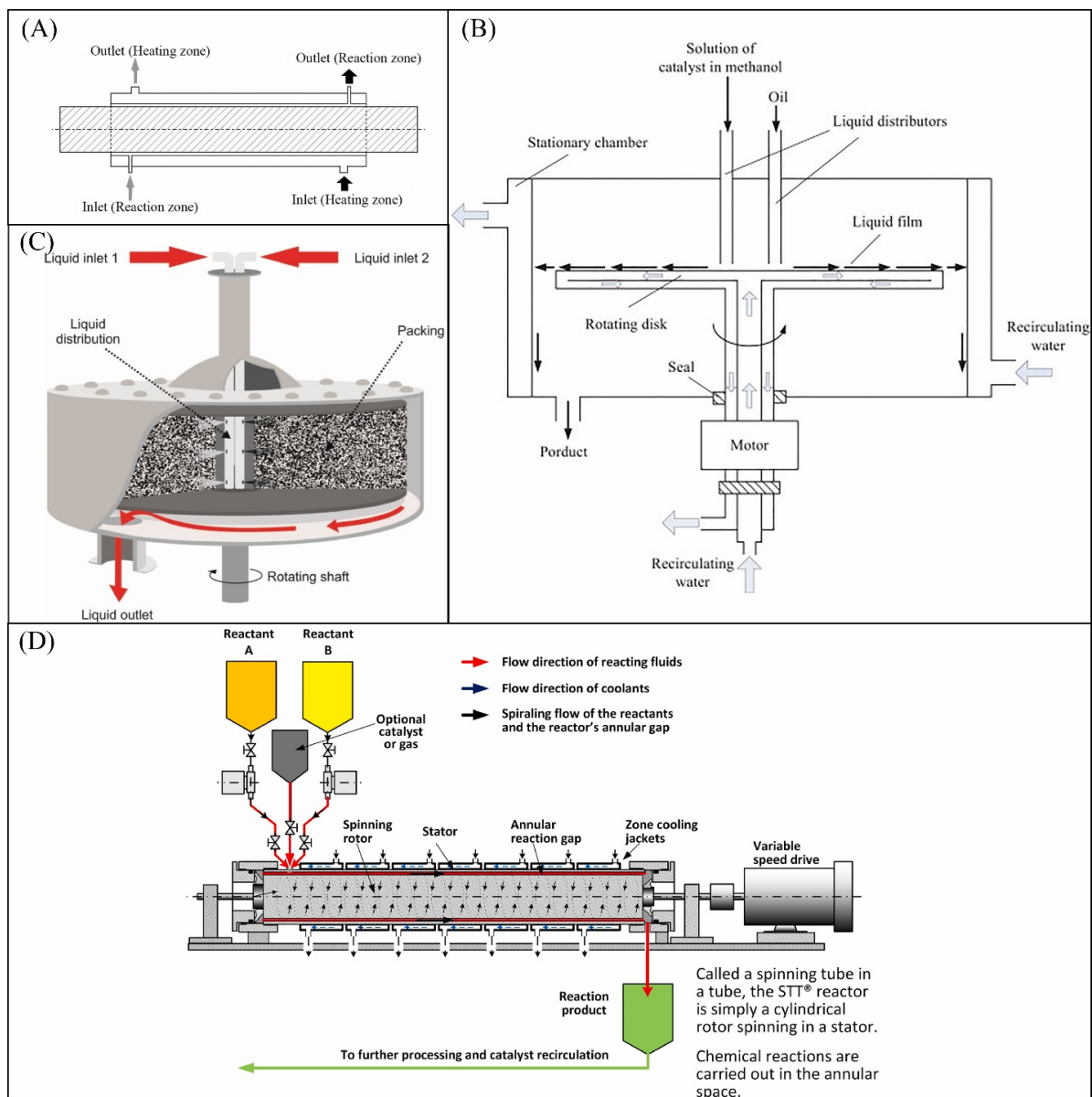


**Figure 11.** Schematic of (A) spinning tube reactor [295], (B) spinning packed bed reactor [296], (C) spinning tube in tube reactor [296], and (D) spinning disc reactor [297].

#### 7.4. Microwave Reactors

Microwave irradiation can be used in reactors to accelerate the rate of chemical reactions by direct transfer of energy into the reactants [298]. This transfer of thermal energy in a microwave reactor involves two mechanisms—dipolar polarisation and ionic conduc-

tion [266]. The use of microwave irradiation for the intensification of biodiesel production reactions has been reported in a number of studies [296,298–301], delivering high FAME yields (95–99%) within 3–5 min. Unlike thermal microreactors, spinning reactors, and ultrasonic reactors, microwaves accelerate reaction rates via efficient and targeted transfer of heat to reactant molecules (and not the reactor vessel), although mechanical stirring is still required to provide mixing. Minimising the reaction times thus necessitates a reactor with multiphase mixing capability coupled with a microwave irradiation unit. An alternative would be to use a tubular plug-flow reactor. Notwithstanding the effectiveness of microwave reactors in intensified processing of biodiesel production, these reactors are challenging to control temperature and reproducibility, bring additional safety issues due to the electrical power demand, and are difficult to scale up [266].

### 7.5. Static Mixers

Static mixers consist of specially designed stationary geometric elements enclosed within a pipe or column [287]. These elements use the energy of the flow stream to create effective radial mixing of the fluids flowing through it. This is also very effective for enhancing the heat transfer. This technology is effective for the dispersion and emulsification of immiscible liquids, such as in biodiesel production. In addition, the energy requirements and operating costs of static mixers are generally low, as they are passive. Static mixers have recently been used for biodiesel processing [287,302,303]. A standalone static mixer with helical mixing elements was reported for the continuous transesterification of canola oil with methanol [287] to produce biodiesel that meets the ASTM D6584 standard [304] for total glycerides (<0.24 wt%) in less than 30 min at a reaction conditions of 6:1 methanol to canola oil molar ratio of 60 °C, 1.5 wt% NaOCH<sub>3</sub>. The study showed that the energy cost associated with mechanical agitation could be greatly reduced. However, the energy cost of the additional pumping requirements required to ensure sufficient superficial flow velocity must be considered [287]. Whether such reactors could be made to work with heterogeneous catalysts is a moot point. This would certainly involve the further development of the catalyst into, e.g., a coating on the elements or in the form of solid beads. This is possible, but other intensified reactors may not require these extra steps in the catalyst formulation (see Section 6). Figure 12 shows a schematic of the experimental setup for the static mixer system.

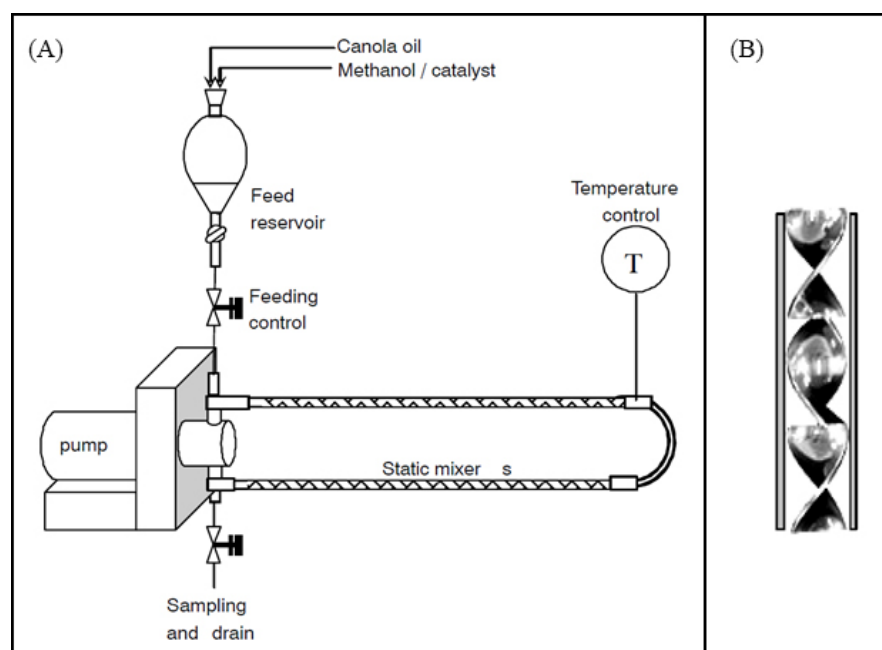


**Figure 12.** Schematic of (A) experimental setup of static mixer system and (B) internal structure of static mixers [287].

### 7.6. Oscillatory Baffled Reactors (OBRs)

An OBR is a continuous reactor consisting of a tube containing equally spaced baffles. Fluid mixing is achieved by imposing an oscillatory motion on the net flow of the fluid. This causes the periodic formation and destruction of toroidal eddies in the baffle cavities [305–309]. This mixing is typically provided by means of diaphragms, bellows or pistons at one end of the tube [308]. The cavities in the baffled tube act like continuous STRs in series, resulting in an approximation of the plug flow. Mixing inside OBRs is finely controlled via oscillatory flow (through amplitude and frequency) and is independent of net flow. This allows reactions of “long” residence times to be performed in oscillatory baffled reactors with a reduced length-to-diameter (L/D) ratio, making them much more compact and practical in size than comparable PFRs, which can be orders of magnitude longer for the same duty.

Applications of OBRs for biodiesel production have been reported at the pilot scale (25 mm diameter, a few litres volume) and mesoscale (typically 4–6 mm diameter) [310–312] with factors of 10–20 reductions in reaction time. The first report [310] of a pilot-scale OBR demonstrated that a reaction with a residence time of ~10 min was possible, resulting in a reduction in reactor size (due to the reduced residence time required and the change from batch to continuous processing) by a factor of over 100. Furthermore, OBR scale up is usually predictable; hence, performance at “mesoscale” usually translates very well to pilot/commercial scale. Phan et al. [313] showed that the residence time in a mesoreactor could be reduced to 5 min or less. In addition, by analysing the reaction scheme, kinetics and judicious choice of operating parameters, they later showed [314] that the reaction time could be reduced to 2 min, and that the base-catalysed reaction could be more tolerant to the presence of water under these conditions. This tolerance was further demonstrated in research by Eze et al. [315]. In addition to these advantages, OBRs can also accommodate solid catalysts of various sizes and shapes by modifying the baffled design, geometry, etc, so as to uniformly suspend solid particles, where necessary. The oscillation conditions required are usually determined by experiments. This was demonstrated in research by Eze et al. [256], in which hexanoic acid was esterified using a suspended  $\text{PrSO}_3\text{H-SBA-15}$  catalyst powder.

In summary, OBRs are an appropriate reaction technology for biodiesel production using homogeneous catalysts; however, they can also, in principle, be used with solid catalysts and perhaps synergistically with other techniques, such as microwaves. Figure 13 shows a schematic of OBRs.

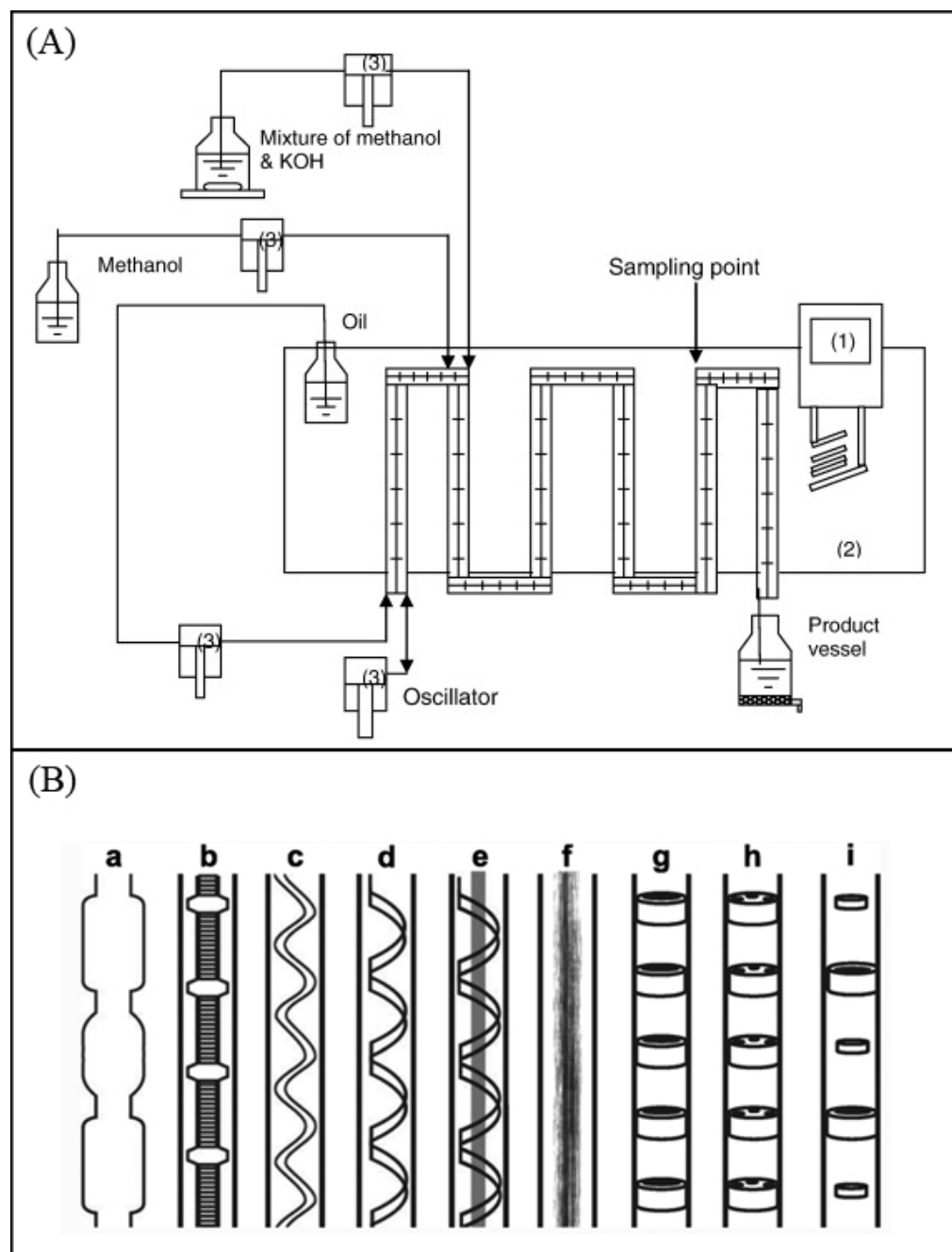


**Figure 13.** Schematic of (A) Oscillatory Baffled Reactor system for continuous biodiesel production [312] and (B) Configurations of oscillatory baffled reactors: (a) integral baffles with periodic constrictions that can be sharp or smooth; (b) central axial baffles; (c) round-edged helical baffles; (d) sharp-edged helical baffles; (e) sharp-edged helical baffles with a central rod; (f) wire-wool baffles; (g) single-orifice baffles; (h) multi-orifice baffles; (i) disc and doughnut baffles [316].

Heterogeneously catalysed biodiesel production involves multiple unit operations (Figure 14) that influence the resulting cetane number, viscosity, and density of the fuel, and hence, its combustion. The cetane number reflects the combustion quality of diesel fuel and is influenced by the FFA composition of the feedstock; longer carbon chains and higher saturation levels favour higher cetane numbers [317]. Viscosity, a fluid's resistance to flow, affects fuel atomisation and combustion and is influenced by the feedstock and the production process. A high viscosity results in poor fuel atomisation and incomplete combustion [318]. Biodiesel density determines its energy content and combustion char-

acteristics, with higher densities being preferred, provided that the engine performance is maintained [319]. Different oil feedstocks have diverse FFA compositions, which affect their cetane number, viscosity, and density [317]. Biodiesel produced from canola and safflower offers higher cetane numbers and lower viscosities compared to those produced from soybean and sunflower oils. Post-production purification, notably washing and drying, also affects biodiesel viscosity and density by removing impurities and residual catalysts; hence, these unit operations must also be optimised to achieve the desired fuel [12]. Özer et al. [320] examined how mixtures of diesel fuel with tall oil, ethanol, methanol, isopropyl alcohol, n-butanol, and fuel oil affected key performance metrics and emission characteristics. Such blended fuels significantly reduce CO and hydrocarbon emissions compared to conventional diesel, particularly at higher engine loads, but are accompanied by an increase in nitrogen oxide emissions.

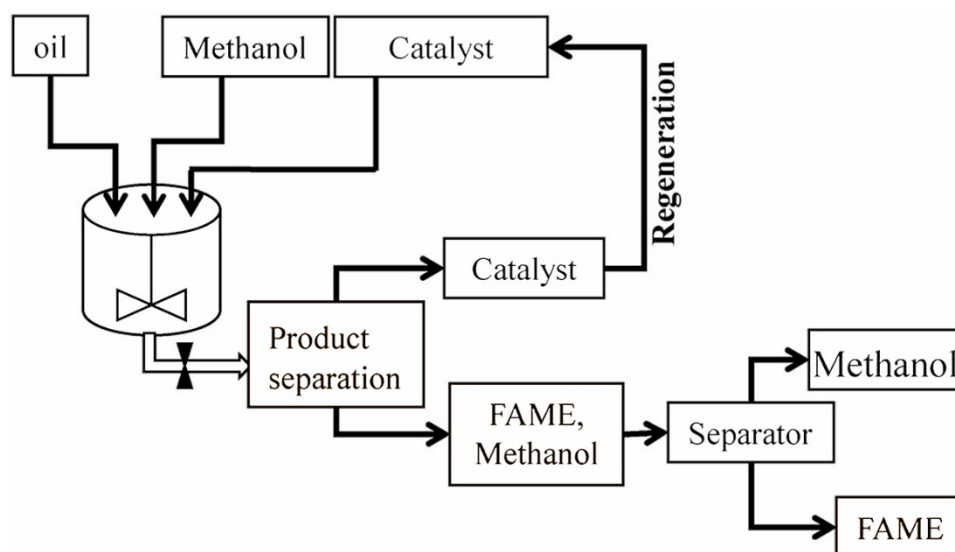


**Figure 14.** Stages of heterogeneously catalysed biodiesel production.

## 8. Chemical and Physical Properties of Biodiesel

Biodiesel derived from the transesterification of vegetable oils or animal fats must meet specific physicochemical properties to ensure its effectiveness and compatibility with diesel engines and adherence to international quality standards, notably viscosity, density, flash point, cold flow characteristics, acid number, cetane number, and stability. Researchers and producers can enhance the quality and performance of biodiesel production.

### 8.1. Viscosity

Viscosity affects the atomisation and combustion of biodiesel in the engine. Biodiesel generally has a higher viscosity compared to petroleum diesel, which hinders fuel injection and combustion efficiency. A high viscosity can lead to injector clogging and poor engine performance. Biodiesel is, therefore, often blended with petroleum diesel or adjusted through transesterification to achieve a viscosity range compatible with engine specifications. Biodiesel viscosity typically ranges from  $4.5$  to  $5.5 \text{ mm}^2 \cdot \text{s}^{-1}$  at  $40 \text{ }^\circ\text{C}$ . For instance, biodiesel derived from *Jatropha curcas* oil was reported to have a viscosity of  $4.8 \text{ mm}^2/\text{s}$ , compared to  $2.5 \text{ mm}^2 \cdot \text{s}^{-1}$  for standard petroleum diesel [321].

### 8.2. Density

Density influences the energy content of biodiesel and its compatibility with existing fuel systems. Biodiesel typically has a higher density than petroleum diesel, which can affect the fuel consumption and engine calibration. Accurate density measurements are crucial for ensuring that biodiesel meets the standard specifications and performs reliably



under various engine conditions. Biodiesel densities range between 860 and 880 kg·m<sup>-3</sup> at 15 °C [322].

### 8.3. Flash Point

The flash point of biodiesel is the temperature at which the vapour pressure of hydrocarbons is sufficient for combustion in the presence of an ignition source; hence, it is an important safety consideration. Biodiesel generally has a higher flash point than petroleum diesel, which can improve the safety during handling and storage. However, extremely high flash points may also affect the ease of ignition during cold weather. Ensuring that the flash point of biodiesel falls within the recommended range is essential for a safe and efficient engine operation. The flash points for biodiesel blends span 150–170 °C [323].

### 8.4. Cold Flow Properties

Cold flow properties, including the pour point and cloud point, determine the biodiesel performance at low temperatures. Biodiesel tends to have higher pour points compared to petroleum diesel, which can lead to gelling or cloud formation in cold weather. To mitigate these issues, biodiesel can be blended with petroleum diesel or treated with additives to enhance its low-temperature performance. Appropriate cold flow characteristics are critical for ensuring reliable engine operation over a range of temperatures. Pour points for biodiesel with additives range from −10 °C to −15 °C. Cloud points for biodiesel blends span from −8 °C to −12 °C [324,325].

### 8.5. Acid Number

The acid number of biodiesel reflects the amount of FFAs present, which impacts the fuel stability and corrosiveness. A high acid number indicates the potential for increased degradation and corrosion of the fuel systems. Monitoring and controlling the acid number through proper production processes and quality control measures are vital for maintaining the longevity and performance of biodiesel. The acid number of high-quality biodiesel is typically <0.5 mg KOH·g<sup>-1</sup> (indicative of a low FFA content) [326,327].

### 8.6. Cetane Number

The cetane number is a measure of the biodiesel's ignition quality, indicating how readily the fuel ignites under compression in the engine. A higher cetane number generally leads to a smoother engine operation, reduced ignition delay, and improved combustion efficiency. Biodiesel typically has a higher cetane number compared to petroleum diesel, which can be beneficial for engine performance. However, the cetane number should be monitored to ensure that it is within the optimal range for a specific engine type to avoid potential starting issues or excessive combustion noise. Cetane numbers for biodiesel from various feedstocks have ranged from 52 to 58, compared to 45–66 for conventional diesel prepared from edible plant oils [328–330].

### 8.7. Stability

Oxidative stability is another crucial property, as it affects the shelf life and performance of biodiesel. Biodiesel is prone to oxidation, which can lead to the formation of peroxides and acids, impacting fuel quality. Antioxidants are often added to enhance stability and prevent degradation during storage. Oxidative stability, measured using the Rancimat test, has been found to range from 6 to 12 h, depending on the biodiesel source and antioxidant content [331–335].

### 8.8. Compliance with Standards

To ensure that biodiesel meets the required quality specifications, it must comply with established standards, such as ASTM D6751 [336] (for biodiesel) and EN 14214 [52] (for European biodiesel). Adherence to these standards ensures that biodiesel has the necessary properties for reliable engine performance and safety. All tested biodiesel samples in recent



studies have met the ASTM D6751 and EN 14214 [52] specifications for key properties, including viscosity, density, and cetane number [337].

## 9. Conclusions and Future Research Focus

FAME-based biodiesel still has an important role to play in the energy mix and in helping hard-to-abate transportation sectors achieve net-zero. While the electrification of passenger vehicles is expanding rapidly, with projections to phase out the sale of new combustion engine cars in the EU by 2035 [338], mandates for biodiesel use as a transportation fuel still exist in oilseed-producing countries, including Brazil and Malaysia. Plans exist to progressively increase usage to 20% and 30% blends by 2030 [339,340], and even higher for heavy-duty vehicles, which are unlikely to be suitable for electrification. FAME is particularly suited for use in marine engines, where blends as high as 30–50% are being advocated for ship operators [341], providing that demand can be met in a sustainable manner. The refocusing of biodiesel on heavy-duty vehicles avoids concerns over engine wear, which is typically problematic for high-performance diesel vehicles [251], meaning that longer chain ( $>C_{18}$ ) FAMEs will also be suitable. Meeting this growing energy demand will necessitate improvements in the technology currently employed for FAME production from oilseed crops and a transition away from the traditional homogeneously catalysed routes. The use of soluble catalysts necessitates multiple neutralisation and washing steps to purify biodiesel, leading to significant wastewater treatment costs, with 1 L of wastewater produced for every litre of fuel. A suitable catalyst and reactor system are necessary to lower the cost of biodiesel production [342]. The advances in catalyst systems and process intensification discussed in this review offer important progress towards next-generation biodiesel production systems. These will provide medium- to long-term solutions to the continuous displacement of hard-to-abate fossil fuels in the transportation sector, while helping to mitigate pollution and CO<sub>2</sub> emissions to help meet net-zero targets.

The development of more efficient and stable heterogeneous catalysts for biodiesel synthesis via transesterification and esterification is currently underway. Solid bases, including alkali earth metal oxides, alkali-doped metal oxides, hydrotalcite, and basic zeolites, are reported for transesterification of high-purity oils, whereas solid acids, including zeolites, doped metal oxides, sulfonated carbons, and heteropoly acids are more applicable for esterification pre-treatments of high fatty acid-containing oils and higher temperature transesterification to FAME. However, the development of a heterogeneously catalysed process requires a better understanding of the structure-reactivity relationships and improved mass transport to enhance productivity. Methods to design pore networks or the use of scaffolds with interconnected macro- and mesoporous channels can significantly enhance reaction rates by improving the in-pore diffusional properties, and is an area for further development [343]. Furthermore, controlling the surface hydrophobicity is critical for esterification reactions where FAME production is limited by reaction equilibria, with reactively formed water or water contained in waste oils hindering the reaction via hydrolysis of FAME. In this instance, the development of catalytic porous materials co-functionalised with surface alkyl groups to tune hydrophobicity offers a promising solution [344]. Reactive distillation is another process-driven approach for converting oils with high FFA levels using a catalytically functionalised distillation column that simultaneously forms and separates products, thereby avoiding equilibrium-limited conversion [345]. However, reactive distillation is only practical if the reaction temperatures and pressures are compatible with those required for distillation, but for the right systems, it can avoid the need for excess alcohol and enable reactions with shorter residence times compared to flow reactors [345]. Alternatively, pretreatment of low-grade high fatty acid-containing oils may be possible by dual-bed continual flow processes using sequential solid-acid and base packed beds for esterification and transesterification [346]. The development of fatty acid-tolerant mixed oxides for simultaneous transesterification and esterification has also been reported, but often involves elevated temperatures ( $>170$  °C) [347,348]. The design of catalysts for simultaneous esterification and transesterification under mild conditions is challenging

but may be possible with superacids [349]. Other options for solid-acid catalysed routes may involve the hydrolysis of TAGs and subsequent esterification of FFAs to FAME [350]. More recently, nanoengineering of hierarchically macro-mesoporous materials led to the discovery of spatially orthogonal acid-base catalysts for FAME production from high FFA-containing oils [121], where acid-functionalised macropores direct the rapid esterification of FFA protecting poisoning of solid base-functionalised mesopores responsible for rapid TAG transesterification. The choice of the catalyst and process will ultimately depend on the available reactor technology and the cost and elemental sustainability of the catalyst, which will be inextricably coupled with the oil composition. Waste or low-grade oils [351] present challenges associated with impurities, which may require improved purification technology [352] or the design of catalysts tolerant to these components.

The design of innovative chemical reactors to facilitate continuous processing of viscous bio-oils is expected to have the greatest impact on the commercial exploitation of heterogeneous catalysts for biodiesel production. Many industrial biodiesel plants still operate in batch mode at a significant scale ( $\sim 7000$  tonnes year<sup>-1</sup>) [353] but are hampered by separation issues of homogeneous catalysts and drawbacks of batch mode (notably increased capital investment required to run at large volumes and increased labour costs of a start/stop process) [354]. A transition towards heterogeneously catalysed, continuous flow reactors would simplify separation and increase the scale of operation (8000–125,000 tonnes year<sup>-1</sup>) [353]. Process optimisation with new reactor geometries will require tailored design of catalyst architectures to suit the mixing capability of alternative reactors, with molecular simulation necessary to take advantage of innovative reactor designs. This review has presented emerging reactor technologies and intensive processing approaches, such as micro-channel reactors, ultrasound-enhanced reactors, rotating beds, microwave reactors, and oscillatory flow reactors, which offer smaller footprints for the more distributed or on-demand production of biodiesel. However, it is essential that technical advances in both materials chemistry and reactor engineering be pursued if biodiesel is to remain a key player in the renewable energy sector during the 21st century. In this regard the 3D printing or micro-chemical reactors/plant is a unique approach to optimise process operations [355].

For slow reactions like FAME synthesis from FFA and TAG (trans)esterification, conventional flow-packed bed flow reactors are not ideal, as long residence times are required, which leads to large footprints and challenges associated with poor mixing at slow flow rates. When considering alternative reactor technologies, powder or particulate heterogeneous catalysts can be readily adopted in ultrasonic, microwave and OBRs; however, other designs, such as spinning tubes or disc reactors, would require further steps in catalyst development, particularly wash coating. The application of OBRs has been proven at the laboratory scale with heterogeneous catalysts and is readily scalable, offering promise for commercial processes. OBRs can also be used with microwaves [356], and although this has been successfully demonstrated for the continuous microwave OBRs production of metal organic frameworks (MOFs), it should be transferrable to biodiesel processing. OBRs are particularly attractive for biodiesel synthesis as the oscillating fluid experiences efficient vortical mixing and plug flow as it passes through the orifice plate baffles [357]. By decoupling the fluid flow and mixing, long reaction times are feasible, with uniform suspensions of porous catalysts entrained under oscillatory flow [256], with reactors readily applied on an industrial scale. This review also outlines the challenges associated with the phase equilibria during biodiesel synthesis and the necessity for efficient separation processes. Long-chain TAG and FFA are poorly miscible with methanol, while the FAME product is miscible, which can lead to poor mass transport and challenges to recover and purify the product mixture, which contains unreacted oil, methanol, glycerol and biodiesel [313]. While the use of co-solvents (e.g., FAME to improve TAG solubility) and OBRs can help improve mixing and overcome miscibility problems, the use of catalytic membrane reactors offers an attractive solution for product separation. The use of a semi-permeable catalytic material to construct the reactor wall allows diffusion of the reactively formed

FAME/glycerol through the barrier, while the unreacted TAG/FFA/MeOH emulsion is retained in the reactor zone for further conversion [358,359].

In summary, biodiesel is a readily implemented renewable and biodegradable fuel that can displace fossil fuel use in hard-to-abate heavy-duty transportation, agricultural vehicles and marine sectors, and still has an important role to play in the energy mix and achieving net-zero. Alternative reactor technologies and process intensification are clearly critical to improve the sustainability of biodiesel synthesis and facilitate distributed biodiesel production in remote areas. However, with the current drive for the use of plant oils to produce first-generation sustainable aviation fuel from hydrotreated esters and fatty acids (HEFA), there will be significant competition for raw feedstock [360]. Technoeconomic and socioeconomic analyses of emerging processes will be essential to avoid the negative impacts of land use changes or increased food prices in agricultural countries and ensure the sustainability of any process [361].

**Author Contributions:** Conceptualisation, A.L. and A.F.L.; writing—original draft preparation, A.L., A.P.H., A.N.P., M.B., K.W. and A.F.L.; writing—review and editing, A.L. and A.F.L.; funding acquisition, K.W. and A.F.L. All authors have read and agreed to the published version of the manuscript.

**Funding:** This research was funded by the Australian Research Council grant numbers DP200100204, DP200100313 and LP190100849, and Australian Government grant number CRCPEIGHT000194.

**Data Availability Statement:** No new data were created or analyzed in this study. Data sharing is not applicable to this article.

**Conflicts of Interest:** The authors declare no conflicts of interest.

## References

1. Pérez-Almada, D.; Galán-Martín, Á.; Contreras, M.d.M.; Castro, E. Integrated techno-economic and environmental assessment of biorefineries: Review and future research directions. *Sustain. Energy Fuels* **2023**, *7*, 4031–4050. [[CrossRef](#)]
2. Jeswani, H.K.; Chilvers, A.; Azapagic, A. Environmental sustainability of biofuels: A review. *Proc. R. Soc. A* **2020**, *476*, 20200351. [[CrossRef](#)] [[PubMed](#)]
3. Ubando, A.T.; Felix, C.B.; Chen, W.-H. Biorefineries in circular bioeconomy: A comprehensive review. *Bioresour. Technol.* **2020**, *299*, 122585. [[CrossRef](#)]
4. Wilson, K.; Lee, A.F. Catalyst design for biorefining. *Philos. Trans. R. Soc. A Math. Phys. Eng. Sci.* **2016**, *374*, 20150081. [[CrossRef](#)]
5. Abbas, A.; Cross, M.; Duan, X.; Jeschke, S.; Konarova, M.; Huber, G.W.; Lee, A.F.; Lovell, E.C.; Lim, J.Y.C.; Polyzos, A.; et al. Catalysis at the intersection of sustainable chemistry and a circular economy. *One Earth* **2024**, *7*, 738–741. [[CrossRef](#)]
6. Atabani, A.E.; Silitonga, A.S.; Badruddin, I.A.; Mahlia, T.M.I.; Masjuki, H.H.; Mekhilef, S. A comprehensive review on biodiesel as an alternative energy resource and its characteristics. *Renew. Sustain. Energy Rev.* **2012**, *16*, 2070–2093. [[CrossRef](#)]
7. Bastan, F.; Kazemeini, M.; Larimi, A.S. Aqueous-phase reforming of glycerol for production of alkanes over Ni/Ce<sub>x</sub>Zr<sub>1-x</sub>O<sub>2</sub> nano-catalyst: Effects of the support's composition. *Renew. Energy* **2017**, *108*, 417–424. [[CrossRef](#)]
8. Larimi, A.; Khorasheh, F. Renewable hydrogen production by ethylene glycol steam reforming over Al<sub>2</sub>O<sub>3</sub> supported Ni-Pt bimetallic nano-catalysts. *Renew. Energy* **2018**, *128*, 188–199. [[CrossRef](#)]
9. Atadashi, I.M.; Aroua, M.K.; Aziz, A.A. Biodiesel separation and purification: A review. *Renew. Energy* **2011**, *36*, 437–443. [[CrossRef](#)]
10. Fayyazi, E.; Ghobadian, B.; Van De Bovenkamp, H.H.; Najafi, G.; Hosseinzadehsamani, B.; Heeres, H.J.; Yue, J. Optimization of Biodiesel Production over Chicken Eggshell-Derived CaO Catalyst in a Continuous Centrifugal Contactor Separator. *Ind. Eng. Chem. Res.* **2018**, *57*, 12742–12755. [[CrossRef](#)]
11. Maleki, H.; Kazemeini, M.; Larimi, A.S.; Khorasheh, F. Transesterification of canola oil and methanol by lithium impregnated CaO-La<sub>2</sub>O<sub>3</sub> mixed oxide for biodiesel synthesis. *J. Ind. Eng. Chem.* **2017**, *47*, 399–404. [[CrossRef](#)]
12. Yaşar, F. Comparison of fuel properties of biodiesel fuels produced from different oils to determine the most suitable feedstock type. *Fuel* **2020**, *264*, 116817. [[CrossRef](#)]
13. Atadashi, I.M.; Aroua, M.K.; Aziz, A.A. High quality biodiesel and its diesel engine application: A review. *Renew. Sustain. Energy Rev.* **2010**, *14*, 1999–2008. [[CrossRef](#)]
14. Salvi, B.L.; Panwar, N.L. Biodiesel resources and production technologies—A review. *Renew. Sustain. Energy Rev.* **2012**, *16*, 3680–3689. [[CrossRef](#)]
15. Zhang, Y.; Dubé, M.A.; McLean, D.D.; Kates, M. Biodiesel production from waste cooking oil: 1. Process design and technological assessment. *Bioresour. Technol.* **2003**, *89*, 1–16. [[CrossRef](#)] [[PubMed](#)]
16. Basso, R.C.; Meirelles, A.J.D.A.; Batista, E.A.C. Experimental data, thermodynamic modeling and sensitivity analyses for the purification steps of ethyl biodiesel from fodder radish oil production. *Braz. J. Chem. Eng.* **2017**, *34*, 341–353. [[CrossRef](#)]

17. Rostami, M.; Raeissi, S.; Mahmoodi, M.; Nowroozi, M. Liquid–Liquid Equilibria in Biodiesel Production. *J. Am. Oil Chem. Soc.* **2013**, *90*, 147–154. [CrossRef]
18. Narasimharao, K.; Lee, A.; Wilson, K. Catalysts in Production of Biodiesel: A Review. *J. Biobased Mater. Bioenergy* **2007**, *1*, 19–30. [CrossRef]
19. Salam, K.A.; Velasquez-Orta, S.B.; Harvey, A.P. A sustainable integrated in situ transesterification of microalgae for biodiesel production and associated co-product—a review. *Renew. Sustain. Energy Rev.* **2016**, *65*, 1179–1198. [CrossRef]
20. Tomasevic, A.V.; Siler-Marinkovic, S.S. Methanolysis of used frying oil. *Fuel Process. Technol.* **2003**, *81*, 1–6. [CrossRef]
21. Wang, Y.; Ou, S.; Liu, P.; Zhang, Z. Preparation of biodiesel from waste cooking oil via two-step catalyzed process. *Energy Convers. Manag.* **2007**, *48*, 184–188. [CrossRef]
22. Zhang, Y.; Dubé, M.A.; McLean, D.D.; Kates, M. Biodiesel production from waste cooking oil: 2. Economic assessment and sensitivity analysis. *Bioresour. Technol.* **2003**, *90*, 229–240. [CrossRef] [PubMed]
23. Chisti, Y. Biodiesel from microalgae. *Biotechnol. Adv.* **2007**, *25*, 294–306. [CrossRef] [PubMed]
24. Kulkarni, M.G.; Dalai, A.K.; Bakhshi, N.N. Transesterification of canola oil in mixed methanol/ethanol system and use of esters as lubricity additive. *Bioresour. Technol.* **2007**, *98*, 2027–2033. [CrossRef] [PubMed]
25. Meher, L.C.; Dharmagadda, V.S.S.; Naik, S.N. Optimization of alkali-catalyzed transesterification of *Pongamia pinnata* oil for production of biodiesel. *Bioresour. Technol.* **2006**, *97*, 1392–1397. [CrossRef]
26. Kumar Tiwari, A.; Kumar, A.; Raheman, H. Biodiesel production from jatropha oil (*Jatropha curcas*) with high free fatty acids: An optimized process. *Biomass Bioenergy* **2007**, *31*, 569–575. [CrossRef]
27. Bošnjaković, M.; Sinaga, N. The Perspective of Large-Scale Production of Algae Biodiesel. *Appl. Sci.* **2020**, *10*, 8181. [CrossRef]
28. USDA National Agricultural Statistics Service. General Economic Reports. Available online: [https://www.nass.usda.gov/Statistics\\_by\\_Subject/index.php?sector=CROPS](https://www.nass.usda.gov/Statistics_by_Subject/index.php?sector=CROPS) (accessed on 12 August 2024).
29. USDA Foreign Agricultural Service. Oilseeds: World Markets and Trade. Available online: <https://www.fas.usda.gov/data/oilseeds-world-markets-and-trade> (accessed on 12 August 2024).
30. USDA Economic Research Service. Oil Crops Yearbook. Available online: <https://www.ers.usda.gov/data-products/oil-crops-yearbook/> (accessed on 14 August 2024).
31. U.S. Department of Energy Alternative Fuels Data Center. Alternative Fuel Price. Available online: <https://afdc.energy.gov/fuels/prices.html> (accessed on 11 August 2024).
32. USDA Foreign Agricultural Service. Available online: <https://www.fas.usda.gov/data> (accessed on 12 August 2024).
33. Choe, E.; Min, D.B. Chemistry of Deep-Fat Frying Oils. *J. Food Sci.* **2007**, *72*, R77–R86. [CrossRef]
34. Kalogianni, E.P.; Karapantsios, T.D.; Miller, R. Effect of repeated frying on the viscosity, density and dynamic interfacial tension of palm and olive oil. *J. Food Eng.* **2011**, *105*, 169–179. [CrossRef]
35. Ruiz-Méndez, M.V.; Marmesat, S.; Liotta, A.; Dobarganes, M.C. Analysis of used frying fats for biodiesel production. *Grasas Aceites* **2008**, *59*, 45–50. [CrossRef]
36. Leung, D.Y.C.; Wu, X.; Leung, M.K.H. A review on biodiesel production using catalyzed transesterification. *Appl. Energy* **2010**, *87*, 1083–1095. [CrossRef]
37. Sendzikiene, E.; Makareviciene, V.; Janulis, P.; Kitrys, S. Kinetics of free fatty acids esterification with methanol in the production of biodiesel fuel. *Eur. J. Lipid Sci. Technol.* **2004**, *106*, 831–836. [CrossRef]
38. Carmo, A.C.; De Souza, L.K.C.; Da Costa, C.E.F.; Longo, E.; Zamian, J.R.; Da Rocha Filho, G.N. Production of biodiesel by esterification of palmitic acid over mesoporous aluminosilicate Al-MCM-41. *Fuel* **2009**, *88*, 461–468. [CrossRef]
39. Srilatha, K.; Lingaiah, N.; Devi, B.L.A.P.; Prasad, R.B.N.; Venkateswar, S.; Prasad, P.S.S. Esterification of free fatty acids for biodiesel production over heteropoly tungstate supported on niobia catalysts. *Appl. Catal. A Gen.* **2009**, *365*, 28–33. [CrossRef]
40. Do Nascimento, L.A.S.; Angélica, R.S.; Da Costa, C.E.F.; Zamian, J.R.; Da Rocha Filho, G.N. Comparative study between catalysts for esterification prepared from kaolins. *Appl. Clay Sci.* **2011**, *51*, 267–273. [CrossRef]
41. Wongjaikham, W.; Wongsawaeng, D.; Ratnitsai, V.; Kamjam, M.; Ngaosuwan, K.; Kiatkittipong, W.; Hosemann, P.; Assabumrungrat, S. Low-cost alternative biodiesel production apparatus based on household food blender for continuous biodiesel production for small communities. *Sci. Rep.* **2021**, *11*, 13827. [CrossRef] [PubMed]
42. Abdulkareem-Alsultan, G.; Asikin-Mijan, N.; Mansir, N.; Lee, H.V.; Zainal, Z.; Islam, A.; Taufiq-Yap, Y.H. Pyro-lytic deoxygenation of waste cooking oil for green diesel production over Ag<sub>2</sub>O<sub>3</sub>-La<sub>2</sub>O<sub>3</sub>/AC nano-catalyst. *J. Anal. Appl. Pyrolysis* **2019**, *137*, 171–184. [CrossRef]
43. Sarve, A.N.; Varma, M.N.; Sonawane, S.S. Ultrasound assisted two-stage biodiesel synthesis from non-edible *Schleichera triguga* oil using heterogeneous catalyst: Kinetics and thermodynamic analysis. *Ultrason. Sonochem.* **2016**, *29*, 288–298. [CrossRef]
44. Bayat, A.; Baghdadi, M.; Bidhendi, G.N. Tailored magnetic nano-alumina as an efficient catalyst for transesterification of waste cooking oil: Optimization of biodiesel production using response surface methodology. *Energy Convers. Manag.* **2018**, *177*, 395–405. [CrossRef]
45. Roy, T.; Sahani, S.; Chandra Sharma, Y. Study on kinetics-thermodynamics and environmental parameter of biodiesel production from waste cooking oil and castor oil using potassium modified ceria oxide catalyst. *J. Clean. Prod.* **2020**, *247*, 119166. [CrossRef]
46. Nautiyal, P.; Subramanian, K.A.; Dastidar, M.G. Kinetic and thermodynamic studies on biodiesel production from *Spirulina platensis* algae biomass using single stage extraction–transesterification process. *Fuel* **2014**, *135*, 228–234. [CrossRef]



47. Wu, L.; Wei, T.; Lin, Z.; Zou, Y.; Tong, Z.; Sun, J. Bentonite-enhanced biodiesel production by NaOH-catalyzed transesterification: Process optimization and kinetics and thermodynamic analysis. *Fuel* **2016**, *182*, 920–927. [[CrossRef](#)]
48. Encinar, J.M.; Pardal, A.; Sánchez, N. An improvement to the transesterification process by the use of co-solvents to produce biodiesel. *Fuel* **2016**, *166*, 51–58. [[CrossRef](#)]
49. Deshmane, V.G.; Adewuyi, Y.G. Synthesis and kinetics of biodiesel formation via calcium methoxide base catalyzed transesterification reaction in the absence and presence of ultrasound. *Fuel* **2013**, *107*, 474–482. [[CrossRef](#)]
50. Sun, C.; Hu, Y.; Sun, F.; Sun, Y.; Song, G.; Chang, H.; Lunprom, S. Comparison of biodiesel production using a novel porous Zn/Al/Co complex oxide prepared from different methods: Physicochemical properties, reaction kinetic and thermodynamic studies. *Renew. Energy* **2022**, *181*, 1419–1430. [[CrossRef](#)]
51. Franca, B.; Villardi, H.; Esteves, T.; Uller, A.M.C.; Pessoa, F.L. Phase equilibrium and emulsion stability on ethyl biodiesel production. *Chem. Eng. Trans.* **2011**, *24*, 745–750.
52. EN 14214; Automotive Fuels—Fatty Acid Methyl Esters (FAME) for Diesel Engines—Requirements and Test Methods. European Committee for Standardization: Brussels, Belgium, 2008.
53. Gonçalves, J.D.; Aznar, M.; Santos, G.R. Liquid–liquid equilibrium data for systems containing Brazil nut biodiesel+methanol+glycerin at 303.15 K and 323.15 K. *Fuel* **2014**, *133*, 292–298. [[CrossRef](#)]
54. Oliveira, M.B.; Varanda, F.R.; Marrucho, I.M.; Queimada, A.J.; Coutinho, J.A.P. Prediction of Water Solubility in Biodiesel with the CPA Equation of State. *Ind. Eng. Chem. Res.* **2008**, *47*, 4278–4285. [[CrossRef](#)]
55. Michelsen, M.L.; Hendriks, E.M. Physical properties from association models. *Fluid Phase Equilib.* **2001**, *180*, 165–174. [[CrossRef](#)]
56. Negi, D.S.; Sobotka, F.; Kimmel, T.; Wozny, G.; Schomäcker, R. Liquid–Liquid Phase Equilibrium in Glycerol–Methanol–Methyl Oleate and Glycerol–Monoolein–Methyl Oleate Ternary Systems. *Ind. Eng. Chem. Res.* **2006**, *45*, 3693–3696. [[CrossRef](#)]
57. Ardila, Y.C.; Pinto, G.M.F.; Machado, A.B.; Wolf Maciel, M.R. Experimental Determination of Binodal Curves and Study of the Temperature in Systems Involved in the Production of Biodiesel with Ethanol. *J. Chem. Eng. Data* **2010**, *55*, 4592–4596. [[CrossRef](#)]
58. Bell, J.C.; Messerly, R.A.; Gee, R.; Harrison, A.; Rowley, R.L.; Wilding, W.V. Ternary Liquid–Liquid Equilibrium of Biodiesel Compounds for Systems Consisting of a Methyl Ester + Glycerin + Water. *J. Chem. Eng. Data* **2013**, *58*, 1001–1004. [[CrossRef](#)]
59. Mazutti, M.A.; Voll, F.A.P.; Cardozo-Filho, L.; Corazza, M.L.; Lanza, M.; Priamo, W.L.; Oliveira, J.V. Thermophysical properties of biodiesel and related systems: (Liquid + liquid) equilibrium data for soybean biodiesel. *J. Chem. Thermodyn.* **2013**, *58*, 83–94. [[CrossRef](#)]
60. Santos, T.; Gomes, J.F.; Puna, J. Liquid-liquid equilibrium for ternary system containing biodiesel, methanol and water. *J. Environ. Chem. Eng.* **2018**, *6*, 984–990. [[CrossRef](#)]
61. Filho, J.C.G.; Bispo, F.B.; Corazza, M.L.; Arce, P.F.; Voll, F.A.P.; de Gusmão Coêlho, D.; Ferreira-Pinto, L.; de Carvalho, S.H.V.; Soletti, J.I. Liquid–Liquid Equilibrium Measurement and Thermodynamic Modeling of the {*Sterculia striata* Biodiesel + Glycerol + Ethanol} System. *J. Chem. Eng. Data* **2021**, *66*, 3293–3299. [[CrossRef](#)]
62. Lee, M.-J.; Lo, Y.-C.; Lin, H.-M. Liquid–liquid equilibria for mixtures containing water, methanol, fatty acid methyl esters, and glycerol. *Fluid Phase Equilib.* **2010**, *299*, 180–190. [[CrossRef](#)]
63. Andreatta, A.E.; Casás, L.M.; Hegel, P.; Bottini, S.B.; Brignole, E.A. Phase Equilibria in Ternary Mixtures of Methyl Oleate, Glycerol, and Methanol. *Ind. Eng. Chem. Res.* **2008**, *47*, 5157–5164. [[CrossRef](#)]
64. Do Carmo, F.R.; Evangelista, N.S.; De Santiago-Aguiar, R.S.; Fernandes, F.A.N.; De Sant’Ana, H.B. Evaluation of optimal activity coefficient models for modeling and simulation of liquid–liquid equilibrium of biodiesel+glycerol+alcohol systems. *Fuel* **2014**, *125*, 57–65. [[CrossRef](#)]
65. Machado, A.B.; Ardila, Y.C.; de Oliveira, L.H.; Aznar, M.; Wolf Maciel, M.R. Liquid–Liquid Equilibria in Ternary and Quaternary Systems Present in Biodiesel Production from Soybean Oil at (298.2 and 333.2) K. *J. Chem. Eng. Data* **2012**, *57*, 1417–1422. [[CrossRef](#)]
66. Silva, W.L.G.D.; Souza, P.T.D.; Shimamoto, G.G.; Tubino, M. Separation of the Glycerol-Biodiesel Phases in an Ethyl Transesterification Synthetic Route Using Water. *J. Braz. Chem. Soc.* **2015**, *26*, 1745–1750. [[CrossRef](#)]
67. Kapil, A.; Wilson, K.; Lee, A.F.; Sadhukhan, J. Kinetic Modeling Studies of Heterogeneously Catalyzed Biodiesel Synthesis Reactions. *Ind. Eng. Chem. Res.* **2011**, *50*, 4818–4830. [[CrossRef](#)]
68. Andreo-Martínez, P.; García-Martínez, N.; Durán-del-Amor, M.D.M.; Quesada-Medina, J. Advances on kinetics and thermodynamics of non-catalytic supercritical methanol transesterification of some vegetable oils to biodiesel. *Energy Convers. Manag.* **2018**, *173*, 187–196. [[CrossRef](#)]
69. Ahmad Farid, M.A.; Hassan, M.A.; Taufiq-Yap, Y.H.; Ibrahim, M.L.; Hasan, M.Y.; Ali, A.A.M.; Othman, M.R.; Shirai, Y. Kinetic and thermodynamic of heterogeneously  $K_3PO_4/AC$ -catalysed transesterification via pseudo-first order mechanism and Eyring-Polanyi equation. *Fuel* **2018**, *232*, 653–658. [[CrossRef](#)]
70. Moradi, G.R.; Mohadesi, M.; Ghanbari, M.; Moradi, M.J.; Hosseini, S.; Davoodbeygi, Y. Kinetic comparison of two basic heterogenous catalysts obtained from sustainable resources for transesterification of waste cooking oil. *Biofuel Res. J.* **2015**, *2*, 236–241. [[CrossRef](#)]
71. Kumar, D.; Ali, A. Transesterification of Low-Quality Triglycerides over a Zn/CaO Heterogeneous Catalyst: Kinetics and Reusability Studies. *Energy Fuels* **2013**, *27*, 3758–3768. [[CrossRef](#)]
72. Kaur, N.; Ali, A. Biodiesel production via ethanolysis of jatropha oil using molybdenum impregnated calcium oxide as solid catalyst. *RSC Adv.* **2015**, *5*, 13285–13295. [[CrossRef](#)]

73. Kaur, N.; Ali, A. Lithium zirconate as solid catalyst for simultaneous esterification and transesterification of low quality triglycerides. *Appl. Catal. A Gen.* **2015**, *489*, 193–202. [[CrossRef](#)]
74. Devaraj Naik, B.; Udayakumar, M. Kinetics and thermodynamic analysis of transesterification of waste cooking sunflower oil using bentonite-supported sodium methoxide catalyst. *Biomass Convers. Biorefin.* **2023**, *13*, 9701–9714. [[CrossRef](#)]
75. Feyzi, M.; Shahbazi, Z. Preparation, kinetic and thermodynamic studies of Al-Sr nanocatalysts for biodiesel production. *J. Taiwan Inst. Chem. Eng.* **2017**, *71*, 145–155. [[CrossRef](#)]
76. Sahani, S.; Roy, T.; Chandra Sharma, Y. Clean and efficient production of biodiesel using barium cerate as a heterogeneous catalyst for the biodiesel production; kinetics and thermodynamic study. *J. Clean. Prod.* **2019**, *237*, 117699. [[CrossRef](#)]
77. Al-Sakkari, E.G.; El-Sheltawy, S.T.; Attia, N.K.; Mostafa, S.R. Kinetic study of soybean oil methanolysis using cement kiln dust as a heterogeneous catalyst for biodiesel production. *Appl. Catal. B Environ.* **2017**, *206*, 146–157. [[CrossRef](#)]
78. Xiao, Y.; Gao, L.; Xiao, G.; Lv, J. Kinetics of the Transesterification Reaction Catalyzed by Solid Base in a Fixed-Bed Reactor. *Energy Fuels* **2010**, *24*, 5829–5833. [[CrossRef](#)]
79. Hattori, H.; Shima, M.; Kabashima, H. Alcoholysis of ester and epoxide catalyzed by solid bases. In *Studies in Surface Science and Catalysis*; Elsevier: Amsterdam, The Netherlands, 2000; Volume 130, pp. 3507–3512.
80. Dossin, T.F.; Reyniers, M.-F.; Berger, R.J.; Marin, G.B. Simulation of heterogeneously MgO-catalyzed transesterification for fine-chemical and biodiesel industrial production. *Appl. Catal. B Environ.* **2006**, *67*, 136–148. [[CrossRef](#)]
81. Malani, R.S.; Patil, S.; Roy, K.; Chakma, S.; Goyal, A.; Moholkar, V.S. Mechanistic analysis of ultrasound-assisted biodiesel synthesis with Cu<sub>2</sub>O catalyst and mixed oil feedstock using continuous (packed bed) and batch (slurry) reactors. *Chem. Eng. Sci.* **2017**, *170*, 743–755. [[CrossRef](#)]
82. Galván Muciño, G.E.; Romero, R.; Ramírez, A.; Ramos, M.J.; Baeza-Jiménez, R.; Natividad, R. Kinetics of Transesterification of Safflower Oil to Obtain Biodiesel Using Heterogeneous Catalysis. *Int. J. Chem. React. Eng.* **2016**, *14*, 929–938. [[CrossRef](#)]
83. Thoai, D.N.; Tongurai, C.; Prasertsit, K.; Kumar, A. A novel two-step transesterification process catalyzed by homogeneous base catalyst in the first step and heterogeneous acid catalyst in the second step. *Fuel Process. Technol.* **2017**, *168*, 97–104. [[CrossRef](#)]
84. Klaewkla, R.; Arend, M.; Hoelderich, W.F. A Review of Mass Transfer Controlling the Reaction Rate in Heterogeneous Catalytic Systems. In *Mass Transfer—Advanced Aspects*; Nakajima, H., Ed.; InTech: London, UK, 2011.
85. Ma, F.; Hanna, M.A. Biodiesel production: A review. *Bioresour. Technol.* **1999**, *70*, 1–15. [[CrossRef](#)]
86. Zakaria, R.; Harvey, A.P. Direct production of biodiesel from rapeseed by reactive extraction/in situ transesterification. *Fuel Process. Technol.* **2012**, *102*, 53–60. [[CrossRef](#)]
87. Porwal, J.; Bangwal, D.; Garg, M.; Kaul, S. Reactive-extraction of pongamia seeds for biodiesel production. *J. Sci. Ind. Res.* **2012**, *71*, 822–828.
88. Amalia Kartika, I.; Yani, M.; Ariono, D.; Evon, P.; Rigal, L. Biodiesel production from jatropha seeds: Solvent extraction and in situ transesterification in a single step. *Fuel* **2013**, *106*, 111–117. [[CrossRef](#)]
89. Silitonga, A.S.; Ong, H.C.; Mahlia, T.M.I.; Masjuki, H.H.; Chong, W.T. Biodiesel Conversion from High FFA Crude *Jatropha curcas*, *Calophyllum inophyllum* and *Ceiba pentandra* Oil. *Energy Procedia* **2014**, *61*, 480–483. [[CrossRef](#)]
90. Dawodu, F.A.; Ayodele, O.O.; Bolanle-Ojo, T. Biodiesel production from *Sesamum indicum* L. seed oil: An optimization study. *Egypt. J. Pet.* **2014**, *23*, 191–199. [[CrossRef](#)]
91. Chen, K.-T.; Wang, J.-X.; Dai, Y.-M.; Wang, P.-H.; Liou, C.-Y.; Nien, C.-W.; Wu, J.-S.; Chen, C.-C. Rice husk ash as a catalyst precursor for biodiesel production. *J. Taiwan Inst. Chem. Eng.* **2013**, *44*, 622–629. [[CrossRef](#)]
92. Savaliya, M.L.; Dhorajiya, B.D.; Dholakiya, B.Z. Current Trends in Separation and Purification of Fatty Acid Methyl Ester. *Sep. Purif. Rev.* **2015**, *44*, 28–40. [[CrossRef](#)]
93. Stojković, I.J.; Stamenković, O.S.; Povrenović, D.S.; Veljković, V.B. Purification technologies for crude biodiesel obtained by alkali-catalyzed transesterification. *Renew. Sustain. Energy Rev.* **2014**, *32*, 1–15. [[CrossRef](#)]
94. Lotero, E.; Liu, Y.; Lopez, D.E.; Suwannakarn, K.; Bruce, D.A.; Goodwin, J.G. Synthesis of Biodiesel via Acid Catalysis. *Ind. Eng. Chem. Res.* **2005**, *44*, 5353–5363. [[CrossRef](#)]
95. Javidialesaadi, A.; Raeissi, S. Biodiesel Production from High Free Fatty Acid-Content Oils: Experimental Investigation of the Pretreatment Step. *APCBEE Procedia* **2013**, *5*, 474–478. [[CrossRef](#)]
96. Brucato, A.; Busciglio, A.; Stefano, F.D.; Grisafi, F.; Micale, G.; Scargiali, F. High temperature solid-catalyzed transesterification for biodiesel production. *Chem. Eng. Trans.* **2010**, *19*, 31–36.
97. Muthu, H.; SathyaSelvabala, V.; Varathachary, T.K.; Kirupha Selvaraj, D.; Nandagopal, J.; Subramanian, S. Synthesis of biodiesel from Neem oil using sulfated zirconia via transesterification. *Braz. J. Chem. Eng.* **2010**, *27*, 601–608. [[CrossRef](#)]
98. Koberg, M.; Gedanken, A. Using Microwave Radiation and SrO as a Catalyst for the Complete Conversion of Oils, Cooked Oils, and Microalgae to Biodiesel. In *New and Future Developments in Catalysis*; Elsevier: Amsterdam, The Netherlands, 2013; pp. 209–227.
99. Musa, I.A. The effects of alcohol to oil molar ratios and the type of alcohol on biodiesel production using transesterification process. *Egypt. J. Pet.* **2016**, *25*, 21–31. [[CrossRef](#)]
100. Mandari, V.; Devarai, S.K. Biodiesel Production Using Homogeneous, Heterogeneous, and Enzyme Catalysts via Transesterification and Esterification Reactions: A Critical Review. *Bioenergy Res.* **2022**, *15*, 935–961. [[CrossRef](#)] [[PubMed](#)]
101. Atadashi, I.M.; Aroua, M.K.; Abdul Aziz, A.R.; Sulaiman, N.M.N. The effects of catalysts in biodiesel production: A review. *J. Ind. Eng. Chem.* **2013**, *19*, 14–26. [[CrossRef](#)]



102. Lam, M.K.; Lee, K.T.; Mohamed, A.R. Homogeneous, heterogeneous and enzymatic catalysis for transesterification of high free fatty acid oil (waste cooking oil) to biodiesel: A review. *Biotechnol. Adv.* **2010**, *28*, 500–518. [[CrossRef](#)] [[PubMed](#)]
103. Sagioglu, A.; Selen, I.; Ozcan, M.; Paluzar, H.; Toprakkiran, N. Comparison of biodiesel productivities of different vegetable oils by acidic catalysis. *Chem. Ind. Chem. Eng. Q.* **2011**, *17*, 53–58. [[CrossRef](#)]
104. Limpanuparb, T.; Punyain, K.; Tantirungrotechai, Y. A DFT investigation of methanolysis and hydrolysis of triacetin. *J. Mol. Struct. Theochem* **2010**, *955*, 23–32. [[CrossRef](#)]
105. Almeida, E.L.; Andrade, C.M.G.; Andreo dos Santos, O. Production of Biodiesel Via Catalytic Processes: A Brief Review. *Int. J. Chem. React. Eng.* **2018**, *16*, 20170130. [[CrossRef](#)]
106. Tan, Y.H.; Abdullah, M.O.; Nolasco-Hipolito, C.; Taufiq-Yap, Y.H. Waste ostrich- and chicken-eggshells as heterogeneous base catalyst for biodiesel production from used cooking oil: Catalyst characterization and biodiesel yield performance. *Appl. Energy* **2015**, *160*, 58–70. [[CrossRef](#)]
107. Vicente, G.; Martínez, M.; Aracil, J. Integrated biodiesel production: A comparison of different homogeneous catalysts systems. *Bioresour. Technol.* **2004**, *92*, 297–305. [[CrossRef](#)]
108. Zhang, M.; Sun, A.; Meng, Y.; Wang, L.; Jiang, H.; Li, G. Catalytic Performance of Biomass Carbon-Based Solid Acid Catalyst for Esterification of Free Fatty Acids in Waste Cooking Oil. *Catal. Surv. Asia* **2015**, *19*, 61–67. [[CrossRef](#)]
109. Lin, L.; Cunshan, Z.; Vittayapadung, S.; Xiangqian, S.; Mingdong, D. Opportunities and challenges for biodiesel fuel. *Appl. Energy* **2011**, *88*, 1020–1031. [[CrossRef](#)]
110. Vasudevan, P.T.; Briggs, M. Biodiesel production—Current state of the art and challenges. *J. Ind. Microbiol. Biotechnol.* **2008**, *35*, 421. [[CrossRef](#)] [[PubMed](#)]
111. Lee, D.-W.; Park, Y.-M.; Lee, K.-Y. Heterogeneous Base Catalysts for Transesterification in Biodiesel Synthesis. *Catal. Surv. Asia* **2009**, *13*, 63–77. [[CrossRef](#)]
112. Md Radzi, M.R.; Manogaran, M.D.; Yusoff, M.H.M.; Zulqarnain; Anuar, M.R.; Shoparwe, N.F.; Rahman, M.F.A. Production of Propanediols through In Situ Glycerol Hydrogenolysis via Aqueous Phase Reforming: A Review. *Catalysts* **2022**, *12*, 945. [[CrossRef](#)]
113. Rattanaphra, D.; Harvey, A.; Srinophakun, P. Simultaneous Conversion of Triglyceride/Free Fatty Acid Mixtures into Biodiesel Using Sulfated Zirconia. *Top. Catal.* **2010**, *53*, 773–782. [[CrossRef](#)]
114. Canakci, M.; Gerpen, J.V. Biodiesel production from oils and fats with high free fatty acids. *Trans. ASAE* **2001**, *44*, 1429–1436. [[CrossRef](#)]
115. Hayyan, A.; Alam, M.Z.; Mirghani, M.E.S.; Kabbashi, N.A.; Hakimi, N.I.N.M.; Siran, Y.M.; Tahiruddin, S. Sludge palm oil as a renewable raw material for biodiesel production by two-step processes. *Bioresour. Technol.* **2010**, *101*, 7804–7811. [[CrossRef](#)]
116. Charoenchaitrakool, M.; Thienmethangkoon, J. Statistical optimization for biodiesel production from waste frying oil through two-step catalyzed process. *Fuel Process. Technol.* **2011**, *92*, 112–118. [[CrossRef](#)]
117. Patil, P.; Deng, S.; Isaac Rhodes, J.; Lammers, P.J. Conversion of waste cooking oil to biodiesel using ferric sulfate and supercritical methanol processes. *Fuel* **2010**, *89*, 360–364. [[CrossRef](#)]
118. Boro, J.; Konwar, L.J.; Deka, D. Transesterification of non edible feedstock with lithium incorporated egg shell derived CaO for biodiesel production. *Fuel Process. Technol.* **2014**, *122*, 72–78. [[CrossRef](#)]
119. Munyentwali, A.; Li, H.; Yang, Q. Review of advances in bifunctional solid acid/base catalysts for sustainable biodiesel production. *Appl. Catal. A Gen.* **2022**, *633*, 118525. [[CrossRef](#)]
120. Al-Saadi, A.; Mathan, B.; He, Y. Biodiesel production via simultaneous transesterification and esterification reactions over SrO–ZnO/Al<sub>2</sub>O<sub>3</sub> as a bifunctional catalyst using high acidic waste cooking oil. *Chem. Eng. Res. Des.* **2020**, *162*, 238–248. [[CrossRef](#)]
121. Isaacs, M.A.; Parlett, C.M.A.; Robinson, N.; Durndell, L.J.; Manayil, J.C.; Beaumont, S.K.; Jiang, S.; Hondow, N.S.; Lamb, A.C.; Jampaiah, D.; et al. A spatially orthogonal hierarchically porous acid–base catalyst for cascade and antagonistic reactions. *Nat. Catal.* **2020**, *3*, 921–931. [[CrossRef](#)]
122. Ding, S.; Fernandez Ainaga, D.L.; Hu, M.; Qiu, B.; Khalid, U.; D’Agostino, C.; Ou, X.; Spencer, B.; Zhong, X.; Peng, Y.; et al. Spatial segregation of catalytic sites within Pd doped H-ZSM-5 for fatty acid hydrodeoxygenation to alkanes. *Nat. Commun.* **2024**, *15*, 7718. [[CrossRef](#)] [[PubMed](#)]
123. Canakci, M.; Gerpen, J.V. Biodiesel production via acid catalysis. *Trans. ASAE* **1999**, *42*, 1203–1210. [[CrossRef](#)]
124. Enweremadu, C.C.; Mbarawa, M.M. Technical aspects of production and analysis of biodiesel from used cooking oil—A review. *Renew. Sustain. Energy Rev.* **2009**, *13*, 2205–2224. [[CrossRef](#)]
125. Romano, S. Vegetable Oils: A New Alternative. In Proceedings of the International Conference on Plant and Vegetable Oils as Fuels, Fargo, ND, USA, 2 August 1982.
126. Iglesias, J.; Melero, J.A.; Bautista, L.F.; Morales, G.; Sánchez-Vázquez, R.; Andreola, M.T.; Lizarraga-Fernández, A. Zr-SBA-15 as an efficient acid catalyst for FAME production from crude palm oil. *Catal. Today* **2011**, *167*, 46–55. [[CrossRef](#)]
127. Parangi, T.; Mishra, M.K. Solid Acid Catalysts for Biodiesel Production. *Comments Inorg. Chem.* **2020**, *40*, 176–216. [[CrossRef](#)]
128. Puna, J.F.; Gomes, J.F.; Correia, M.J.N.; Soares Dias, A.P.; Bordado, J.C. Advances on the development of novel heterogeneous catalysts for transesterification of triglycerides in biodiesel. *Fuel* **2010**, *89*, 3602–3606. [[CrossRef](#)]
129. Chouhan, A.P.S.; Sarma, A.K. Modern heterogeneous catalysts for biodiesel production: A comprehensive review. *Renew. Sustain. Energy Rev.* **2011**, *15*, 4378–4399. [[CrossRef](#)]

130. Diamantopoulos, N. Comprehensive Review on the Biodiesel Production using Solid Acid Heterogeneous Catalysts. *J. Therm. Catal.* **2015**, *6*, 1–8. [[CrossRef](#)]
131. Sani, Y.M.; Daud, W.M.A.W.; Abdul Aziz, A.R. Activity of solid acid catalysts for biodiesel production: A critical review. *Appl. Catal. A Gen.* **2014**, *470*, 140–161. [[CrossRef](#)]
132. Erika, L.P.A.; Ochoa-Herrera, V.; Quintanilla, F.; Egas, D.A.; Mora, J.R. Optimization of a Gas Chromatography Methodology for Biodiesel Analysis. *J. Anal. Chem.* **2021**, *76*, 106–111. [[CrossRef](#)]
133. Ramos, K.; Riddell, A.; Tsiagras, H.; Hupp, A.M. Analysis of biodiesel-diesel blends: Does ultrafast gas chromatography provide for similar separation in a fraction of the time? *J. Chromatogr. A* **2022**, *1667*, 462903. [[CrossRef](#)] [[PubMed](#)]
134. Syed, M.B. Analysis of biodiesel by high performance liquid chromatography using refractive index detector. *MethodsX* **2017**, *4*, 256–259. [[CrossRef](#)]
135. Torres, A.; Fuentes, B.; Rodríguez, K.E.; Brito, A.; Díaz, L. Analysis of the Content of Fatty Acid Methyl Esters in Biodiesel by Fourier-Transform Infrared Spectroscopy: Method and Comparison with Gas Chromatography. *J. Am. Oil Chem. Soc.* **2020**, *97*, 651–661. [[CrossRef](#)]
136. Bligaard, T.; Bullock, R.M.; Campbell, C.T.; Chen, J.G.; Gates, B.C.; Gorte, R.J.; Jones, C.W.; Jones, W.D.; Kitchin, J.R.; Scott, S.L. Toward Benchmarking in Catalysis Science: Best Practices, Challenges, and Opportunities. *ACS Catal.* **2016**, *6*, 2590–2602. [[CrossRef](#)]
137. Schüth, F.; Ward, M.D.; Buriak, J.M. Common Pitfalls of Catalysis Manuscripts Submitted to Chemistry of Materials. *Chem. Mater.* **2018**, *30*, 3599–3600. [[CrossRef](#)]
138. Guo, F.; Fang, Z. Biodiesel Production with Solid Catalysts. In *Biodiesel—Feedstocks and Processing Technologies*; Stoytcheva, M., Ed.; InTech: London, UK, 2011.
139. Chung, K.-H.; Park, B.-G. Esterification of oleic acid in soybean oil on zeolite catalysts with different acidity. *J. Ind. Eng. Chem.* **2009**, *15*, 388–392. [[CrossRef](#)]
140. Chung, K.-H.; Chang, D.-R.; Park, B.-G. Removal of free fatty acid in waste frying oil by esterification with methanol on zeolite catalysts. *Bioresour. Technol.* **2008**, *99*, 7438–7443. [[CrossRef](#)]
141. Hassani, M.; Najafpour, G.D.; Mohammadi, M.; Rabiee, M. Preparation, characterization and application of zeolite-based catalyst for production of biodiesel from waste cooking oil. *J. Sci. Ind. Res.* **2014**, *73*, 120–133.
142. Brito, A.; Borges, M.E.; Arvelo, R.; Garcia, F.; Diaz, M.C.; Otero, N. Reuse of Fried Oil to Obtain Biodiesel: Zeolites Y as a Catalyst. *Int. J. Chem. React. Eng.* **2007**, *5*. [[CrossRef](#)]
143. Medina-Valtierra, J.; Ramirez-Ortiz, J. Biodiesel production from waste frying oil in sub- and supercritical methanol on a zeolite Y solid acid catalyst. *Front. Chem. Sci. Eng.* **2013**, *7*, 401–407. [[CrossRef](#)]
144. Prinsen, P.; Luque, R.; González-Arellano, C. Zeolite catalyzed palmitic acid esterification. *Micropor. Mesoporous Mater.* **2018**, *262*, 133–139. [[CrossRef](#)]
145. Septiani, U.; Putri, R.; Jamarun, N. Synthesis of Zeolite ZSM-5 from rice husk ash as catalyst in vegetable oil transesterification for biodiesel production. *Der Pharmacia Lettre* **2016**, *8*, 86–91.
146. Védrine, J. Heterogeneous Catalysis on Metal Oxides. *Catalysts* **2017**, *7*, 341. [[CrossRef](#)]
147. Abreu, W.C.D.; Moura, B.C.V.R.D.; Costa, J.C.S.; Moura, E.M.D. Strontium and Nickel Heterogeneous Catalysts for Biodiesel Production from Macaw Oil. *J. Braz. Chem. Soc.* **2017**, *28*, 319–327. [[CrossRef](#)]
148. Khder, A.S.; El-Sharkawy, E.A.; El-Hakam, S.A.; Ahmed, A.I. Surface characterization and catalytic activity of sulfated tin oxide catalyst. *Catal. Commun.* **2008**, *9*, 769–777. [[CrossRef](#)]
149. Istadi, I.; Anggoro, D.D.; Buchori, L.; Rahmawati, D.A.; Intaningrum, D. Active Acid Catalyst of Sulphated Zinc Oxide for Transesterification of Soybean Oil with Methanol to Biodiesel. *Procedia Environ. Sci.* **2015**, *23*, 385–393. [[CrossRef](#)]
150. Shao, G.N.; Sheikh, R.; Hilonga, A.; Lee, J.E.; Park, Y.-H.; Kim, H.T. Biodiesel production by sulfated mesoporous titania–silica catalysts synthesized by the sol–gel process from less expensive precursors. *Chem. Eng. J.* **2013**, *215–216*, 600–607. [[CrossRef](#)]
151. Jitputti, J.; Kitiyanan, B.; Rangsunvigit, P.; Bunyakiat, K.; Attanatho, L.; Jenvanitpanjakul, P. Transesterification of crude palm kernel oil and crude coconut oil by different solid catalysts. *Chem. Eng. J.* **2006**, *116*, 61–66. [[CrossRef](#)]
152. Noda, L.K.; Almeida, R.M.D.; Gonçalves, N.S.; Probst, L.F.D.; Sala, O. TiO<sub>2</sub> with a high sulfate content—Thermogravimetric analysis, determination of acid sites by infrared spectroscopy and catalytic activity. *Catal. Today* **2003**, *85*, 69–74. [[CrossRef](#)]
153. Zhang, H.; Yu, H.; Zheng, A.; Li, S.; Shen, W.; Deng, F. Reactivity Enhancement of 2-Propanol Photocatalysis on SO<sub>4</sub><sup>2-</sup>/TiO<sub>2</sub>: Insights from Solid-State NMR Spectroscopy. *Environ. Sci. Technol.* **2008**, *42*, 5316–5321. [[CrossRef](#)] [[PubMed](#)]
154. Li, Z.; Wnetrzak, R.; Kwapinski, W.; Leahy, J.J. Synthesis and Characterization of Sulfated TiO<sub>2</sub> Nanorods and ZrO<sub>2</sub>/TiO<sub>2</sub> Nanocomposites for the Esterification of Biobased Organic Acid. *ACS Appl. Mater. Interfaces* **2012**, *4*, 4499–4505. [[CrossRef](#)]
155. Zhao, J.; Yue, Y.; Hua, W.; He, H.; Gao, Z. Catalytic activities and properties of sulfated zirconia supported on mesostructured  $\gamma$ -Al<sub>2</sub>O<sub>3</sub>. *Appl. Catal. A Gen.* **2008**, *336*, 133–139. [[CrossRef](#)]
156. Wang, J.; Yang, P.; Fan, M.; Yu, W.; Jing, X.; Zhang, M.; Duan, X. Preparation and characterization of novel magnetic ZrO<sub>2</sub>/TiO<sub>2</sub>/Fe<sub>3</sub>O<sub>4</sub> solid superacid. *Mater. Lett.* **2007**, *61*, 2235–2238. [[CrossRef](#)]
157. Li, C.; Tan, J.; Fan, X.; Zhang, B.; Zhang, H.; Zhang, Q. Magnetically separable one dimensional Fe<sub>3</sub>O<sub>4</sub>/P(MAA-DVB)/TiO<sub>2</sub> nanochains: Preparation, characterization and photocatalytic activity. *Ceram. Int.* **2015**, *41*, 3860–3868. [[CrossRef](#)]
158. Jiang, Y.-X.; Chen, X.-M.; Mo, Y.-F.; Tong, Z.-F. Preparation and properties of Al-PILC supported SO<sub>4</sub><sup>2-</sup>/TiO<sub>2</sub> superacid catalyst. *J. Mol. Catal. A Chem.* **2004**, *213*, 231–234. [[CrossRef](#)]

159. Lai, D.-M.; Deng, L.; Guo, Q.-X.; Fu, Y. Hydrolysis of biomass by magnetic solid acid. *Energy Environ. Sci.* **2011**, *4*, 3552–3557. [[CrossRef](#)]
160. Wu, L.; Zhou, Y.; Nie, W.; Song, L.; Chen, P. Synthesis of highly monodispersed teardrop-shaped core-shell SiO<sub>2</sub>/TiO<sub>2</sub> nanoparticles and their photocatalytic activities. *Appl. Surf. Sci.* **2015**, *351*, 320–326. [[CrossRef](#)]
161. Shen, J.; Zhu, Y.; Yang, X.; Li, C. Magnetic composite microspheres with exposed {001} faceted TiO<sub>2</sub> shells: A highly active and selective visible-light photocatalyst. *J. Mater. Chem.* **2012**, *22*, 13341–13347. [[CrossRef](#)]
162. Jacinto, M.J.; Santos, O.H.C.F.; Jardim, R.F.; Landers, R.; Rossi, L.M. Preparation of recoverable Ru catalysts for liquid-phase oxidation and hydrogenation reactions. *Appl. Catal. A Gen.* **2009**, *360*, 177–182. [[CrossRef](#)]
163. Lu, A.-H.; Salabas, E.L.; Schüth, F. Magnetic Nanoparticles: Synthesis, Protection, Functionalization, and Application. *Angew. Chem. Int. Ed.* **2007**, *46*, 1222–1244. [[CrossRef](#)]
164. Sobhani, S.; Parizi, Z.P.; Razavi, N. Nano n-propylsulfonated  $\gamma$ -Fe<sub>2</sub>O<sub>3</sub> as magnetically recyclable heterogeneous catalyst for the efficient synthesis of  $\beta$ -phosphonomalonates. *Appl. Catal. A Gen.* **2011**, *409–410*, 162–166. [[CrossRef](#)]
165. Tang, S.; Wang, L.; Zhang, Y.; Li, S.; Tian, S.; Wang, B. Study on preparation of Ca/Al/Fe<sub>3</sub>O<sub>4</sub> magnetic composite solid catalyst and its application in biodiesel transesterification. *Fuel Process. Technol.* **2012**, *95*, 84–89. [[CrossRef](#)]
166. Xin, T.; Ma, M.; Zhang, H.; Gu, J.; Wang, S.; Liu, M.; Zhang, Q. A facile approach for the synthesis of magnetic separable Fe<sub>3</sub>O<sub>4</sub>@TiO<sub>2</sub> core-shell nanocomposites as highly recyclable photocatalysts. *Appl. Surf. Sci.* **2014**, *288*, 51–59. [[CrossRef](#)]
167. Moghanian, H.; Mobinikhaledi, A.; Blackman, A.G.; Sarough-Farahani, E. Sulfanilic acid-functionalized silica-coated magnetite nanoparticles as an efficient, reusable and magnetically separable catalyst for the solvent-free synthesis of 1-amido- and 1-aminoalkyl-2-naphthols. *RSC Adv.* **2014**, *4*, 28176–28185. [[CrossRef](#)]
168. Qin, S.; Cai, W.; Tang, X.; Yang, L. Sensitively monitoring photodegradation process of organic dye molecules by surface-enhanced Raman spectroscopy based on Fe<sub>3</sub>O<sub>4</sub>@SiO<sub>2</sub>@TiO<sub>2</sub>@Ag particle. *Analyst* **2014**, *139*, 5509–5515. [[CrossRef](#)]
169. Petchmala, A.; Laosiripojana, N.; Jongsomjit, B.; Goto, M.; Panpranot, J.; Mekasuwandumrong, O.; Shotipruk, A. Transesterification of palm oil and esterification of palm fatty acid in near- and super-critical methanol with SO<sub>4</sub><sup>2-</sup>-ZrO<sub>2</sub> catalysts. *Fuel* **2010**, *89*, 2387–2392. [[CrossRef](#)]
170. Yee, K.F.; Lee, K.T.; Ceccato, R.; Abdullah, A.Z. Production of biodiesel from *Jatropha curcas* L. oil catalyzed by SO<sub>4</sub><sup>2-</sup>/ZrO<sub>2</sub> catalyst: Effect of interaction between process variables. *Bioresour. Technol.* **2011**, *102*, 4285–4289. [[CrossRef](#)]
171. Jiménez-Morales, I.; Santamaría-González, J.; Maireles-Torres, P.; Jiménez-López, A. Calcined zirconium sulfate supported on MCM-41 silica as acid catalyst for ethanolysis of sunflower oil. *Appl. Catal. B Environ.* **2011**, *103*, 91–98. [[CrossRef](#)]
172. Li, Y.; Zhang, X.-D.; Sun, L.; Xu, M.; Zhou, W.-G.; Liang, X.-H. Solid superacid catalyzed fatty acid methyl esters production from acid oil. *Appl. Energy* **2010**, *87*, 2369–2373.
173. Yan, F.; Yuan, Z.; Lu, P.; Luo, W.; Yang, L.; Deng, L. Fe–Zn double-metal cyanide complexes catalyzed biodiesel production from high-acid-value oil. *Renew. Energy* **2011**, *36*, 2026–2031. [[CrossRef](#)]
174. Kafuku, G.; Lam, M.K.; Kansedo, J.; Lee, K.T.; Mbarawa, M. *Croton megalocarpus* oil: A feasible non-edible oil source for biodiesel production. *Bioresour. Technol.* **2010**, *101*, 7000–7004. [[CrossRef](#)]
175. Kafuku, G.; Lam, M.K.; Kansedo, J.; Lee, K.T.; Mbarawa, M. Heterogeneous catalyzed biodiesel production from *Moringa oleifera* oil. *Fuel Process. Technol.* **2010**, *91*, 1525–1529. [[CrossRef](#)]
176. Athar, M.; Zaidi, S.; Hassan, S.Z. Intensification and optimization of biodiesel production using microwave-assisted acid-organocatalyzed transesterification process. *Sci. Rep.* **2020**, *10*, 21239. [[CrossRef](#)]
177. Lee, A.F.; Bennett, J.A.; Manayil, J.C.; Wilson, K. Heterogeneous catalysis for sustainable biodiesel production via esterification and transesterification. *Chem. Soc. Rev.* **2014**, *43*, 7887–7916. [[CrossRef](#)]
178. Manayil, J.C.; Inocencio, C.V.M.; Lee, A.F.; Wilson, K. Mesoporous sulfonic acid silicas for pyrolysis bio-oil upgrading via acetic acid esterification. *Green Chem.* **2016**, *18*, 1387–1394. [[CrossRef](#)]
179. Guldhe, A.; Singh, P.; Ansari, F.A.; Singh, B.; Bux, F. Biodiesel synthesis from microalgal lipids using tungstated zirconia as a heterogeneous acid catalyst and its comparison with homogeneous acid and enzyme catalysts. *Fuel* **2017**, *187*, 180–188. [[CrossRef](#)]
180. Gardy, J.; Hassanpour, A.; Lai, X.; Ahmed, M.H.; Rehan, M. Biodiesel production from used cooking oil using a novel surface functionalised TiO<sub>2</sub> nano-catalyst. *Appl. Catal. B Environ.* **2017**, *207*, 297–310. [[CrossRef](#)]
181. Furuta, S.; Matsuhashi, H.; Arata, K. Biodiesel fuel production with solid amorphous-zirconia catalysis in fixed bed reactor. *Biomass Bioenergy* **2006**, *30*, 870–873. [[CrossRef](#)]
182. De Almeida, R.M.; Noda, L.K.; Gonçalves, N.S.; Meneghetti, S.M.P.; Meneghetti, M.R. Transesterification reaction of vegetable oils, using superacid sulfated TiO<sub>2</sub>-base catalysts. *Appl. Catal. A Gen.* **2008**, *347*, 100–105. [[CrossRef](#)]
183. Lam, M.K.; Lee, K.T.; Mohamed, A.R. Sulfated tin oxide as solid superacid catalyst for transesterification of waste cooking oil: An optimization study. *Appl. Catal. B Environ.* **2009**, *93*, 134–139. [[CrossRef](#)]
184. Guan, D.; Fan, M.; Wang, J.; Zhang, Y.; Liu, Q.; Jing, X. Synthesis and properties of magnetic solid superacid: SO<sub>4</sub><sup>2-</sup>/ZrO<sub>2</sub>-B<sub>2</sub>O<sub>3</sub>-Fe<sub>3</sub>O<sub>4</sub>. *Mater. Chem. Phys.* **2010**, *122*, 278–283. [[CrossRef](#)]
185. Wen, Z.; Yu, X.; Tu, S.-T.; Yan, J.; Dahlquist, E. Biodiesel production from waste cooking oil catalyzed by TiO<sub>2</sub>-MgO mixed oxides. *Bioresour. Technol.* **2010**, *101*, 9570–9576. [[CrossRef](#)]
186. Valle-Vigón, P.; Sevilla, M.; Fuertes, A.B. Sulfonated mesoporous silica-carbon composites and their use as solid acid catalysts. *Appl. Surf. Sci.* **2012**, *261*, 574–583. [[CrossRef](#)]



187. Madhuvilakku, R.; Piraman, S. Biodiesel synthesis by TiO<sub>2</sub>–ZnO mixed oxide nanocatalyst catalyzed palm oil transesterification process. *Bioresour. Technol.* **2013**, *150*, 55–59. [CrossRef]
188. Osatiashtiani, A.; Durndell, L.J.; Manayil, J.C.; Lee, A.F.; Wilson, K. Influence of alkyl chain length on sulfated zirconia catalysed batch and continuous esterification of carboxylic acids by light alcohols. *Green Chem.* **2016**, *18*, 5529–5535. [CrossRef]
189. Alhassan, F.H.; Rashid, U.; Taufiq-Yap, Y.H. Synthesis of waste cooking oil-based biodiesel via effectual recyclable bi-functional Fe<sub>2</sub>O<sub>3</sub>MnOSO<sub>4</sub><sup>2-</sup>/ZrO<sub>2</sub> nanoparticle solid catalyst. *Fuel* **2015**, *142*, 38–45. [CrossRef]
190. Raia, R.Z.; Da Silva, L.S.; Marcucci, S.M.P.; Arroyo, P.A. Biodiesel production from *Jatropha curcas* L. oil by simultaneous esterification and transesterification using sulphated zirconia. *Catal. Today* **2017**, *289*, 105–114. [CrossRef]
191. Fu, X.-B.; Chen, J.; Song, X.-L.; Zhang, Y.-M.; Zhu, Y.; Yang, J.; Zhang, C.-W. Biodiesel Production Using a Carbon Solid Acid Catalyst Derived from β-Cyclodextrin. *J. Am. Oil Chem. Soc.* **2015**, *92*, 495–502. [CrossRef]
192. Dehkhoda, A.M.; West, A.H.; Ellis, N. Biochar based solid acid catalyst for biodiesel production. *Appl. Catal. A Gen.* **2010**, *382*, 197–204. [CrossRef]
193. Zhang, D.-Y.; Duan, M.-H.; Yao, X.-H.; Fu, Y.-J.; Zu, Y.-G. Preparation of a novel cellulose-based immobilized heteropoly acid system and its application on the biodiesel production. *Fuel* **2016**, *172*, 293–300. [CrossRef]
194. Ryu, Y.-J.; Kim, Z.-H.; Lee, S.G.; Yang, J.-H.; Shin, H.-Y.; Lee, C.-G. Development of Carbon-Based Solid Acid Catalysts Using a Lipid-Extracted Alga, *Dunaliella tertiolecta*, for Esterification. *J. Microbiol. Biotechnol.* **2018**, *28*, 732–738. [CrossRef]
195. Shu, Q.; Gao, J.; Nawaz, Z.; Liao, Y.; Wang, D.; Wang, J. Synthesis of biodiesel from waste vegetable oil with large amounts of free fatty acids using a carbon-based solid acid catalyst. *Appl. Energy* **2010**, *87*, 2589–2596. [CrossRef]
196. Gupta, J.; Agarwal, M.; Dalai, A.K. An overview on the recent advancements of sustainable heterogeneous catalysts and prominent continuous reactor for biodiesel production. *J. Ind. Eng. Chem.* **2020**, *88*, 58–77. [CrossRef]
197. Cao, F.; Chen, Y.; Zhai, F.; Li, J.; Wang, J.; Wang, X.; Wang, S.; Zhu, W. Biodiesel production from high acid value waste frying oil catalyzed by superacid heteropolyacid. *Biotechnol. Bioeng.* **2008**, *101*, 93–100. [CrossRef]
198. Chai, F.; Cao, F.; Zhai, F.; Chen, Y.; Wang, X.; Su, Z. Transesterification of Vegetable Oil to Biodiesel using a Heteropolyacid Solid Catalyst. *Adv. Synth. Catal.* **2007**, *349*, 1057–1065. [CrossRef]
199. Alcañiz-Monge, J.; Bakkali, B.E.; Trautwein, G.; Reinoso, S. Zirconia-supported tungstophosphoric heteropolyacid as heterogeneous acid catalyst for biodiesel production. *Appl. Catal. B Environ.* **2018**, *224*, 194–203. [CrossRef]
200. Thangaraj, B.; Solomon, P.R.; Muniyandi, B.; Ranganathan, S.; Lin, L. Catalysis in biodiesel production—A review. *Clean Energy* **2019**, *3*, 2–23. [CrossRef]
201. Marwaha, A.; Dhir, A.; Mahla, S.K.; Mohapatra, S.K. An overview of solid base heterogeneous catalysts for biodiesel production. *Catal. Rev.* **2018**, *60*, 594–628. [CrossRef]
202. Di Serio, M.; Tesser, R.; Pengmei, L.; Santacesaria, E. Heterogeneous Catalysts for Biodiesel Production. *Energy Fuels* **2008**, *22*, 207–217. [CrossRef]
203. Li, Z.; Ding, S.; Chen, C.; Qu, S.; Du, L.; Lu, J.; Ding, J. Recyclable Li/NaY zeolite as a heterogeneous alkaline catalyst for biodiesel production: Process optimization and kinetics study. *Energy Convers. Manag.* **2019**, *192*, 335–345. [CrossRef]
204. Baskar, G.; Aiswarya, R. Trends in catalytic production of biodiesel from various feedstocks. *Renew. Sustain. Energy Rev.* **2016**, *57*, 496–504. [CrossRef]
205. Refaat, A.A. Biodiesel production using solid metal oxide catalysts. *Int. J. Environ. Sci. Technol.* **2011**, *8*, 203–221. [CrossRef]
206. MacLeod, C.S.; Harvey, A.P.; Lee, A.F.; Wilson, K. Evaluation of the activity and stability of alkali-doped metal oxide catalysts for application to an intensified method of biodiesel production. *Chem. Eng. J.* **2008**, *135*, 63–70. [CrossRef]
207. Jothiramalingam, R.; Wang, M.K. Review of Recent Developments in Solid Acid, Base, and Enzyme Catalysts (Heterogeneous) for Biodiesel Production via Transesterification. *Ind. Eng. Chem. Res.* **2009**, *48*, 6162–6172. [CrossRef]
208. Yang, G.; Yu, J. Advancements in Basic Zeolites for Biodiesel Production via Transesterification. *Chemistry* **2023**, *5*, 438–451. [CrossRef]
209. Shan, R.; Lu, L.; Shi, Y.; Yuan, H.; Shi, J. Catalysts from renewable resources for biodiesel production. *Energy Convers. Manag.* **2018**, *178*, 277–289. [CrossRef]
210. Borges, M.E.; Díaz, L. Recent developments on heterogeneous catalysts for biodiesel production by oil esterification and transesterification reactions: A review. *Renew. Sustain. Energy Rev.* **2012**, *16*, 2839–2849. [CrossRef]
211. Viriya-empikul, N.; Krasae, P.; Puttasawat, B.; Yoosuk, B.; Chollacoop, N.; Faungnawakij, K. Waste shells of mollusk and egg as biodiesel production catalysts. *Bioresour. Technol.* **2010**, *101*, 3765–3767. [CrossRef]
212. Zhu, H.; Wu, Z.; Chen, Y.; Zhang, P.; Duan, S.; Liu, X.; Mao, Z. Preparation of Biodiesel Catalyzed by Solid Super Base of Calcium Oxide and Its Refining Process. *Chin. J. Chem.* **2006**, *27*, 391–396. [CrossRef]
213. Kouzu, M.; Kasuno, T.; Tajika, M.; Sugimoto, Y.; Yamanaka, S.; Hidaka, J. Calcium oxide as a solid base catalyst for transesterification of soybean oil and its application to biodiesel production. *Fuel* **2008**, *87*, 2798–2806. [CrossRef]
214. Marinković, D.M.; Stanković, M.V.; Veličković, A.V.; Avramović, J.M.; Miladinović, M.R.; Stamenković, O.O.; Veljković, V.B.; Jovanović, D.M. Calcium oxide as a promising heterogeneous catalyst for biodiesel production: Current state and perspectives. *Renew. Sustain. Energy Rev.* **2016**, *56*, 1387–1408. [CrossRef]
215. Liu, X.; He, H.; Wang, Y.; Zhu, S. Transesterification of soybean oil to biodiesel using SrO as a solid base catalyst. *Catal. Commun.* **2007**, *8*, 1107–1111. [CrossRef]
216. López, D.E.; Goodwin, J.G.; Bruce, D.A.; Lotero, E. Transesterification of triacetin with methanol on solid acid and base catalysts. *Appl. Catal. A Gen.* **2005**, *295*, 97–105. [CrossRef]

217. Meher, L.C.; Kulkarni, M.G.; Dalai, A.K.; Naik, S.N. Transesterification of karanja (*Pongamia pinnata*) oil by solid basic catalysts. *Eur. J. Lipid Sci. Technol.* **2006**, *108*, 389–397. [CrossRef]
218. Gurunathan, B.; Ravi, A. Process optimization and kinetics of biodiesel production from neem oil using copper doped zinc oxide heterogeneous nanocatalyst. *Bioresour. Technol.* **2015**, *190*, 424–428. [CrossRef]
219. Torres-Rodríguez, D.A.; Romero-Ibarra, I.C.; Ibarra, I.A.; Pfeiffer, H. Biodiesel production from soybean and *Jatropha* oils using cesium impregnated sodium zirconate as a heterogeneous base catalyst. *Renew. Energy* **2016**, *93*, 323–331. [CrossRef]
220. Kaur, M.; Ali, A. An efficient and reusable Li/NiO heterogeneous catalyst for ethanolysis of waste cottonseed oil. *Eur. J. Lipid Sci. Technol.* **2015**, *117*, 550–560. [CrossRef]
221. Taufiq-Yap, Y.H.; Lee, H.V.; Hussein, M.Z.; Yunus, R. Calcium-based mixed oxide catalysts for methanolysis of *Jatropha curcas* oil to biodiesel. *Biomass Bioenergy* **2011**, *35*, 827–834. [CrossRef]
222. Xie, W.; Peng, H.; Chen, L. Calcined Mg–Al hydrotalcites as solid base catalysts for methanolysis of soybean oil. *J. Mol. Catal. A Chem.* **2006**, *246*, 24–32. [CrossRef]
223. Wang, Y.-T.; Fang, Z.; Zhang, F.; Xue, B.-J. One-step production of biodiesel from oils with high acid value by activated Mg–Al hydrotalcite nanoparticles. *Bioresour. Technol.* **2015**, *193*, 84–89. [CrossRef] [PubMed]
224. Navajas, A.; Campo, I.; Moral, A.; Echave, J.; Sanz, O.; Montes, M.; Odriozola, J.A.; Arzamendi, G.; Gandía, L.M. Outstanding performance of rehydrated Mg–Al hydrotalcites as heterogeneous methanolysis catalysts for the synthesis of biodiesel. *Fuel* **2018**, *211*, 173–181. [CrossRef]
225. Brito, A.; Borges, M.E.; Garín, M.; Hernández, A. Biodiesel Production from Waste Oil Using Mg–Al Layered Double Hydroxide Catalysts. *Energy Fuels* **2009**, *23*, 2952–2958. [CrossRef]
226. Cantrell, D.G.; Gillie, L.J.; Lee, A.F.; Wilson, K. Structure-reactivity correlations in MgAl hydrotalcite catalysts for biodiesel synthesis. *Appl. Catal. A Gen.* **2005**, *287*, 183–190. [CrossRef]
227. Tajuddin, N.A.; Manayil, J.C.; Lee, A.F.; Wilson, K. Alkali-Free Hydrothermally Reconstructed NiAl Layered Double Hydroxides for Catalytic Transesterification. *Catalysts* **2022**, *12*, 286. [CrossRef]
228. Tajuddin, N.A.; Manayil, J.C.; Isaacs, M.A.; Parlett, C.M.A.; Lee, A.F.; Wilson, K. Alkali-Free Zn–Al Layered Double Hydroxide Catalysts for Triglyceride Transesterification. *Catalysts* **2018**, *8*, 667. [CrossRef]
229. Du, L.; Ding, S.; Li, Z.; Lv, E.; Lu, J.; Ding, J. Transesterification of castor oil to biodiesel using NaY zeolite-supported La<sub>2</sub>O<sub>3</sub> catalysts. *Energy Convers. Manag.* **2018**, *173*, 728–734. [CrossRef]
230. Babajide, O.; Musyoka, N.; Petrik, L.; Ameer, F. Novel zeolite Na-X synthesized from fly ash as a heterogeneous catalyst in biodiesel production. *Catal. Today* **2012**, *190*, 54–60. [CrossRef]
231. Al-Jammal, N.; Al-Hamamre, Z.; Alnaief, M. Manufacturing of zeolite based catalyst from zeolite tuft for biodiesel production from waste sunflower oil. *Renew. Energy* **2016**, *93*, 449–459. [CrossRef]
232. Xie, J.; Zheng, X.; Dong, A.; Xiao, Z.; Zhang, J. Biont shell catalyst for biodiesel production. *Green Chem.* **2009**, *11*, 355–364. [CrossRef]
233. Yang, L.; Zhang, A.; Zheng, X. Shrimp Shell Catalyst for Biodiesel Production. *Energy Fuels* **2009**, *23*, 3859–3865. [CrossRef]
234. Rezaei, R.; Mohadesi, M.; Moradi, G.R. Optimization of biodiesel production using waste mussel shell catalyst. *Fuel* **2013**, *109*, 534–541. [CrossRef]
235. Nakatani, N.; Takamori, H.; Takeda, K.; Sakugawa, H. Transesterification of soybean oil using combusted oyster shell waste as a catalyst. *Bioresour. Technol.* **2009**, *100*, 1510–1513. [CrossRef]
236. Chakraborty, R.; Bepari, S.; Banerjee, A. Transesterification of soybean oil catalyzed by fly ash and egg shell derived solid catalysts. *Chem. Eng. J.* **2010**, *165*, 798–805. [CrossRef]
237. Nair, P.; Singh, B.; Upadhyay, S.N.; Sharma, Y.C. Synthesis of biodiesel from low FFA waste frying oil using calcium oxide derived from *Meretrix meretrix* as a heterogeneous catalyst. *J. Clean. Prod.* **2012**, *29–30*, 82–90. [CrossRef]
238. Liu, X.H.; Bai, H.X.; Zhu, D.J.; Cao, G. Green Catalyzing Transesterification of Soybean Oil with Methanol for Biodiesel Based on the Reuse of Waste River-Snail Shell. *Adv. Mater. Res.* **2010**, *148–149*, 794–798.
239. Gupta, J.; Agarwal, M. Preparation and characterization of highly active solid base catalyst from snail shell for biodiesel production. *Biofuels* **2019**, *10*, 315–324. [CrossRef]
240. Ngamcharussrivichai, C.; Nunthasanti, P.; Tanachai, S.; Bunyakiat, K. Biodiesel production through transesterification over natural calciums. *Fuel Process. Technol.* **2010**, *91*, 1409–1415. [CrossRef]
241. Aktas, A.; Ozer, S. Biodiesel production from leftover olive cake. *Parameters* **2012**, *10*, 11.
242. Al-Hamamre, Z. Potential of Utilizing Olive Cake Oil for Biodiesel Manufacturing. *Energy Sources Part A Recovery Util. Environ. Eff.* **2015**, *37*, 2609–2615. [CrossRef]
243. Sandouqa, A.; Al-Hamamre, Z.; Asfar, J. Preparation and performance investigation of a lignin-based solid acid catalyst manufactured from olive cake for biodiesel production. *Renew. Energy* **2019**, *132*, 667–682. [CrossRef]
244. Elnasr, T.A.S.; Al-Enezi, A.T.; Hussein, M.F.; Bielal, H.; Alhumaimess, M.S.; El-Ossaily, Y.A.; Hassan, H.M.A.; AlNahwa, L.H.M.; Aldawsari, A.M.; Alsohaimi, I.H. Sustainable biodiesel production from waste olive oil: Utilizing olive pulp-derived catalysts for environmental and economic benefits. *Sustain. Chem. Pharm.* **2024**, *37*, 101426. [CrossRef]
245. Behzadi, S.; Farid, M.M. Production of biodiesel using a continuous gas–liquid reactor. *Bioresour. Technol.* **2009**, *100*, 683–689. [CrossRef]
246. Chen, Y.-H.; Wang, L.-C.; Tsai, C.-H.; Shang, N.-C. Continuous-flow Esterification of Free Fatty Acids in a Rotating Packed Bed. *Ind. Eng. Chem. Res.* **2010**, *49*, 4117–4122. [CrossRef]

247. Veljković, V.B.; Avramović, J.M.; Stamenković, O.S. Biodiesel production by ultrasound-assisted transesterification: State of the art and the perspectives. *Renew. Sustain. Energy Rev.* **2012**, *16*, 1193–1209. [[CrossRef](#)]
248. Qiu, Z.; Zhao, L.; Weatherley, L. Process intensification technologies in continuous biodiesel production. *Chem. Eng. Process.* **2010**, *49*, 323–330. [[CrossRef](#)]
249. Perego, C.; Ricci, M. Diesel fuel from biomass. *Catal. Sci. Technol.* **2012**, *2*, 1776–1786. [[CrossRef](#)]
250. Badday, A.S.; Abdullah, A.Z.; Lee, K.T.; Khayoon, M.S. Intensification of biodiesel production via ultrasonic-assisted process: A critical review on fundamentals and recent development. *Renew. Sustain. Energy Rev.* **2012**, *16*, 4574–4587. [[CrossRef](#)]
251. Knothe, G. Improving biodiesel fuel properties by modifying fatty ester composition. *Energy Environ. Sci.* **2009**, *2*, 759–766. [[CrossRef](#)]
252. Srivastava, A.; Prasad, R. Triglycerides-based diesel fuels. *Renew. Sustain. Energy Rev.* **2000**, *4*, 111–133. [[CrossRef](#)]
253. Gerpen, J.V. Biodiesel processing and production. *Fuel Process. Technol.* **2005**, *86*, 1097–1107. [[CrossRef](#)]
254. Gole, V.L.; Gogate, P.R. Intensification of synthesis of biodiesel from non-edible oil using sequential combination of microwave and ultrasound. *Fuel Process. Technol.* **2013**, *106*, 62–69. [[CrossRef](#)]
255. Gole, V.L.; Gogate, P.R. Intensification of glycerolysis reaction of higher free fatty acid containing sustainable feedstock using microwave irradiation. *Fuel Process. Technol.* **2014**, *118*, 110–116. [[CrossRef](#)]
256. Eze, V.C.; Phan, A.N.; Pirez, C.; Harvey, A.P.; Lee, A.F.; Wilson, K. Heterogeneous catalysis in an oscillatory baffled flow reactor. *Catal. Sci. Technol.* **2013**, *3*, 2373–2379. [[CrossRef](#)]
257. Ghayal, D.; Pandit, A.B.; Rathod, V.K. Optimization of biodiesel production in a hydrodynamic cavitation reactor using used frying oil. *Ultrason. Sonochem.* **2013**, *20*, 322–328. [[CrossRef](#)]
258. Santacesaria, E.; Di Serio, M.; Tesser, R.; Turco, R.; Tortorelli, M.; Russo, V. Biodiesel process intensification in a very simple microchannel device. *Chem. Eng. Process.* **2012**, *52*, 47–54. [[CrossRef](#)]
259. Wen, Z.; Yu, X.; Tu, S.-T.; Yan, J.; Dahlquist, E. Intensification of biodiesel synthesis using zigzag micro-channel reactors. *Bioresour. Technol.* **2009**, *100*, 3054–3060. [[CrossRef](#)]
260. Dimian, A.C.; Bildea, C.S.; Omota, F.; Kiss, A.A. Innovative process for fatty acid esters by dual reactive distillation. *Comput. Chem. Eng.* **2009**, *33*, 743–750. [[CrossRef](#)]
261. Demirbas, A. Biodiesel from Vegetable Oils with MgO Catalytic Transesterification in Supercritical Methanol. *Energy Sources Part A Recovery Util. Environ. Eff.* **2008**, *30*, 1645–1651. [[CrossRef](#)]
262. Lim, S.; Lee, K.T. Process intensification for biodiesel production from *Jatropha curcas* L. seeds: Supercritical reactive extraction process parameters study. *Appl. Energy* **2013**, *103*, 712–720. [[CrossRef](#)]
263. Kobayashi, J.; Mori, Y.; Kobayashi, S. Multiphase Organic Synthesis in Microchannel Reactors. *Chem. Asian J.* **2006**, *1*, 22–35. [[CrossRef](#)] [[PubMed](#)]
264. Kockmann, N. Process Engineering Methods and Microsystem Technology. In *Advanced Micro and Nanosystems*, 1st ed.; Kockmann, N., Ed.; Wiley: Hoboken, NJ, USA, 2006; pp. 1–45.
265. Dessimoz, A.-L.; Cavin, L.; Renken, A.; Kiwi-Minsker, L. Liquid–liquid two-phase flow patterns and mass transfer characteristics in rectangular glass microreactors. *Chem. Eng. Sci.* **2008**, *63*, 4035–4044. [[CrossRef](#)]
266. Mazubert, A.; Poux, M.; Aubin, J. Intensified processes for FAME production from waste cooking oil: A technological review. *Chem. Eng. J.* **2013**, *233*, 201–223. [[CrossRef](#)]
267. Kalu, E.E.; Chen, K.S.; Gedris, T. Continuous-flow biodiesel production using slit-channel reactors. *Bioresour. Technol.* **2011**, *102*, 4456–4461. [[CrossRef](#)] [[PubMed](#)]
268. Sun, J.; Ju, J.; Ji, L.; Zhang, L.; Xu, N. Synthesis of Biodiesel in Capillary Microreactors. *Ind. Eng. Chem. Res.* **2008**, *47*, 1398–1403. [[CrossRef](#)]
269. Xie, T.; Zhang, L.; Xu, N. Biodiesel synthesis in microreactors. *Green Process. Synth.* **2012**, *1*, 61–70. [[CrossRef](#)]
270. Fernandez Rivas, D.; Kuhn, S. Synergy of Microfluidics and Ultrasound: Process Intensification Challenges and Opportunities. *Top. Curr. Chem.* **2016**, *374*, 70. [[CrossRef](#)]
271. Santana, H.S.; Silva, J.L.; Taranto, O.P. Development of microreactors applied on biodiesel synthesis: From experimental investigation to numerical approaches. *J. Ind. Eng. Chem.* **2019**, *69*, 1–12. [[CrossRef](#)]
272. Tiwari, A.; Rajesh, V.M.; Yadav, S. Biodiesel production in micro-reactors: A review. *Energy Sustain. Dev.* **2018**, *43*, 143–161. [[CrossRef](#)]
273. Chueluecha, N.; Kaewchada, A.; Jaree, A. Biodiesel synthesis using heterogeneous catalyst in a packed-microchannel. *Energy Convers. Manag.* **2017**, *141*, 145–154. [[CrossRef](#)]
274. Madhawan, A.; Arora, A.; Das, J.; Kuila, A.; Sharma, V. Microreactor technology for biodiesel production: A review. *Biomass Convers. Biorefin.* **2018**, *8*, 485–496. [[CrossRef](#)]
275. Gopi, R.; Thangarasu, V.; Ramanathan, A. A critical review of recent advancements in continuous flow reactors and prominent integrated microreactors for biodiesel production. *Renew. Sustain. Energy Rev.* **2022**, *154*, 111869.
276. Abdulla Yusuf, H.; Hossain, S.M.Z.; Aloraibi, S.; Alzaabi, N.J.; Alfayhani, M.A.; Almedfaie, H.J. Fabrication of novel microreactors in-house and their performance analysis via continuous production of biodiesel. *Chem. Eng. Process.* **2022**, *172*, 108792. [[CrossRef](#)]
277. Gole, V.L.; Gogate, P.R. A review on intensification of synthesis of biodiesel from sustainable feed stock using sonochemical reactors. *Chem. Eng. Process.* **2012**, *53*, 1–9. [[CrossRef](#)]
278. Gogate, P.R. Cavitation reactors for process intensification of chemical processing applications: A critical review. *Chem. Eng. Process.* **2008**, *47*, 515–527. [[CrossRef](#)]



279. Gole, V.L.; Gogate, P.R. Intensification of Synthesis of Biodiesel from Nonedible Oils Using Sonochemical Reactors. *Ind. Eng. Chem. Res.* **2012**, *51*, 11866–11874. [[CrossRef](#)]
280. Santos, F.F.P.; Malveira, J.Q.; Cruz, M.G.A.; Fernandes, F.A.N. Production of biodiesel by ultrasound assisted esterification of *Oreochromis niloticus* oil. *Fuel* **2010**, *89*, 275–279. [[CrossRef](#)]
281. Boffito, D.C.; Mansi, S.; Leveque, J.-M.; Pirola, C.; Bianchi, C.L.; Patience, G.S. Ultrafast Biodiesel Production Using Ultrasound in Batch and Continuous Reactors. *ACS Sustain. Chem. Eng.* **2013**, *1*, 1432–1439. [[CrossRef](#)]
282. Mahamuni, N.N.; Adewuyi, Y.G. Optimization of the Synthesis of Biodiesel via Ultrasound-Enhanced Base-Catalyzed Transesterification of Soybean Oil Using a Multifrequency Ultrasonic Reactor. *Energy Fuels* **2009**, *23*, 2757–2766. [[CrossRef](#)]
283. Boffito, D.C.; Galli, F.; Pirola, C.; Bianchi, C.L.; Patience, G.S. Ultrasonic free fatty acids esterification in tobacco and canola oil. *Ultrason. Sonochem.* **2014**, *21*, 1969–1975. [[CrossRef](#)]
284. Pirola, C.; Bianchi, C.L.; Boffito, D.C.; Carvoli, G.; Ragaini, V. Vegetable Oil Deacidification by Amberlyst: Study of the Catalyst Lifetime and a Suitable Reactor Configuration. *Ind. Eng. Chem. Res.* **2010**, *49*, 4601–4606. [[CrossRef](#)]
285. Pirola, C.; Galli, F.; Bianchi, C.L.; Boffito, D.C.; Comazzi, A.; Manenti, F. Vegetable Oil Deacidification by Methanol Heterogeneously Catalyzed Esterification in (Monophasic Liquid)/Solid Batch and Continuous Reactors. *Energy Fuels* **2014**, *28*, 5236–5240. [[CrossRef](#)]
286. Kardos, N.; Luche, J.-L. Sonochemistry of carbohydrate compounds. *Carbohydr. Res.* **2001**, *332*, 115–131. [[CrossRef](#)]
287. Thompson, J.C.; He, B.B. Biodiesel Production Using Static Mixers. *Trans. ASABE* **2007**, *50*, 161–165. [[CrossRef](#)]
288. Avramović, J.M.; Stamenković, O.S.; Todorović, Z.B.; Lazić, M.L.; Veljković, V.B. The optimization of the ultrasound-assisted base-catalyzed sunflower oil methanolysis by a full factorial design. *Fuel Process. Technol.* **2010**, *91*, 1551–1557. [[CrossRef](#)]
289. Kumar, D.; Kumar, G.; Poonam; Singh, C.P. Fast, easy ethanolysis of coconut oil for biodiesel production assisted by ultrasonication. *Ultrason. Sonochem.* **2010**, *17*, 555–559. [[CrossRef](#)]
290. Thanh, L.T.; Okitsu, K.; Sadanaga, Y.; Takenaka, N.; Maeda, Y.; Bandow, H. Ultrasound-assisted production of biodiesel fuel from vegetable oils in a small scale circulation process. *Bioresour. Technol.* **2010**, *101*, 639–645. [[CrossRef](#)] [[PubMed](#)]
291. Colucci, J.A.; Borrero, E.E.; Alape, F. Biodiesel from an alkaline transesterification reaction of soybean oil using ultrasonic mixing. *J. Am. Oil Chem. Soc.* **2005**, *82*, 525–530. [[CrossRef](#)]
292. Chen, X.; Qian, W.-W.; Lu, X.-P.; Han, P.-F. Preparation of biodiesel catalysed by KF/CaO with ultrasound. *Nat. Prod. Res.* **2012**, *26*, 1249–1256. [[CrossRef](#)] [[PubMed](#)]
293. Qiu, Z.; Petera, J.; Weatherley, L.R. Biodiesel synthesis in an intensified spinning disk reactor. *Chem. Eng. J.* **2012**, *210*, 597–609. [[CrossRef](#)]
294. Pask, S.D.; Nuyken, O.; Cai, Z. The spinning disk reactor: An example of a process intensification technology for polymers and particles. *Polym. Chem.* **2012**, *3*, 2698–2707. [[CrossRef](#)]
295. Chanthon, N.; Ngaosuwan, K.; Kiatkittipong, W.; Wongsawaeng, D.; Appamana, W.; Quitain, A.T.; Assabumrungrat, S. High-efficiency biodiesel production using rotating tube reactor: New insight of operating parameters on hydrodynamic regime and biodiesel yield. *Renew. Sustain. Energy Rev.* **2021**, *151*, 111430. [[CrossRef](#)]
296. Tabatabaei, M.; Aghbashlo, M.; Dehghani, M.; Panahi, H.K.S.; Mollahosseini, A.; Hosseini, M.; Soufiyan, M.M. Reactor technologies for biodiesel production and processing: A review. *Prog. Energy Combust. Sci.* **2019**, *74*, 239–303. [[CrossRef](#)]
297. Chen, K.-J.; Chen, Y.-S. Intensified production of biodiesel using a spinning disk reactor. *Chem. Eng. Process.* **2014**, *78*, 67–72. [[CrossRef](#)]
298. Motasemi, F.; Ani, F.N. A review on microwave-assisted production of biodiesel. *Renew. Sustain. Energy Rev.* **2012**, *16*, 4719–4733. [[CrossRef](#)]
299. Azcan, N.; Danisman, A. Alkali catalyzed transesterification of cottonseed oil by microwave irradiation. *Fuel* **2007**, *86*, 2639–2644. [[CrossRef](#)]
300. Lin, Y.-C.; Hsu, K.-H.; Lin, J.-F. Rapid palm-biodiesel production assisted by a microwave system and sodium methoxide catalyst. *Fuel* **2014**, *115*, 306–311. [[CrossRef](#)]
301. Liao, C.-C.; Chung, T.-W. Optimization of process conditions using response surface methodology for the microwave-assisted transesterification of Jatropha oil with KOH impregnated CaO as catalyst. *Chem. Eng. Res. Des.* **2013**, *91*, 2457–2464. [[CrossRef](#)]
302. Boucher, M.B.; Weed, C.; Leadbeater, N.E.; Wilhite, B.A.; Stuart, J.D.; Parnas, R.S. Pilot Scale Two-Phase Continuous Flow Biodiesel Production via Novel Laminar Flow Reactor-Separator. *Energy Fuels* **2009**, *23*, 2750–2756. [[CrossRef](#)]
303. Frascari, D.; Zuccaro, M.; Pinelli, D.; Paglianti, A. A Pilot-Scale Study of Alkali-Catalyzed Sunflower Oil Transesterification with Static Mixing and with Mechanical Agitation. *Energy Fuels* **2008**, *22*, 1493–1501. [[CrossRef](#)]
304. ASTM 6584; Standard Test Method for Determination of Total Monoglycerides, Total Diglycerides, Total Triglycerides, and Free and Total Glycerin in B-100 Biodiesel Methyl Esters by Gas Chromatography. ASTM: West Conshohocken, PA, USA, 2022.
305. Brunold, C.R.; Hunns, J.C.B.; Mackley, M.R.; Thompson, J.W. Experimental observations on flow patterns and energy losses for oscillatory flow in ducts containing sharp edges. *Chem. Eng. Sci.* **1989**, *44*, 1227–1244. [[CrossRef](#)]
306. Dickens, A.W.; Mackley, M.R.; Williams, H.R. Experimental residence time distribution measurements for unsteady flow in baffled tubes. *Chem. Eng. Sci.* **1989**, *44*, 1471–1479. [[CrossRef](#)]
307. Howes, T.; Mackley, M.R.; Roberts, E.P.L. The simulation of chaotic mixing and dispersion for periodic flows in baffled channels. *Chem. Eng. Sci.* **1991**, *46*, 1669–1677. [[CrossRef](#)]

308. Ni, X.; Jian, H.; Fitch, A.W. Computational fluid dynamic modelling of flow patterns in an oscillatory baffled column. *Chem. Eng. Sci.* **2002**, *57*, 2849–2862. [\[CrossRef\]](#)
309. Harvey, A.P.; Mackley, M.R.; Stonestreet, P. Operation and Optimization of an Oscillatory Flow Continuous Reactor. *Ind. Eng. Chem. Res.* **2001**, *40*, 5371–5377. [\[CrossRef\]](#)
310. Harvey, A.P.; Mackley, M.R.; Seliger, T. Process intensification of biodiesel production using a continuous oscillatory flow reactor. *J. Chem. Technol. Biotechnol.* **2003**, *78*, 338–341. [\[CrossRef\]](#)
311. Zheng, M.; Skelton, R.L.; Mackley, M.R. Biodiesel Reaction Screening Using Oscillatory Flow Meso Reactors. *Process Saf. Environ. Prot.* **2007**, *85*, 365–371. [\[CrossRef\]](#)
312. Phan, A.N.; Harvey, A.P.; Rawcliffe, M. Continuous screening of base-catalysed biodiesel production using New designs of mesoscale oscillatory baffled reactors. *Fuel Process. Technol.* **2011**, *92*, 1560–1567. [\[CrossRef\]](#)
313. Phan, A.N.; Harvey, A.P.; Eze, V. Rapid Production of Biodiesel in Mesoscale Oscillatory Baffled Reactors. *Chem. Eng. Technol.* **2012**, *35*, 1214–1220. [\[CrossRef\]](#)
314. Eze, V.C.; Phan, A.N.; Harvey, A.P. A more robust model of the biodiesel reaction, allowing identification of process conditions for significantly enhanced rate and water tolerance. *Bioresour. Technol.* **2014**, *156*, 222–231. [\[CrossRef\]](#) [\[PubMed\]](#)
315. Eze, V.C.; Phan, A.N.; Harvey, A.P. Intensified one-step biodiesel production from high water and free fatty acid waste cooking oils. *Fuel* **2018**, *220*, 567–574. [\[CrossRef\]](#)
316. Bianchi, P.; Williams, J.D.; Kappe, C.O. Oscillatory flow reactors for synthetic chemistry applications. *J. Flow Chem.* **2020**, *10*, 475–490. [\[CrossRef\]](#)
317. Moser, B.R. Biodiesel Production, Properties, and Feedstocks. In *Biofuels: Global Impact on Renewable Energy, Production Agriculture, and Technological Advancements*; Tomes, D., Lakshmanan, P., Songstad, D., Eds.; Springer: New York, NY, USA, 2011; pp. 285–347.
318. Lin, C.-Y.; Ma, L. Influences of Water Content in Feedstock Oil on Burning Characteristics of Fatty Acid Methyl Esters. *Processes* **2020**, *8*, 1130. [\[CrossRef\]](#)
319. Kumar, S.; Singhal, M.K.; Sharma, M.P. Predictability of Biodiesel Fuel Properties from the Fatty Acid Composition of the Feedstock Oils. *Arab. J. Sci. Eng.* **2022**, *47*, 5671–5691. [\[CrossRef\]](#)
320. Özer, S. The effect of diesel fuel-tall oil/ethanol/methanol/isopropyl/n-butanol/fusel oil mixtures on engine performance and exhaust emissions. *Fuel* **2020**, *281*, 118671. [\[CrossRef\]](#)
321. Aketo, T.; Waga, K.; Yabu, Y.; Maeda, Y.; Yoshino, T.; Hanada, A.; Sano, K.; Kamiya, T.; Takano, H.; Tanaka, T. Algal biomass production by phosphorus recovery and recycling from wastewater using amorphous calcium silicate hydrates. *Bioresour. Technol.* **2021**, *340*, 125678. [\[CrossRef\]](#)
322. Im, K.; Choi, K.H.; Park, B.J.; Yoo, S.J.; Kim, J. Tofu-derived heteroatom-doped carbon for oxygen reduction reaction in an anion exchange membrane–fuel cell. *Energy Convers. Manag.* **2022**, *265*, 115754. [\[CrossRef\]](#)
323. Tomić, M.; Đurišić-Mladenović, N.; Mičić, R.; Simikić, M.; Savin, L. Effects of accelerated oxidation on the selected fuel properties and composition of biodiesel. *Fuel* **2019**, *235*, 269–276. [\[CrossRef\]](#)
324. Masudi, A.; Muraza, O.; Jusoh, N.W.C.; Ubaidillah, U. Improvements in the stability of biodiesel fuels: Recent progress and challenges. *Environ. Sci. Pollut. Res.* **2023**, *30*, 14104–14125. [\[CrossRef\]](#)
325. Verma, T.N.; Shrivastava, P.; Rajak, U.; Dwivedi, G.; Jain, S.; Zare, A.; Shukla, A.K.; Verma, P. A comprehensive review of the influence of physicochemical properties of biodiesel on combustion characteristics, engine performance and emissions. *J. Traffic Transp. Eng. (Engl. Ed.)* **2021**, *8*, 510–533. [\[CrossRef\]](#)
326. Saluja, R.K.; Kumar, V.; Sham, R. Stability of biodiesel—A review. *Renew. Sustain. Energy Rev.* **2016**, *62*, 866–881. [\[CrossRef\]](#)
327. Wang, Y.; Wu, B.; Ma, T.; Mi, Y.; Jiang, H.; Yan, H.; Zhao, P.; Zhang, S.; Wu, L.; Chen, L.; et al. Efficient conversion of hemicellulose into 2,3-butanediol by engineered psychrotrophic *Raoultella terrigena*: Mechanism and efficiency. *Bioresour. Technol.* **2022**, *359*, 127453. [\[CrossRef\]](#) [\[PubMed\]](#)
328. Oliveira, L.; Da Silva, M. Relationship between cetane number and calorific value of biodiesel from Tilapia visceral oil blends with mineral diesel. In Proceedings of the International Conference on Renewable Energies and Power Quality (ICREPO'13), Bilbao, Spain, 20–22 March 2013; pp. 20–23.
329. Mekonnen, K.D.; Endris, Y.A.; Abdu, K.Y. Alternative Methods for Biodiesel Cetane Number Valuation: A Technical Note. *ACS Omega* **2024**, *9*, 6296–6304. [\[CrossRef\]](#)
330. Lin, C.-Y.; Wu, X.-E. Determination of Cetane Number from Fatty Acid Compositions and Structures of Biodiesel. *Processes* **2022**, *10*, 1502. [\[CrossRef\]](#)
331. Sharma, A.K.; Sharma, P.K.; Chintala, V.; Khatri, N.; Patel, A. Environment-Friendly Biodiesel/Diesel Blends for Improving the Exhaust Emission and Engine Performance to Reduce the Pollutants Emitted from Transportation Fleets. *Int. J. Environ. Res. Public Health* **2020**, *17*, 3896. [\[CrossRef\]](#)
332. de Menezes, L.C.; de Sousa, E.R.; da Silva, G.S.; Marques, A.L.B.; Viegas, H.D.C.; dos Santos, M.J.C. Investigations on Storage and Oxidative Stability of Biodiesel from Different Feedstocks Using the Rancimat Method, Infrared Spectroscopy, and Chemometry. *ACS Omega* **2022**, *7*, 30746–30755. [\[CrossRef\]](#)
333. Knothe, G. Some aspects of biodiesel oxidative stability. *Fuel Process. Technol.* **2007**, *88*, 669–677. [\[CrossRef\]](#)
334. Longanesi, L.; Pereira, A.P.; Johnston, N.; Chuck, C.J. Oxidative stability of biodiesel: Recent insights. *Biofuels Bioprod. Biorefin.* **2022**, *16*, 265–289. [\[CrossRef\]](#)

335. Neves, C.V.; Módenes, A.N.; Scheufele, F.B.; Rocha, R.P.; Pereira, M.F.R.; Figueiredo, J.L.; Borba, C.E. Dibenzothiophene adsorption onto carbon-based adsorbent produced from the coconut shell: Effect of the functional groups density and textural properties on kinetics and equilibrium. *Fuel* **2021**, *292*, 120354. [CrossRef]
336. ASTM D6751; Standard Specification for Biodiesel Fuel Blend Stock (B100) for Middle Distillate Fuels. ASTM: West Conshohocken, PA, USA, 2023.
337. Sakthivel, R.; Ramesh, K.; Purnachandran, R.; Mohamed Shameer, P. A review on the properties, performance and emission aspects of the third generation biodiesels. *Renew. Sustain. Energy Rev.* **2018**, *82*, 2970–2992. [CrossRef]
338. EU Ban on the Sale of New Petrol and Diesel Cars from 2035 Explained. Available online: <https://www.europarl.europa.eu/topics/en/article/20221019STO44572/eu-ban-on-sale-of-new-petrol-and-diesel-cars-from-2035-explained> (accessed on 17 August 2024).
339. Ang, R. Malaysia Targets B30 Mandate for Heavy Vehicles by 2030. Available online: <https://www.argusmedia.com/en/news-and-insights/latest-market-news/2484262-malaysia-targets-b30-mandate-for-heavy-vehicles-by-2030> (accessed on 17 August 2024).
340. Pakulski, L. Brazil's Chamber of Deputies Approves Proposal to Raise Biodiesel Mandate to 20% in 2030. Available online: <https://www.fastmarkets.com/insights/brazil-approves-proposal-to-raise-biodiesel-mandate/> (accessed on 17 August 2024).
341. Stamatopoulos, B. The Role of Biofuels in the New Regulations Landscape. Available online: <https://safety4sea.com/cm-the-role-of-biofuels-in-the-new-regulations-landscape/> (accessed on 17 August 2024).
342. U.S. Department of Agriculture. Waste Management in Biodiesel Production. Available online: <https://farm-energy.extension.org/waste-management-in-biodiesel-production/> (accessed on 17 August 2024).
343. Dhainaut, J.; Dacquin, J.-P.; Lee, A.F.; Wilson, K. Hierarchical macroporous–mesoporous SBA-15 sulfonic acid catalysts for biodiesel synthesis. *Green Chem.* **2010**, *12*, 296–303. [CrossRef]
344. Pirez, C.; Lee, A.F.; Jones, C.; Wilson, K. Can surface energy measurements predict the impact of catalyst hydrophobicity upon fatty acid esterification over sulfonic acid functionalised periodic mesoporous organosilicas? *Catal. Today* **2014**, *234*, 167–173. [CrossRef]
345. Albuquerque, A.A.; Ng, F.T.T.; Danielski, L.; Stragevitch, L. Phase equilibrium modeling in biodiesel production by reactive distillation. *Fuel* **2020**, *271*, 117688. [CrossRef]
346. He, B.; Shao, Y.; Ren, Y.; Li, J.; Cheng, Y. Continuous biodiesel production from acidic oil using a combination of cation- and anion-exchange resins. *Fuel Process. Technol.* **2015**, *130*, 1–6. [CrossRef]
347. Zhang, G.; Xie, W. ZrMo oxides supported catalyst with hierarchical porous structure for cleaner and sustainable production of biodiesel using acidic oils as feedstocks. *J. Clean. Prod.* **2023**, *384*, 135594. [CrossRef]
348. Li, K.; Xie, W. Enhanced biodiesel production from low-value acidic oils using ordered hierarchical macro–mesoporous MoAl@H-SiO<sub>2</sub> catalyst. *Fuel* **2024**, *364*, 131105. [CrossRef]
349. Luque, R.; Clark, J.H. Biodiesel-Like Biofuels from Simultaneous Transesterification/Esterification of Waste Oils with a Biomass-Derived Solid Acid Catalyst. *ChemCatChem* **2011**, *3*, 594–597. [CrossRef]
350. Suwannakarn, K.; Lotero, E.; Ngaosuwan, K.; Goodwin, J.G. Simultaneous Free Fatty Acid Esterification and Triglyceride Transesterification Using a Solid Acid Catalyst with in Situ Removal of Water and Unreacted Methanol. *Ind. Eng. Chem. Res.* **2009**, *48*, 2810–2818. [CrossRef]
351. Morales, G.; Fernando Bautista, L.; Melero, J.A.; Iglesias, J.; Sanchez-Vazquez, R. Low-grade oils and fats: Effect of several impurities on biodiesel production over sulfonic acid heterogeneous catalysts. *Bioresour. Technol.* **2011**, *102*, 9571–9578. [CrossRef]
352. Mata, T.M.; Cardoso, N.; Ornelas, M.; Neves, S.; Caetano, N.S. Evaluation of Two Purification Methods of Biodiesel from Beef Tallow, Pork Lard, and Chicken Fat. *Energy Fuels* **2011**, *25*, 4756–4762. [CrossRef]
353. Aransiola, E.F.; Ojumu, T.V.; Oyekola, O.O.; Madzimbamuto, T.F.; Ikhu-Omoregbe, D.I.O. A review of current technology for biodiesel production: State of the art. *Biomass Bioenergy* **2014**, *61*, 276–297. [CrossRef]
354. Tasić, M.B.; Stamenković, O.S.; Veljković, V.B. Cost analysis of simulated base-catalyzed biodiesel production processes. *Energy Convers. Manag.* **2014**, *84*, 405–413. [CrossRef]
355. Lopes, M.G.M.; Santana, H.S.; Andolphato, V.F.; Russo, F.N.; Silva, J.L.; Taranto, O.P. 3D printed micro-chemical plant for biodiesel synthesis in millireactors. *Energy Convers. Manag.* **2019**, *184*, 475–487. [CrossRef]
356. Laybourn, A.; López-Fernández, A.M.; Thomas-Hillman, I.; Katrib, J.; Lewis, W.; Dodds, C.; Harvey, A.P.; Kingman, S.W. Combining continuous flow oscillatory baffled reactors and microwave heating: Process intensification and accelerated synthesis of metal-organic frameworks. *Chem. Eng. J.* **2019**, *356*, 170–177. [CrossRef]
357. Ni, X.; Mackley, M.R.; Harvey, A.P.; Stonestreet, P.; Baird, M.H.I.; Rama Rao, N.V. Mixing Through Oscillations and Pulsations—A Guide to Achieving Process Enhancements in the Chemical and Process Industries. *Chem. Eng. Res. Des.* **2003**, *81*, 373–383. [CrossRef]
358. Taherian, T.; Hemmati, A. Synthesis of the novel catalytic membrane of KOH/ Fe<sub>3</sub>O<sub>4</sub>-graphene oxide/PVDF for the production of biodiesel in a membrane reactor: Optimization with response surface methodology (RSM). *Renew. Energy* **2024**, *225*, 120219. [CrossRef]
359. Wandscher Busanello, F.; Sérgio Gomes, M.C.; Paschoal, S.M.; Rodrigues da Silva Baumgärtner, T.; Barp, G.; Fiorentin-Ferrari, L.D. The influence of membrane separation technique in the biodiesel and bioethanol production process: A review. *Biofuels* **2024**, *15*, 903–928. [CrossRef]

360. Lau, J.I.C.; Wang, Y.S.; Ang, T.; Seo, J.C.F.; Khadaroo, S.N.B.A.; Chew, J.J.; Ng Kay Lup, A.; Sunarso, J. Emerging technologies, policies and challenges toward implementing sustainable aviation fuel (SAF). *Biomass Bioenergy* **2024**, *186*, 107277. [[CrossRef](#)]
361. Fiorini, A.C.O.; Angelkorte, G.; Maia, P.L.; Bergman-Fonte, C.; Vicente, C.; Morais, T.; Carvalho, L.; Zanon-Zotin, M.; Szklo, A.; Schaeffer, R.; et al. Sustainable aviation fuels must control induced land use change: An integrated assessment modelling exercise for Brazil. *Environ. Res. Lett.* **2023**, *18*, 014036. [[CrossRef](#)]

**Disclaimer/Publisher's Note:** The statements, opinions and data contained in all publications are solely those of the individual author(s) and contributor(s) and not of MDPI and/or the editor(s). MDPI and/or the editor(s) disclaim responsibility for any injury to people or property resulting from any ideas, methods, instructions or products referred to in the content.